PH.D. IN ELECTRONIC AND COMPUTER ENGINEERING
Dept. of Electrical and Electronic Engineering
University of Cagliari

Advanced Random Access Techniques for Satellite Communications

Ing. Alessio Meloni

Advisor: Prof. Maurizio Murroni

Curriculum: ING-INF/03 Telecomunicazioni

XXVI Cycle
March 2014

In loving memory of my father
to whom I owe my engineer attitude

Ringraziamenti

La conclusione del dottorato segna in un certo senso la fine del mio periodo di formazione universitaria. Un po' per questo e un po' perché non ho mai ringraziato nessuno nelle occasioni precedenti, voglio concedermi di essere prolisso per nominare tutti quelli che, in modo diretto o meno, mi hanno aiutato e mi sono stati vicini in questi anni, sperando di non dimenticare nessuno. Innanzitutto parlando di istruzione, vorrei iniziare col ringraziare tutti quegli insegnanti che hanno preso parte alla mia formazione, partendo dalle maestre delle elementari come maestra Laura e maestra Luisella che fin da piccolo hanno piantato in me il seme della curiosità che professori delle medie prima e professori delle superiori poi hanno contribuito a far crescere con la loro passione per l'insegnamento.

Gli anni di università sono stati per me indimenticabili. E lo sono stati anche grazie alla compagnia dei miei ex-coinquilini Enrico, Nicola e Maurizio con i quali ho condiviso tanti momenti belli e divertenti. E come non citare Serra, coinquilino aggiunto che puntualmente si univa a noi per le partite di calcio infrasettimanali e non. Ringrazio tutti quei colleghi con la quale ho condiviso il percorso di studi e uno su tutti Mattia, con la quale ho passato innumerevoli giornate in biblioteca a studiare e ho condiviso innumerevoli pasti alla mensa universitaria. Inoltre vorrei ricordare Luigi, collega e amico tragicamente scomparso durante gli studi il cui ricordo porterò sempre nel cuore. Vorrei anche ringraziare tutti gli amici del mio paese e gli amici di Cagliari per esserci sempre stati quando avevo bisogno di prendere un po' d'aria e di bere qualche birretta. Un grande ringraziamento va anche tutte quelle persone che ho conosciuto in Erasmus come Uroš, Alok e Sören che hanno reso questa esperienza unica e che sono diventati per me come fratelli. Dicono che l'Erasmus apre la mente e ti forma al di là dell'esperienza accademica, ma non se ne capisce appieno il senso finché non la si vive. E io ringrazio per aver avuto la possibilità di viverla.

Per quanto riguarda il mio dottorato ringrazio immensamente il prof. Maurizio Murroni per avermi dato questa possibilità ed essermi stato vicino non solo dal punto di vista professionale ma anche umano. Ringrazio anche il prof. Atzori e tutti i colleghi dell'MCLab grazie ai quali ho capito quanto sia importante un ambiente lavorativo sereno e stimolante. Un ringraziamento va anche ai miei tutor esteri Matteo e Christian che mi hanno supervisionato durante il mio periodo

di ricerca all'Agenzia Aerospaziale Tedesca, nonchè a tutti i colleghi del gruppo di Digital Networks e ai miei due compagni d'ufficio in Germania: Giuliano e Tom. Ringrazio anche Sebastiano, Francesco, Delia e Giorgia con la quale ho vissuto per gran parte del mio dottorato e che per me sono una seconda famiglia ancor prima che amici. Ringrazio inoltre le mie attuali coinquiline Giorgia e Linda, soprattutto per essermi state vicine in un momento tragico come la scomparsa di mio padre. E ringrazio anche i miei compagni di squadra dell'Ichnos Flying Disc per avermi fatto amare l'Ultimate e avermi fatto capire che dopo una giornata nera, fare sport in bella compagnia è uno dei migliori antidoti. Un grazie va anche a tutti i miei parenti che mi hanno sostenuto in questi anni e in particolare a zia Adriana, Roberta e Oreste per essere stati così vicini e di così grande supporto per la mia famiglia.

Ultimo ringraziamento e per me anche più grande e più importante va alle due donne della mia vita: mia madre e la mia ragazza. Dicono che dietro ogni grande uomo c'è sempre una grande donna. Ma siccome io sono un piccolo uomo avevo bisogno di due grandi donne. Ringrazio mia mamma per tutto, perché a lei devo quello che sono, per avermi supportato in ogni scelta della mia vita, per avermi confortato nei momenti di sconforto, per avermi sostenuto economicamente e non solo in tutti questi anni. Ringrazio la mia ragazza per essere sempre stata al mio fianco fin dall'inizio dell'università, per aver gioito con me nei momenti di felicità e avermi dato forza nei momenti di difficoltà. Grazie di cuore.

Contents

List of Figures

List of Tables

Introduction

In a multi-access scenario [1] [2] for satellite uplink communications where pre-assignment of the available resources [3] is not possible or not convenient, the channel can basically be shared in two different manners: 1) the channel is accessed in a dedicated manner and managed by a central entity that gives permission to transmit; 2) no central entity or algorithm for coordination among users exists, therefore each user sends its data according to a local algorithm. The first option is known as Demand Assignment Multiple Access (DAMA) [4] [5] [6] and avoids the case of collisions among data sent from different terminals. However, reservation mechanisms need time to be accomplished, since a three-way handshake or similar is needed. In other words, each user sends a capacity request and has to wait for feedback in order to know whether it can transmit or not. This waiting time is not negligible and sometimes not acceptable when long propagation delay is present as in satellite communications [7]. As a matter of fact, in a typical scenario with bent-pipe Geostationary Earth Orbit (GEO) satellites, the minimum achievable delay from the moment a packet is generated till reception at the gateway using DAMA corresponds to a three-hop delay that is approximately $750\ ms$ [8]. Moreover, in scenarios such as the return channel over satellite of Digital Video Broadcasting (DVB) the transmission from each application is generally composed of short packets (e.g. DNS requests, HTTP web requests) so that the amount of data transmitted upon reservation of the channel does not pay off the cost of negotiation thus wasting capacity. Therefore DAMA is convenient only when single users have a medium or high amount of traffic to send while, if transmission from users is bursty [9] [10] as in the case of consumer type of interactive satellite terminals, the second alternative known as Random Access (RA) may be preferred, although the possibility of burst collision among terminals is present because of the nature of the channel that does not allow carrier sensing [11] and collision avoidance (as for example in 802.11 [12]).

RA techniques such as Slotted Aloha (SA) [13] [14] [15] and Diversity Slotted Aloha (DSA) [16] have been largely used especially in satellite communications mainly for initial terminal login. Their almost 40 years long success resides in the capability to work nicely in peculiar conditions such as long propagation delay [17] [18] and directional transmissions that do not allow transmitting terminals to have an immediate feedback either about the state of the

channel in terms of occupancy or about the outcome of their transmission. However, as already mentioned, the absence of coordination among terminals introduces the possibility of collision among bursts sent from different users and the subsequent loss of the transmitted content. For this reason, ALOHA-based techniques have been generally used when the expected load on the channel is small enough to ensure a sufficiently low packet loss probability [19].

Recently, Aloha-based techniques have gained increasingly new attention due to the introduction of the concept of Interference Cancellation (IC), already investigated in [20] for Code Division Multiple Access (CDMA), as a mean to exploit the diversity advantages brought by DSA. In particular this new technique, called Contention Resolution Diversity Slotted Aloha (CRDSA), was firstly introduced in [21] and allows to restore the content of colliding packets based on the fact that if two identical copies of the same packet are sent and each one contains a pointer to the position of the other one, the interference contribution due to the remaining copy of the decoded packet can be removed in order to restore previously interfering bursts. Subsequently, the same concept has been extended to more than two copies per packet [22] [23] and to the case of variable burst degree, known as Irregular Repetition Slotted Aloha (IRSA) [24] [25] [26], in which the number of copies sent per packet varies according to a given probability distribution. Moreover, the concept of contention resolution has also been extended to the case of unslotted ALOHA [27] and to the case in which bursts are segmented and encoded prior to transmission [28] [29] [30] [31] [32].

Consider G_{IN} as the normalized logical Medium Access Control (MAC) channel load, i.e. the average number of different packet contents sent per slot and G_{OUT} as the throughput, i.e. the average number of different packet contents correctly received over a slot period. While for SA the maximum throughput value is $G_{OUT} \simeq 0.36[pkt/slot]$ (obtained for $G_{IN} = 1$) and DSA ensures smaller packet loss probability up to moderate loads, CRDSA and its evolutions can reach throughput values even close to $1[pkt/slot]$. Moreover, the use of IC can also benefit from power unbalance among different sources [33] [34]. Considering the advantages mentioned above, these techniques were investigated within the DVB committee for its use in the Return Channel over Satellite (RCS) of the next generation of interactive satellite services [35][36] and have been recently approved in the specification for the Digital Video Broadcasting - Return Channel over Satellite version 2 (DVB-RCS2) [37], in which the possibility of sending logon, control and even user traffic using RA in timeslots specified by the Network Control Center (NCC) is provided to Return Channel Satellite Terminals (RCST) in light of the increasingly need of high-speed bidirectional networks [38] [39] for consumer interactivity [40] [41].

After the birth of SA a significant number of research studies on possible applications [42] [37], optimizations [43] and stability [44] [45] [46] [47] [48] have been carried out. Also the

birth of CRDSA has given place to the same interests among the scientific community. The work presented in this thesis operates in this direction providing contributions in some of these research branches such as optimization [49] [50] [51] and stability modelling [52] [53] [54] for Aloha-based techniques using IC and employed in the context of satellite communications. In particular, the remainder of this thesis is organized as follows:

- Chapter 1 deals with the state of the art of RCS satellite communications and gives an overview of RA techniques with particular emphasis on Aloha-based ones;

- in Chapter 2 RA communication design in DVB-RCS2 is considered with regard to CRDSA. In particular, a model for stability computation is presented and some crucial evaluation parameters for such a model are defined; a thorough analysis of the design aspects to take into account in such a system is also presented and the use of dynamic control limit policies is discussed both for finite and infinite population;

- in Chapter 3 the results obtained in the previous chapter for synchronous RA techniques are extended to the case of asynchronous ones and a comparison between the two in terms of stability as well as delay and throughput performance is put in place;

- in Chapter 4 a new technique is introduced, in which CRDSA is used in an unframed manner in order to lower the overall packet delay of received packets. Found results demonstrate that this new access scheme is also beneficial for the throughput of the communication;

- Chapter 5 concludes the paper resuming the work presented in this thesis and its contribution in the field of Advanced Random Access Techniques for Satellite Communications.

Chapter 1

State of the Art

Since the early 1990s, commercial satellite communications have emerged to support bidirectional services [38] [39] through Very Small Aperture Terminals (VSAT) systems. Its success resides in the exploitation of communication gaps in terrestrial networks as for example remote and rural area communications. For this reason, a range of commercial systems support broadband satellite access: Digital Video Broadcasting - Return Channel over Satellite (DVB-RCS) [35], Internet Protocol over Satellite (IPoS) [42], Data over Cable Service Interface Specification over Satellites (S-DOCSIS) [55] and Regenerative Satellite Mesh (RSM-A) [56]. Among these, DVB-RCS is the only open specification and is considered the reference architecture for broadband satellite systems.

The DVB-RCS standard [35] defines an air interface specification for two-way satellite communications later extended to support mobile applications [57] [58]. Moreover, recent advances in satellite systems such as Digital Signal Processors (DSP)-based demodulation, advanced Forward Error Correction (FEC), availability of new flexible high-power satellites, and commercial access to Ka-Band frequency spectrum have provided an opportunity for a new generation of low-cost interactive satellite broadband access [59] [60]. These advances together with renewed interest in supporting a wider range of Internet Protocol (IP)-based traffic, have resulted in the inclusion of an RA channel in the DVB-RCS2 specification [37]. This specification comprises a part dealing with the Lower Layer (LL) and a part dealing with the Higher Layer (HL). The Medium Access Control (MAC) mechanisms are specified in the LL and are responsible for signaling and resource reservation using Demand Assigned Multiple Access (DAMA) as well as for logon, control and user traffic using RA mode.

In the followings multiple access methods are summarized. In particular, protocols based on dedicated access with particular regard to the DAMA case and fundamental RA techniques linked to satellite communications are reviewed. The last two sections briefly describe the role of Dedicated Access and RA respectively in Digital Video Broadcasting - Return Channel over

Satellite (DVB-RCS) [41] and DVB-RCS2 [61].

1.1 Demand Assignment Satellite Protocols

Dedicated Access based on reservation aim to completely avoid collisions by preventing terminals from accessing the channel until a reservation is made. These protocols can achieve very high throughput, but the combination of reservation delay and satellite Round Trip Time (RTT) can be too high for some user applications, espcially if using GEO satellites. Among the protocols of this family, dynamic reservation based on Time Division Multiple Access (TDMA) is popular in modern satellite networks, because it is flexible and can adapt to changing traffic patterns. When a NCC is used, RCSTs send reservation requests to the NCC through the reservation channel. Even though reservation-based channels operate collision free, there is however a need for each terminal to send capacity request messages to the NCC. Therefore, four basic DAMA request methods are generally defined:

- Constant Rate Allocation (CRA) is static capacity allocated by the NCC according to the Service Level Agreement (SLA). The allocation is constant as long as the user remains active.
- Rate Based Dynamic Capacity (RBDC) provides a predictive capacity request, based on an estimate of the arrival rate. The NCC assigns capacity at the start of each superframe to sustain requested rate. This rate must be refreshed before expiration of a timer, or a new request is made.
- Volume Based Dynamic Capacity (VBDC) is capacity request derived from the occupancy of the RCST transmit buffers. The NCC allocates capacity when available, based on some fairness criteria. Each request is cumulative. New requests add to any previous backlogs until all requested timeslots are allocated to the RCST. Absolute VBDC (AVBDC) is used to periodically resynchronize the allocations.
- Free Capacity Allocation (FCA) is an additional capacity allocated by the NCC actually without any explicit request from an RCST. It assigns unallocated timeslots to specific RCSTs based on a combination of heuristics and traffic models.

1.2 Random Access Satellite Protocols

The family of Carrier Sense Multiple Access (CSMA) protocols cannot be used in satellite systems because the propagation delay is much longer than packet transmission time and terminals

have not immediate sense of the state of the channel. For this reason protocols presented hereinafter are mainly based on Aloha or other concepts that do not require immediate sensing of the channel state.

1.2.1 Aloha Protocol

The Aloha protocol is one of the simplest and earliest methods used to share satellite capacity. In this protocol, terminals transmit packets immediately to the satellite in an unsynchronized manner. After each transmission, a terminal waits for acknowledgement of successful transmission on the downlink path. In case no acknowledgement is observed, the packet is assumed to have suffered collision, which occurs when transmission from more than one terminal overlap in time. Therefore the terminal waits a random interval (known as backoff time) to retransmit the packet. Figure 1.1 shows on a time axis, an example of transmission using Aloha in which transmission from a terminal is correctly received (e.g. Pkt 1) or suffered interference (e.g. Pkt 2). Consider an infinite number of users transmitting independently (so that packet arrivals can be modelled as a Poisson process) and a channel in which packets can be lost only by means of interference. In [13] it has been shown that such a protocol can have a throughput up to $G_{OUT} \simeq 0.18$ when $G_{IN} = 0.5$.

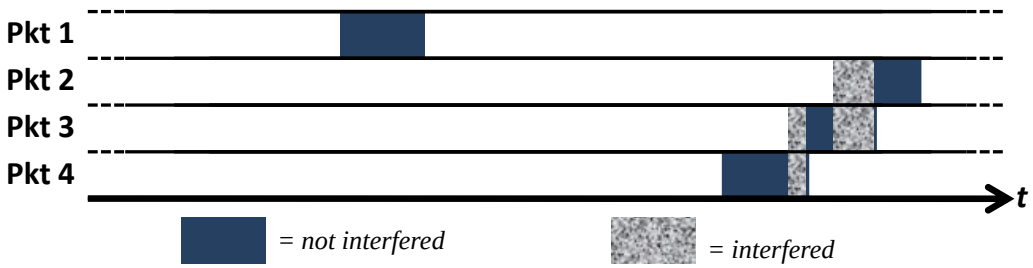

Figure 1.1: Example of Aloha channel

1.2.2 Slotted Aloha (SA) Protocol

The maximum throughput of an Aloha protocol may be increased by synchronizing all transmissions to a common channel clock as in Figure 1.2. In satellite systems this is usually performed by a broadcast reference clock [14]. Packets are transmitted in a synchronised manner at the start of timeslots thus eliminating the possibility of partial collision of packets from different terminals. With such an expedient, this protocol doubles the maximum achievable throughput to $G_{OUT} \simeq 0.36$ when $G_{IN} = 1$. At very low loads SA delay performance is worse than Aloha because ready packets have to wait for the start of a timeslot. However when load increases, fewer collisions reduce the number of retransmissions necessary and hence reduce average delay.

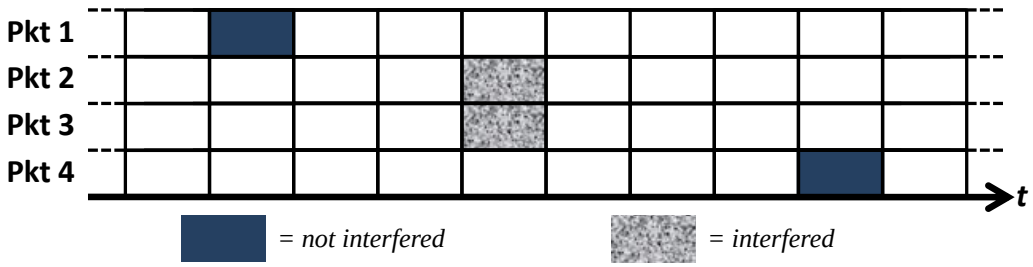

Figure 1.2: Example of SA channel

1.2.3 SREJ-Aloha Protocol

This version of the Aloha protocol approaches the theoretical SA throughput limit of $G_{OUT} \simeq 0.36$ for asynchronous multiple access by sub-packetizing messages into independently receivable segments and using a control feedback to retransmit only those sub-packets that are lost in a collision [62]. The main advantage of SREJ-Aloha over SA is the ability to achieve similar throughput performance without synchronization between data terminals. However this also incurs additional delay and the need for a control feedback loop. In practice the useful throughput achieved varies depending on the packet length and overhead required for each sub-packet.

1.2.4 Diversity Slotted Aloha (DSA) Protocol

DSA is an enhanced SA protocol that allows a terminal to randomly transmit multiple copies of the same packet either on different frequency channels or spaced apart by random time intervals (as in Figure 1.3). This increases the probability that at least one replica (see Pkt 3) will be received after one or few transmission attempts, hence resulting in low average delay. In fact throughput is an important performance criterion, but for GEO satellite networks delay performance is equally important. It has been shown [16] that sending replicas results in better delay performance for light traffic. However this performance degrades rapidly once the maximum throughput is obtained due to multiple packet transmission that increases the overall

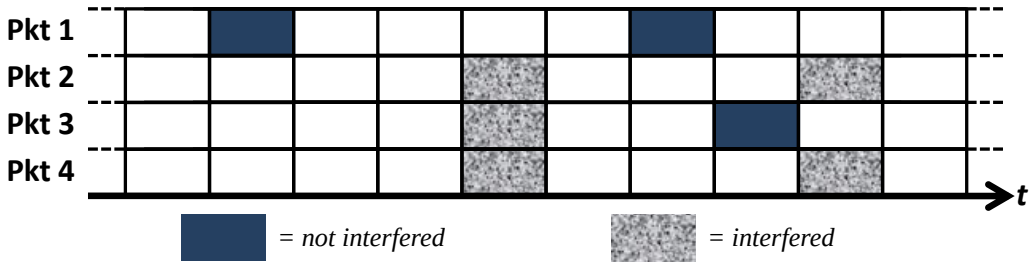

Figure 1.3: Example of DSA channel

physical[1] channel load. The resulting delay performance is relatively good over a large range of input traffic when sending two replicas of a packet. A larger number of replicas results in more robustness to loss, but at the cost of lower overall capacity.

1.2.5 Contention Resolution Diversity Slotted Aloha (CRDSA) Protocol

Consider a multi-access channel populated by a total number of users M. Users are synchronized so that the channel is divided into slots and N_s consecutive slots are grouped in a frame. The probability that at the beginning of a frame an idle user will send a new packet is p_0. When a frame starts, users willing to transmit place 2 copies of the same packet over the N_s slots of that frame. Packet copies are nothing else that redundant replicas except for the fact that each one contains a pointer to the location of the others. These pointers are used in order to attempt restoring collided packets at the receiver by means of IC, i.e. by subtracting the interfering content of already decoded packets through DSP thanks to their location's knowledge.

Assuming perfect IC and a channel without disturbances such as noise that might require SNR estimation [63], the only cause of unsuccessful decoding of packets is interference among them[2]. Given these conditions, consider the example in Figure 1.4 where each slot can be in one of three states:

- no packet's copies have been placed in a given slot, thus the slot is empty;
- only 1 packet's copy has been placed in a given slot, thus the packet is correctly decoded;
- more than 1 packet's copy has been placed in a given slot, thus resulting in collision.

In DSA, if all copies of a given packet collided the packet is surely lost. In CRDSA, if at least one copy of a certain packet has been correctly received (see User 4), the contribution of the other copies of the same packet can be removed from the other slots thanks to the knowledge of their location provided by the pointers contained in the decoded packet. This process might allow to restore the content of packets that had all their copies colliding (see User 2) and iteratively other packets may be correctly decoded up to a point in which no more packets can be restored (see User 1 and 3) or until the maximum number of iterations I_{max} for the SIC process is reached, if a limit has been fixed. The increased throughput allows CRDSA to be practically operated at logical loads of up to 0.55, thus allowing the transmission of small/medium sized packets in a timely manner [21].

[1] The term *physical* means the number of bursts sent and it has been specified here with regard to the *logical* channel, i.e. the load generated from different payload contents regardless of the number of copies.

[2] For the case in which non-ideal channel estimation is considered, the reader can refer to [21] where it has been demonstrated that there is no appreciable impact on the CRDSA performance for moderate SNR.

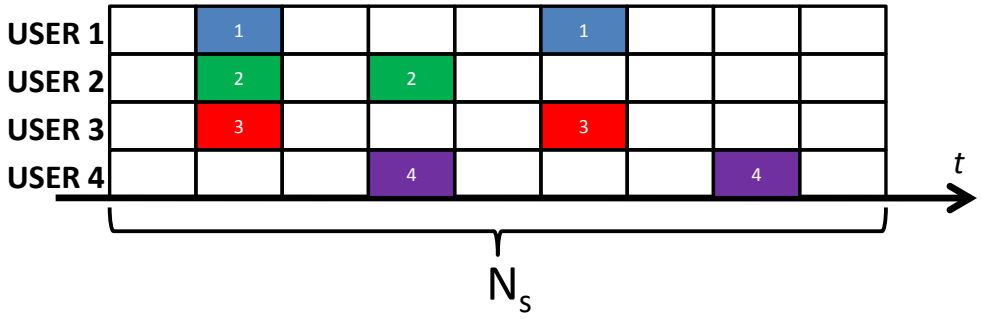

Figure 1.4: Example of frame at the receiver for CRDSA

1.2.6 CRDSA++ Protocol

An enhanced version of CRDSA [22] generates more than 2 replicas per packet and can also attempt to decode collisions by exploiting the power unbalance of received packets. It has been demonstrated that despite a higher probability of collision due to more packets in a frame, the increased diversity of CRDSA++ increases the protocol's ability to recover collisions, providing a throughput up to 0.7 [23].

1.2.7 Irregular Repetition Slotted Aloha (IRSA) Protocol

A further extension of CRDSA [26] called IRSA considers the case in which for each packet, the transmitting terminal chooses a number of copies accordingly to a predefined probability mass function. The intuition beyond this enhancement resides in the similarities between DSA-based transmission and Low Density Parity Check (LDPC) codes [64].

As a matter of fact, each frame can be described as a bipartite graph $G = (B, S, E)$ in which B is the set of burst nodes representing sent packets, S is the set of sum nodes representing each slot, and E is the set of archs connecting each packet b_i to the corresponding slot s_j in which a copy of b_i has been placed. Therefore a burst node b_i with degree d represents a packet for which d copies were sent while the degree of a generic sum node s_j indicates how many different packets have been sent in that slot. Figure 1.5 illustrates the IC process of IRSA on the corresponding bipartite graph. Removable archs (i.e. belonging to removable packets) are marked as 1, the other archs are marked as 0. Results shown in [26] demonstrated that IRSA can reach throughput values close to 1 for an asymptotic setting and around 0.8 for realistic settings.

Figure 1.6 and Figure 1.7 show respectively throughput and PLR results for all the SA-based techniques described so far, showing that in the case of high loads IRSA appears to be the best choice while for low loads a regular number of copies such as in CRDSA++ has to be prefered.

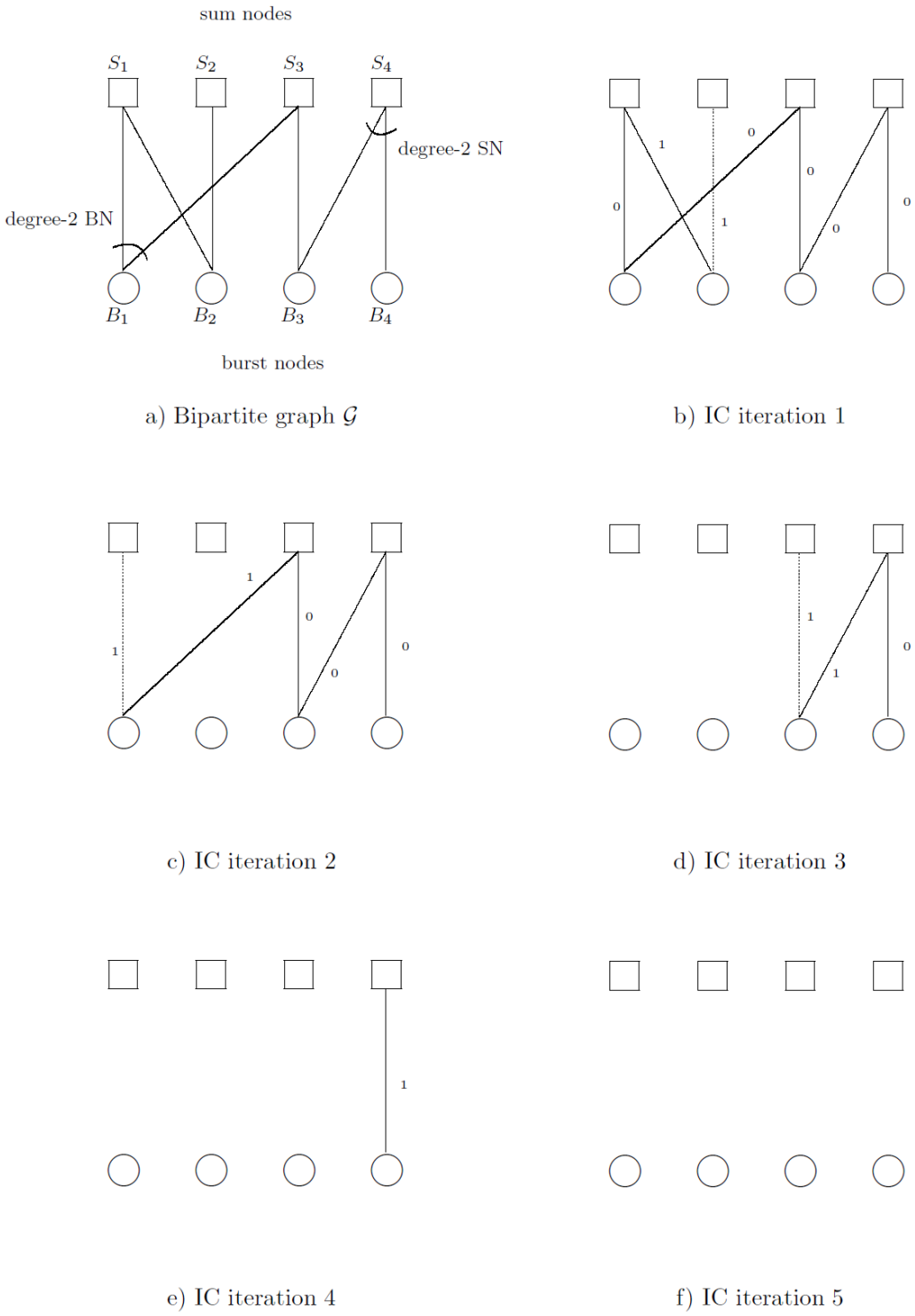

Figure 1.5: Graph representation of the IC iterative process [26]

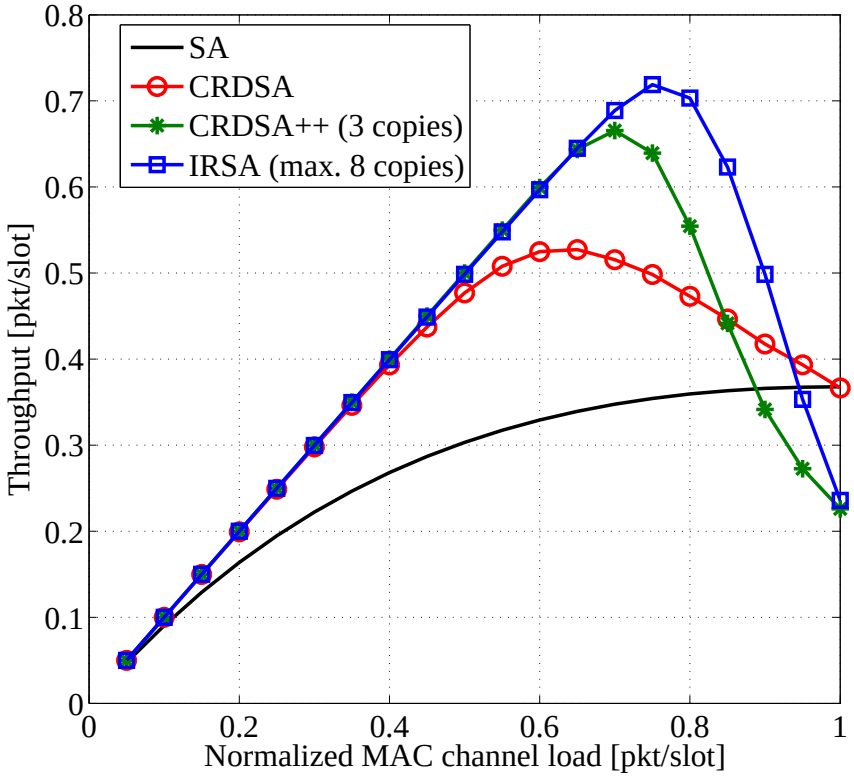

Figure 1.6: Throughput for SA-based schemes

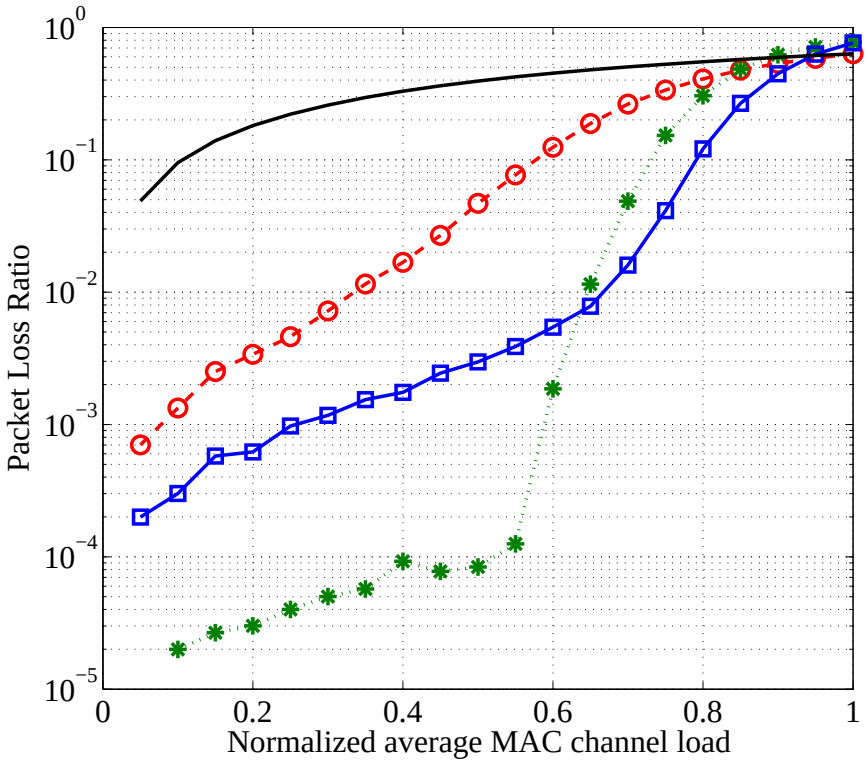

Figure 1.7: Packet Loss Ratio for SA based schemes

1.2.8 Tree Algorithms

Tree algorithms are a general class of multiple access protocols, which are based upon the observation that a channel contention is resolved if, and only if, all the terminals are divided into sets such that each set contains at most one terminal with a packet to transmit. One protocol in this category is the binary tree algorithm [65] in which each data terminal corresponds to a leaf on a binary tree (equivalent to having a unique binary address). At the start of contention for channel access, all the leaves in the tree belong to one of two branches. The channel is slotted and the slots are paired such that each of the two slots is contended for by one group of terminals. If there is more than one terminal with data to transmit on the first slot (branch), then the branch is successively divided into two until each branch has exactly one leaf on it. Terminals choose the branch in which attempt the next transmission with a certain probability, therefore a certain probability to choose the same leaf leaving the other one empty exists (see Figure 1.8). Terminals belonging to the second slot are blocked from transmitting until all contentions in first slot are resolved and follow the same method. These algorithms have been shown to be stable with maximum throughput of 0.43 and have good average delay properties.

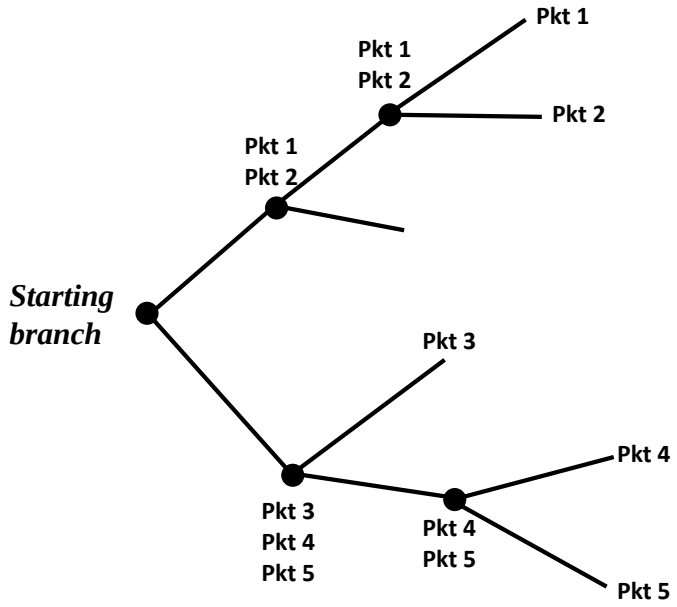

Figure 1.8: Example of binary tree contention

1.3 Hybrid protocols

In general DAMA reservation protocols can coordinate access to achieve high efficiency and throughput. This makes them attractive for commercial satellite systems where resources must be optimized. In contrast, RA protocols can achieve better delay performance at the expense of the possibility of interference that lowers the throughput. The level of compromise largely depends on the channel traffic characteristics. Hybrid protocols attempt to integrate the advantages of RA and reservation protocols into one system. An example could be to rely primarily on DAMA for active terminals with sustained traffic and to introduce RA for variable load, e.g. to offer low delay at the start of a transmission, and to issue a DAMA request as the load increases. Another option may be to dynamically reserve timeslots in an RA frame, using feedback from a previous transmission to implicitly reserve the same timeslot for a terminal. This allows the RA channel to gradually converge to contention free operation. Examples of hybrid protocols include the Reservation Aloha (R-Aloha) protocol [66], Selective Reject Aloha/First Come First Served (SREJ-Aloha/FCFS) protocol [67] and Optimal Adaptive Scheme for multiple access broadcast communication [68].

1.4 Dedicated and Random Access in DVB-RCS

Consider Figure 1.9, DVB-RCS basic operation provides a Time Division Multiplexed (TDM) broadcast link that carries data and signaling from the NCC co-located with the gateway, which is received by all the RCSTs. The Gateway provides the connectivity between each RCST and the attached network (e.g. Internet). Moreover, an RCST may support single or multiple users via the Local Area Network (LAN) interface. A set of Multi-Frequency Time Division Multiple Access (MF-TDMA) satellite channels is used for communication towards the gateway. Channels are coordinated using DAMA to share the satellite capacity between the set of active RCSTs. The NCC controls when each RCST may transmit by allocating inbound capacity to an RCST. Only one RCST can access one timeslot in the return channel. If allocation is made to an RCST that has no data to transmit the capacity is wasted, conversely an RCST with data, but no allocated timeslots has to wait until the next allocation is received. Although many early VSAT systems provided other multiple access methods [69] [70], Constant Rate Allocation (CRA), Dynamic Assignment using Bandwidth on Demand (BoD) and Free Capacity Allocation (FCA) were the only ones specified for RCS in [35].

DVB-RCS provides highly efficient use of satellite capacity with the VBDC DAMA method, ensuring there are no collisions and no capacity is unused. In contrast, the RBDC and CRA and FCA methods can provide contention-free lower access delay than VBDC, but do so at the risk

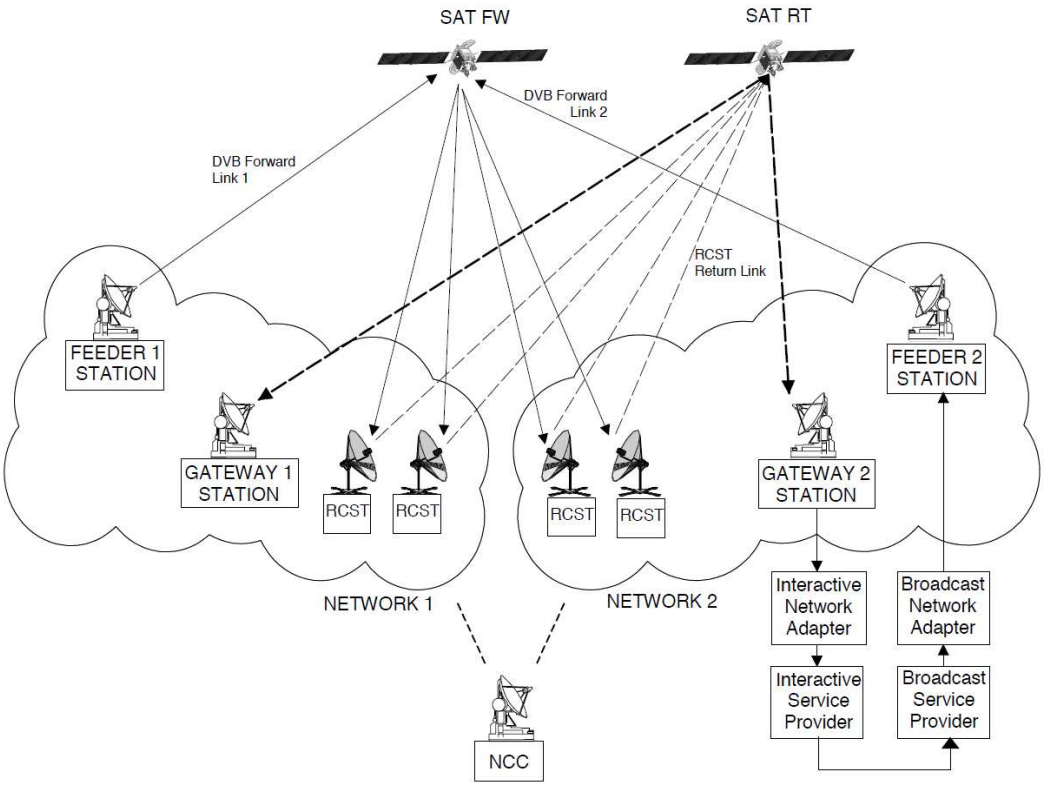

Figure 1.9: DVB-RCS Reference Model [35]

of allocating a timeslot that is not subsequently used by an RCST. A practical system will often experience fewer requests at the NCC than the total capacity to be allocated. In this case, a typical DVB-RCS system will use FCA to allocate the unused capacity to specific RCSTs. While this additional capacity can reduce the access time for the RCST, it has a high probability of being unused since the RCST did not request the capacity. For this reason, the introduction of an RA channel was thought as a way to improve this system especially for interactive Internet applications.

Two important performance criteria for interactive Internet applications are throughput (rate of transmission) and response time (time to complete transfer of an object or set of objects). TCP employs extensive handshaking between sender and receiver for establishing a connection [71]. Slow-start congestion control algorithm [72] can then be used to slowly probe the network for available capacity, limiting the initial throughput before it is gradually increased to its maximum value. This initial connection delay and limited short-term throughput during slowstart has a noticeable negative effect on response time for short-lived connections that end during the slow start phase such as web page requests [73]. This results in a long delay which is a particularly sensitive issue for satellite systems.

1.5 Dedicated and Random Access in DVB-RCS2

The DVB-RCS2 dictates mandatory support for MF-TDMA channel access method on the return link. Thus, transmission bursts from RCSTs are expected at the gateway receiver antenna within allocated timeslots on one of several carriers. DVB-RCS2 supports dedicated access to these timeslots, where each timeslot is exclusively allocated to an individual RCST. The allocation procedure may be solicited or unsolicited. Solicited allocation is equivalent to the DAMA mechanism in DVB-RCS; whereby, RCSTs must send to the NCC volume-based and/or rate-based dynamic Capacity Request (CR)s before being allocated timeslots. In unsolicited allocation, the NCC allocates timeslots to RCSTs without prior CRs. The NCC may allocate such timeslots to provide a minimum guaranteed rate for each RCST or to share excess return link capacity among RCSTs. Unsolicited allocation is equivalent to CRA and FCA assignment in DVB-RCS. Unlike DVB-RCS, DVB-RCS2 optionally supports RA to return link timeslots for user traffic transmission as well as control and logon traffic. Both SA and CRDSA are included in the specification. Also note that implementation-dependent support can be introduced for IRSA by defining the necessary forward link signalling descriptors in the user space.

1.5.1 Random Access

For CRDSA, RA block definition is a key concept. RA slots of a given channel are grouped in blocks according to their locations along the time axis. RA block definition, which is in the broadcast RA traffic method descriptor, indicates the start and the end time of each RA block in each superframe sequence for each RA channel. It is important to note that the RA traffic method descriptor may not contain RA block definitions. In this case, the default RA block duration corresponds to the whole superframe, and all RA slots of the same RA channel in the superframe belong to the same RA block. RA blocks are equivalent to CRDSA frames. The RCST randomizes CRDSA replica locations across the RA block. At the gateway, the CRDSA decoder applies IC independently across each RA block.

1.5.2 Dedicated Access

Definition of CRA, VBDC, AVBDC and FCA in DVB-RCS2 are the same as in DVB-RCS [35] and have their roots in [5]. Modifications related to dedicated access in DVB-RCS2 have primarily to do with the CR generation and signalling.

Capacity request generation

The DVB-RCS2, like DVB-RCS, does not define a standard algorithm to generate CRs. This is intentionally left out as an implementation decision. However, in a multi-vendor DVB-RCS2 network with RCSTs possibly running different CR generation algorithms, maintaining resource allocation fairness among RCSTs can be difficult. As a solution, DVB-RCS2 imposes limitation on the level of resources that can be requested. The DVB-RCS2 dictates that the RCST must ensure for each request class that (1) the resources requested (for all capacity categories combined), (2) the resources accessed via RA and (3) the resources allocated via CRA, do not exceed the 110% of the resources required to carry the input traffic. Note that this limitation applies at the FEC frame payload level. In other words, the current FEC coding rate has no impact on whether or not this limitation is met.

Capacity request signalling

In DVB-RCS2 volume-based CRs are expressed as 8-bit integers and four scaling factors are defined: 1x, 8x, 64x and 512x. DVB-RCS2 VBDC CRs are in units of bytes as opposed to slots, which is the convention adopted in the first generation of the standard [35]. Accordingly, NCC resource allocation algorithms of the first generation DVB-RCS, which expected VBDC requests in timeslots and allocated timeslots, will need to be modified to handle byte-based DVB-RCS2 VBDC requests. Rate-based CRs in DVB-RCS2 are also expressed as 8-bit integers with 1x, 4x, 16x and 64x scaling factors and in units of kilobits per second.

Chapter 2

Stability in Contention Resolution Diversity Slotted Aloha

In the current DVB generation, satellite terminals are expected to be interactive and capable of transmission in the return channel with satisfying quality. Considering the bursty nature of their traffic and the long propagation delay, the use of a RA technique is a viable solution for such a MAC scenario. In this chapter RA communication design in DVB-RCS2 is considered with particular regard to the recently introduced CRDSA technique. In particular, the main contributions of this chapter are: the presentation of a stability model and of some crucial evaluation parameters such as packet delay and First Exit Time (FET) developed in [46] for SA and here adapted to CRDSA; a thorough analysis of the design aspects to take into account in such a system; the adaptation of the dynamic control limit policies developed for SA and the analysis of their convenience when compared to static CRDSA design; the extension of all these results to the case of infinite population that is usually not considered even though in some scenarios is the most appropriate population representation.

The remainder of this chapter is organized as follows. In 2.1 the stability model used for analysis and design is presented and the concept of stability is defined while in 2.2 some practical study cases are shown in order to validate the stability model. Paragraph 2.3 deals with the definition of a Markov chain for packet delay computation and its validation. In paragraph 2.4 the definition of FET is given and the formulas for its calculation are presented; moreover the adaptation of the model for computation reduction and for the extension to the case of infinite population are discussed. Paragraph 2.5 exploits the model and the evaluation parameters introduced in the previous paragraphs by giving a general overview of how they are used in the design phase. Paragraph 2.6 compares the advantages and disadvantages of various Aloha-based RA techniques and packet degree choices. Finally Paragraph 2.7 introduces some dynamic control policies while paragraph 2.8 and 2.9 discuss their application respectively to the case of finite and infinite population. Paragraph 2.10 concludes the chapter.

2.1 Stability Model

Consider the RA communication system presented in chapter 1. Each user can be in one of two states [74]: Thinking (T) or Backlogged (B). Users in T state generate a new packet for transmission with probability p_0 over a frame interval; if so, no other packets are generated until successful transmission for that packet has been acknowledged. Users in B state have unsuccessfully transmitted their packet and keep attempting to retransmit it with probability p_r over a frame interval. In the followings, we assume that users are acknowledged about the success of their transmission at the end of the frame in which the packet has been transmitted (i.e. immediate feedback). Nevertheless this constraint will be relaxed in the last sections.

2.1.1 Equilibrium Contour

Defining

- N_B^f : backlogged users at the end of frame f
- $G_B^f = \frac{N_B^{(f-1)} p_r}{N_s}$: expected logical [1] channel load of frame f due to users in B state
- G_T^f : expected channel load of frame f due to users in T state
- $G_{IN}^f = G_T^f + G_B^f$: expected total channel load of frame f
- $PLR^f(G_{IN}^f, N_s, d, I_{max})$: expected packet loss ratio of frame f
- $G_{OUT}^f = G_{IN}^f(1 - PLR(G_{IN}^f, N_s, d, I_{max}))$: part of load successfully transmitted in frame f, i.e. throughput.

The equilibrium contour [75] can be written as

$$G_T = G_{OUT} = G_{IN}(1 - PLR(G_{IN}, N_s, d, I_{max})) \tag{2.1}$$

that represents the *locus of points for which at any time the expected channel load due to users in T state is equal to the expected throughput* G_{OUT}. Notice that the frame number f has been omitted, since in equilibrium state this condition is expected to hold for any frame.

From the definition above we can also gather that the expected number of backlogged users remains the same frame after frame. Therefore

[1] The word logical refers to the fact that the number of packets considered are those with different payload contents, thus regardless of the number of copies sent per packet.

$$N_B = \frac{G_{IN} PLR(G_{IN}, N_s, d, I_{max}) N_s}{p_r} \tag{2.2}$$

Equations (2.1) and (2.2) completely describe the *equilibrium contour* on the (G_T,N_B) plane for different values of G_{IN}[2].

2.1.2 Channel load line

Notice that the equilibrium contour itself is an infinite set of equilibrium points. In fact, we have not considered M and p_0 so far. This two essential parameters constitute the channel load line and provide the knowledge of the actual stability points for a certain scenario.

Consider M and p_0 to be constant (i.e. stationary input). Given a certain number of backlogged packets, the channel load line expresses the expected value of channel load due to users in T state. For the finite population case, the *channel load line* can be defined as

$$G_T = \frac{M - N_B}{N_s} p_0 \tag{2.3}$$

while for $M \to \infty$ the channel input can be described as a Poisson process with expected value of λ thinking users [15] so that

$$G_T = \frac{\lambda}{N_s} \tag{2.4}$$

for any N_B (i.e. the expected channel input is constant and independent of the number of backlogged packets).

2.1.3 Definition of stability

Figure 2.1 shows the equilibrium contour and the channel load line for various cases. The equilibrium contour divides the (N_B,G_T) plane in two parts and each channel load line can have one or more intersections with the equilibrium contour. These intersections are referred to as equilibrium points since $G_{OUT} = G_T$. The rest of the points of the channel load line belong to one of two sets: those on the left of the equilibrium contour represent points for which $G_{OUT} > G_T$, thus situations that yield to decrease of the backlogged population; those on the right represent points for which $G_{OUT} < G_T$, thus situations that yield to growth of the backlogged population.

Therefore we can gather that an intersection point where the channel load line enters the left part for increasing backlogged population corresponds to a *stable equilibrium point*. In

[2]Concerning the values used for the PLR, it is known from the literature [21] that the relation between $PLR(G_{IN})$ and G_{IN} can not be tightly described in an analytical manner. For this reason PLR values used in this work are taken from simulations. However, once simulations for the open loop case are accomplished, they can be used in the stability model to see how the performance changes when modifying some crucial parameters such as p_r, p_0 and M without the need of running brand new simulations. Moreover simulated values can be substituted with tight analytical equations in case any will be found in the future.

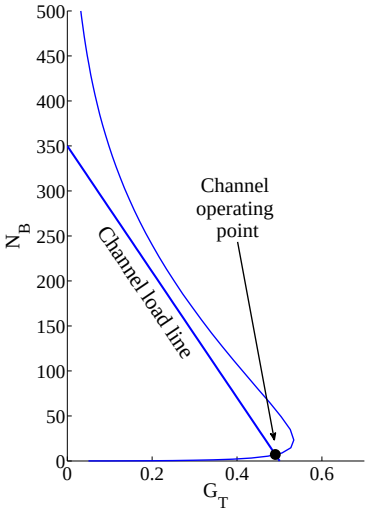

(a) Stable channel

$$p_0 = 0.143$$
$$p_r = 0.5$$
$$M = 350$$
$$(G_T^G, N_B^G) = (0.49, 8.2)$$

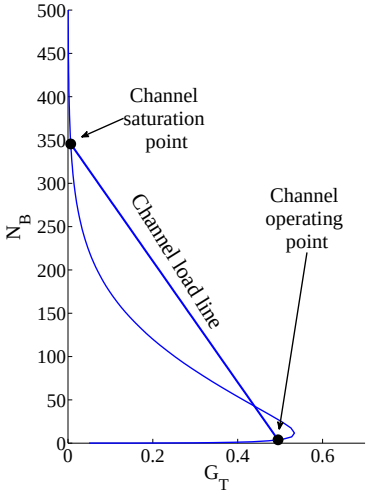

(b) Unstable channel (finite M)

$$p_0 = 0.143$$
$$p_r = 1$$
$$M = 350$$
$$(G_T^{S1}, N_B^{S1}) = (0.495, 3.9)$$
$$(G_T^U, N_B^U) = (0.44, 42.7)$$
$$(G_T^{S2}, N_B^{S2}) = (6 \cdot 10^{-3}, 346)$$

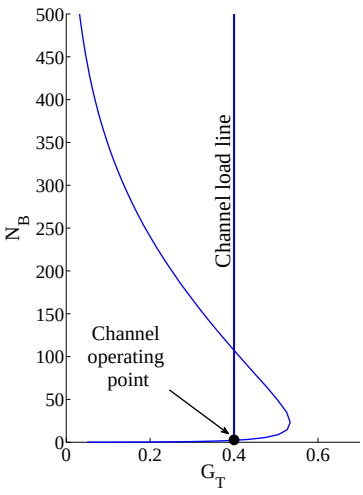

(c) Unstable channel (infinite M)

$$\lambda = 40$$
$$p_r = 0.5$$
$$M \to \infty$$
$$(G_T^{S1}, N_B^{S1}) = (0.4, 1.7)$$
$$(G_T^U, N_B^U) = (0.4, 107.32)$$
$$(G_T^{S2}, N_B^{S2}) = (0.4, \infty)$$

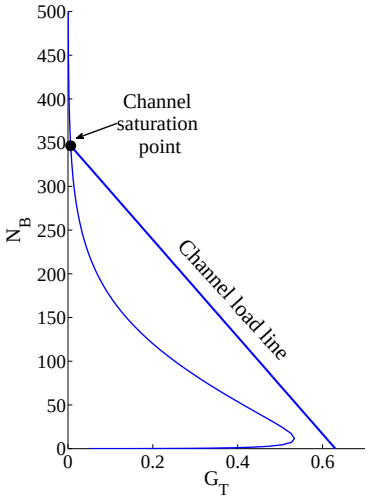

(d) Overloaded channel

$$p_0 = 0.18$$
$$p_r = 1$$
$$M = 350$$
$$(G_T^S, N_B^S) = (6 \cdot 10^{-3}, 346)$$

Figure 2.1: Examples of stable and unstable channels for CRDSA with $N_s = 100$ and $I_{max} = 20$. Stable equilibrium points are marked with a black dot.

particular, if the intersection is the only one, the point is a *globally stable equilibrium point* (indicated as G_T^G,N_B^G) while if more than one intersection is present, it is a *locally stable equilibrium point* (indicated as G_T^S,N_B^S). If an intersection point enters the right part for increasing backlogged population, it is said to be an *unstable equilibrium point* (indicated as G_T^U,N_B^U) [76].

2.1.4 Channel state definition

Figure 2.1(a) shows a stable channel. The globally stable equilibrium point can be referred as *channel operating point* in the sense that we expect the channel to operate around that point. With the word around we mean that due to statistical fluctuations, the actual G_T and G_B (and thus also G_{IN} and G_{OUT}) may differ from the expected values. In fact, the actual values have binomially distributed probability for G_B and G_T with finite M

$$Pr\left\{G_B = \frac{b}{N_s}\right\} = \frac{\binom{N_B}{b} \cdot p_r^b \cdot (1-p_r)^{N_B-b}}{N_s} \tag{2.5}$$

$$Pr\left\{G_T = \frac{t}{N_s}\right\} = \frac{\binom{M-N_B}{t} \cdot p_0^t \cdot (1-p_0)^{N_B-t}}{N_s} \tag{2.6}$$

and Poisson distributed probability for G_T with infinite M

$$Pr\left\{G_T = \frac{t}{N_s}\right\} = \frac{(\lambda^t \cdot e^{-\lambda})/(t!)}{N_s} \tag{2.7}$$

where b and t are respectively the number of backlogged and thinking users transmitting in a certain frame. Nevertheless, this assumption will be validated in the next paragraph.

Figures 2.1(b) and 2.1(c) show two unstable channels respectively for finite and infinite number of users. Analyzing this two figures for increasing number of backlogged packets, the first equilibrium point is a stable equilibrium point. Therefore the communication will tend to keep around it as for the stable equilibrium point in Figure 2.1(a) and we can refer to it once again as *channel operating point*. However, due to the abovementioned statistical fluctuations, the number of backlogged users could pass the second intersection and start to monotonically increase.

In the case of finite M, this increment goes on till a new intersection point is reached, while in the case of infinite M the expected number of backlogged users increases without any bound. In the former case, this third intersection point is another stable equilibrium point known as *channel saturation point*, so called because it is a condition in which almost any user is in B state and G_{OUT} approaches zero. In the latter case, we can say that a *channel saturation point* is present for $N_B \to \infty$ [77].

Finally Figure 2.1(d) shows the case of an overloaded channel. In this case there is only one equilibrium point corresponding to the channel saturation point. Therefore, even though the channel is nominally stable, the point of stability occurs in a non-desired region. For this reason this case is separated and distinguished from what is intended in this work as *stable channel*.

2.2 Stability Model Validation

In this paragraph, the results of simulations are shown in order to validate the stability model described above. The simulator has been built according to the system description given in the previous paragraphs, therefore perfect IC and channel estimation [78] are assumed. Moreover, neither the possibility of FEC nor power unbalance have been considered for our simulations.

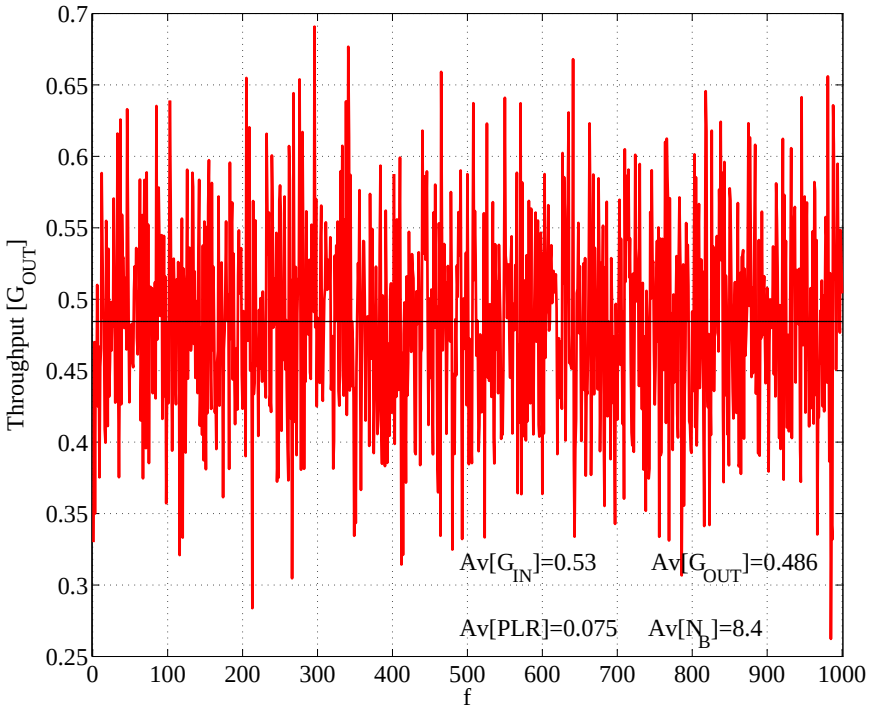

Figure 2.2: Simulated throughput for CRDSA with $N_f = 100$ $slots$, $I_{max} = 20$, $p_0 = 0.143$, $p_r = 0.5$, $M = 350$

Figure 2.2 shows the result of simulations for a communication scenario with the same parameters as the example of stable channel described in Figure 2.1(a). It can be seen that due to the aforementioned statistical variations, the throughput oscillates around a certain value. This value is the equilibrium point. In fact the horizontal line represents the value $Av[G_{OUT}] = 0.486$, that is the value obtained averaging the throughput over the entire simulation and is, as expected, a value really close to the one claimed in Figure 2.1(a).

Figure 2.3 illustrates an outcome of simulations for the communication scenario of the

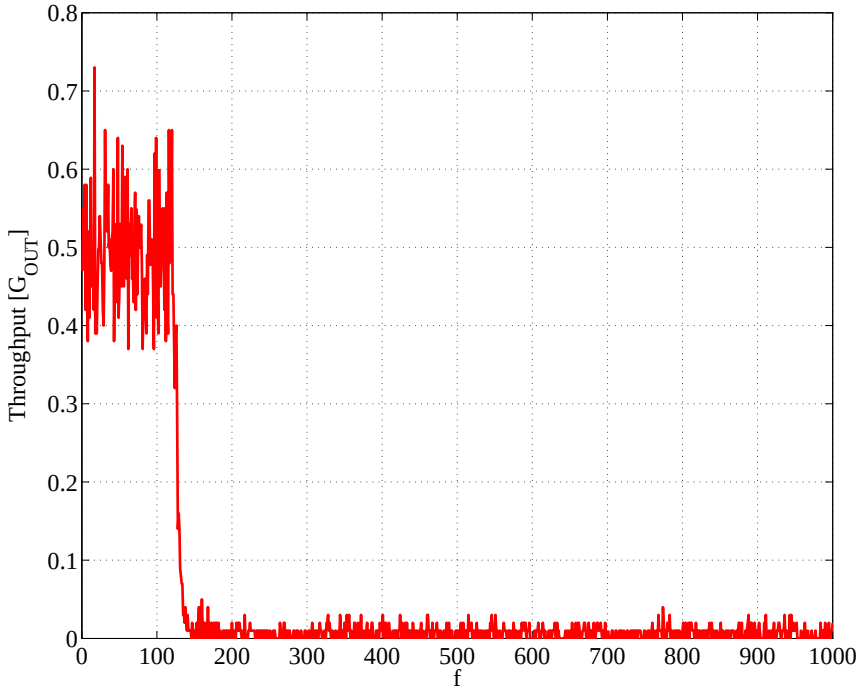

Figure 2.3: Simulated throughput for CRDSA with $N_f = 100\ slots$, $I_{max} = 20$, $p_0 = 0.143$, $p_r = 1$, $M = 350$

unstable channel described in Figure 2.1(b). In this case, the initial behaviour of the channel is such that the throughput oscillates around the channel operating point. However, differently from the previous example, this is not a globally stable equilibrium point. Therefore statistical fluctuations will sooner or later cause divergence from the channel operating point and the subsequent saturation of the channel with an average throughput that approaches zero. The time it takes for the channel to diverge from the channel operating point varies from simulation to simulation. In literature [44] the expected time of divergence for SA is known as First Exit Time (FET) and its computation will be presented in paragraph 2.4.

Finally, Figure 2.4 illustrates an outcome of simulations for the case illustrated in Figure 2.1(c), that is the case of infinite population. In particular, this outcome shows an occurrence in which divergence from the channel operating point has not occurred yet. As we can see, as long as the communication takes place around the channel operating point, the same throughput and delay considerations as for the stable channel are valid. This example highlights that depending on the communication parameters, even though the channel is unstable, the FET could be so big that instability might be acceptable depending on the application. However, if this is not the case, the communication will soon exit the stability region and the number of backlogged users N_B will grow fast and indefinitely as shown in Figure 2.5.

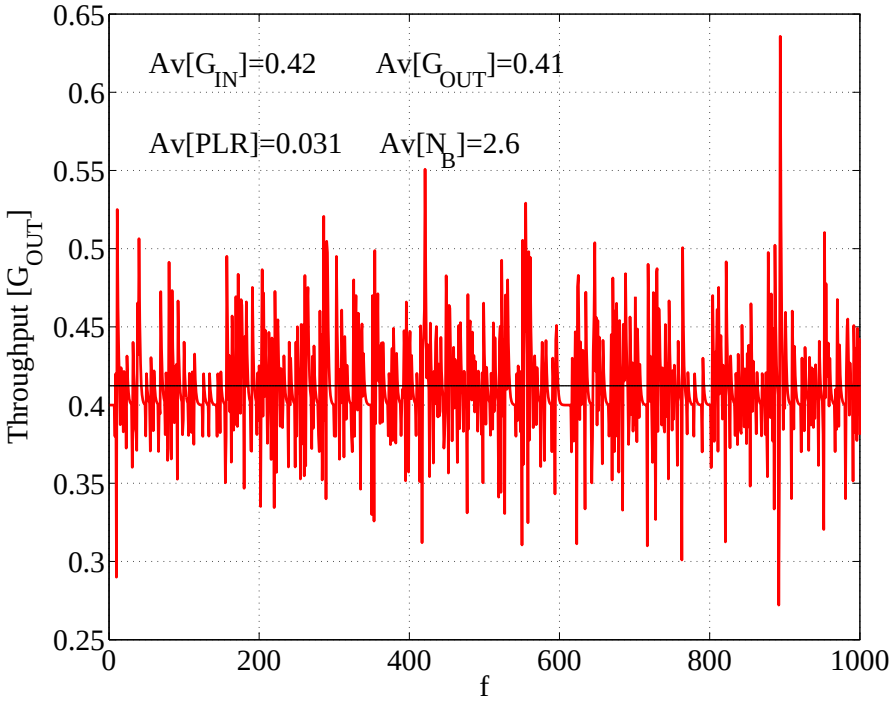

Figure 2.4: Simulated throughput for CRDSA with $N_f = 100\ slots$, $I_{max} = 20$, $\lambda = 0.4$, $p_r = 0.5$, $M \to \infty$ when divergence from the operating point has not occurred yet

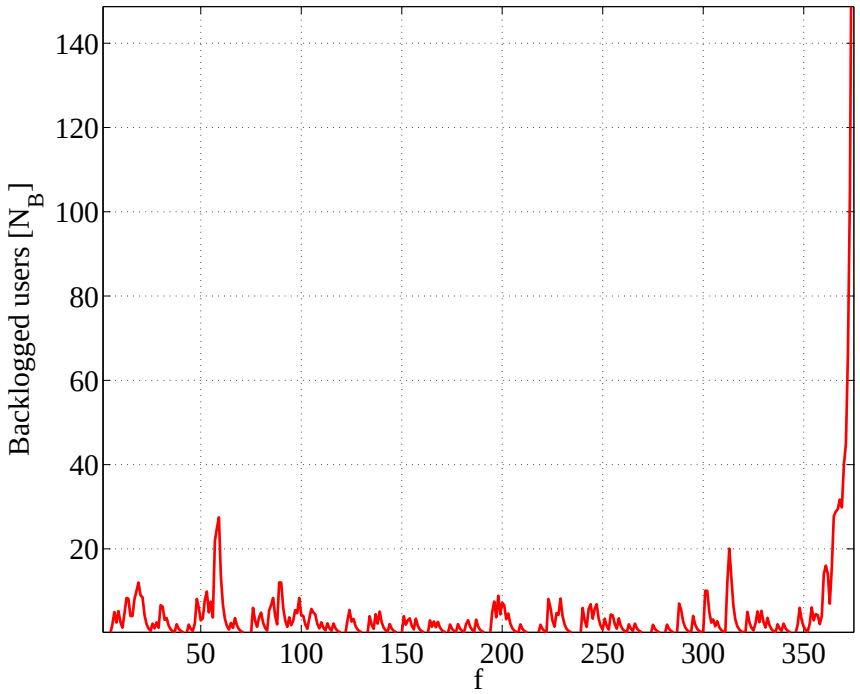

Figure 2.5: Number of backlogged users for CRDSA with $N_f = 100\ slots$, $I_{max} = 20$, $\lambda = 0.4$, $p_r = 0.5$, $M \to \infty$ with divergence from the operating point after a certain time

2.3 Packet Delay Model

Once we are sure that the channel is working at its *channel operating point*, we would like to know what is the expected distribution and average delay associated to packets that are successfully received at the gateway. This can be described using a discrete-time Markov chain with the two states B and T (Figure 2.6).

The edges emanating from the states represent the state transitions occurring to users which depend on p_r and the expected PLR at the channel operating point. If a packet transmitting for the first time receives a positive acknowledgment the user stays in T state while in case of negative acknowledgment the user switches to B state until successful retransmission has been accomplished. We assume a frame duration to be the discrete time unit of this Markov chain. Therefore the packet delay D_{pkt} is calculated as the number of frames that elapse from the beginning of the frame in which the packet was transmitted for the first time, till the end of the one in which the packet was correctly received.

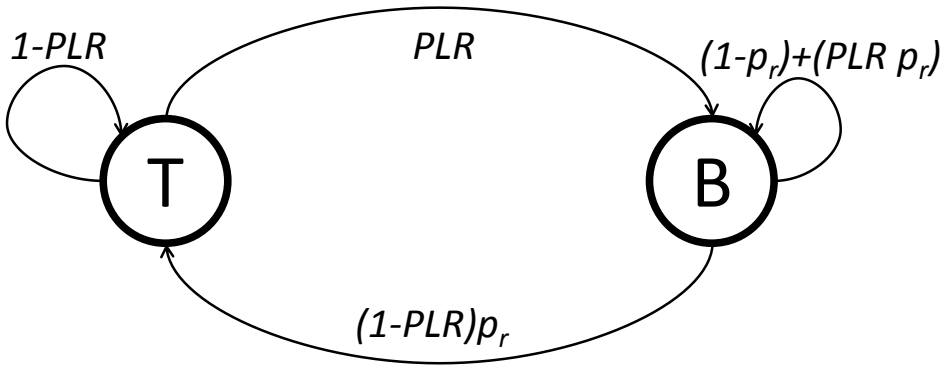

Figure 2.6: Markov Chain for the Packet Delay analysis

According to the definition above, packet delay distribution is entirely described by

$$Pr\{D_{pkt} = f\} = \begin{cases} 1 - PLR & \text{for } f = 1 \\ PLR\,[p_r\,(1 - PLR)] \cdot [1 - p_r + PLR\,p_r]^{f-2} & \text{for } f > 1 \end{cases} \tag{2.8}$$

which results in the average delay

$$Av[D_{pkt}] = \sum_{f=1}^{\infty} f \cdot Pr\{D_{pkt} = f\} \tag{2.9}$$

Equation 2.9 can alternatively be rewritten in a simpler and more intuitive form by means of Little's Theorem [44][79] [80] considering that the average number of backlogged users in

a stable system is equal to the average time spent in backlogged state, multiplied by the arrival rate of new packets G_T (that we know to be equal to G_{OUT} at the operational point). Therefore

$$Av[D_{pkt}] = \frac{N_B}{G_{OUT} \cdot N_s} \tag{2.10}$$

where the presence of N_s in the formula has the aim of normalizing the delay to the frame unit.

p_r	$Av[D_{pkt}]_{ana}$	$Av[D_{pkt}]_{sim}$	PLR
1	543.48	541.89	0.99816
0.4	3.17	3.16	0.465
0.2	2.01	2.12	0.168
0.05	2.53	2.66	0.0713
0.005	5.08	5.22	0.02

Table 2.1: Analytic and simulated average packet delay at the channel operating point for CRDSA with $N_s = 100\ slots$, $I_{max} = 20$, $M = 350$ and $p_0 = 0.18$

2.3.1 Model validation and retransmission probability's effect

Figures 2.7 and 2.8 show some results based on the example of overloaded channel given in paragraph 2.1, in order to validate the model and demonstrate the effect of p_r on the packet delay [81]. In particular p_r is progressively decreased in order to evaluate how distribution and average packet delay change. Figure 2.7 represents the channel load line and equilibrium curves for several p_r values.

When p_r is decreased, the equilibrium contour moves upwards and the point of equilibrium is found for bigger values of throughput while N_B decreases. Therefore, from Little's theorem, it is intuitive to expect that users will spend less time in B state. If we keep decreasing p_r after the throughput peak is reached, the throughput starts to decrease while the number of backlogged users increases again thus yielding to an increase of the average packet delay. This is confirmed by the results given in Table 2.1.

Figure 2.8 shows that while having a small p_r is beneficial for the PLR, it also means that users in B state will generally wait longer before retransmitting a packet. As a consequence, the smaller the p_r value the less steep the cumulative distribution curve is, so that at a certain point curves with bigger p_r overcome it in terms of probability to receive a packet before a certain time deadline. Finally the simulated average packet delay associated to the examples in Figure 2.8 is reported in Table 2.1 together with the expected results, demonstrating the validity of the model.

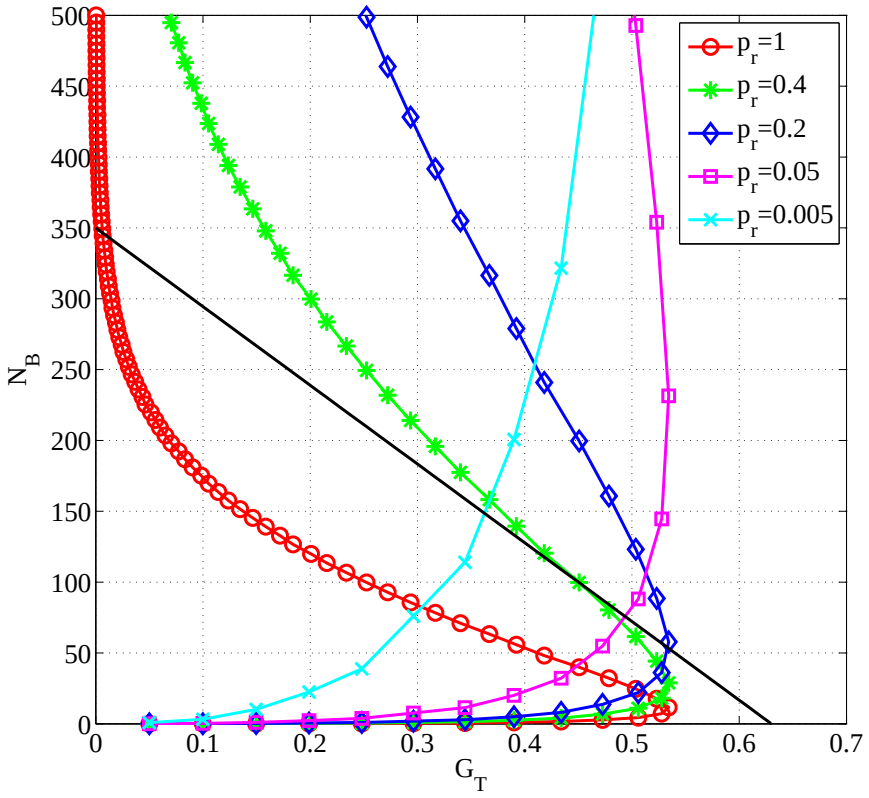

Figure 2.7: Equilibrium curves for CRDSA with $N_s = 100\ slots$, $I_{max} = 20$, $M = 350$ and $p_0 = 0.18$

2.4 First Exit Time

In paragraph 2.1 the concept of unstable channel has been introduced. Beside knowing that a certain channel is unstable, it is also of big interest to quantify how much the channel is unstable. The First Exit Time (FET) calculates the time spent around the operational point by an unstable channel before leaving the stability region. To calculate this parameter we consider a discrete-time Markov chain [82] [83] which uses the number of backlogged users N_B as describing state, since equilibrium points and more generally the state of the communication can be uniquely identified with it.

2.4.1 Transition matrix definition

Let us define P as the transition matrix for this Markov chain, with each element p_{ij} denoting the probability to pass from a number of backlogged users $N_B = j$ to a number of backlogged users $N_B = i$. To calculate each p_{ij} value we need to know the probability that having a certain number of backlogged users j and a certain number of thinking users $M - j$, respectively b backlogged users and t thinking users have transmitted and $s = t - (i - j)$ out of $t + b$ packets

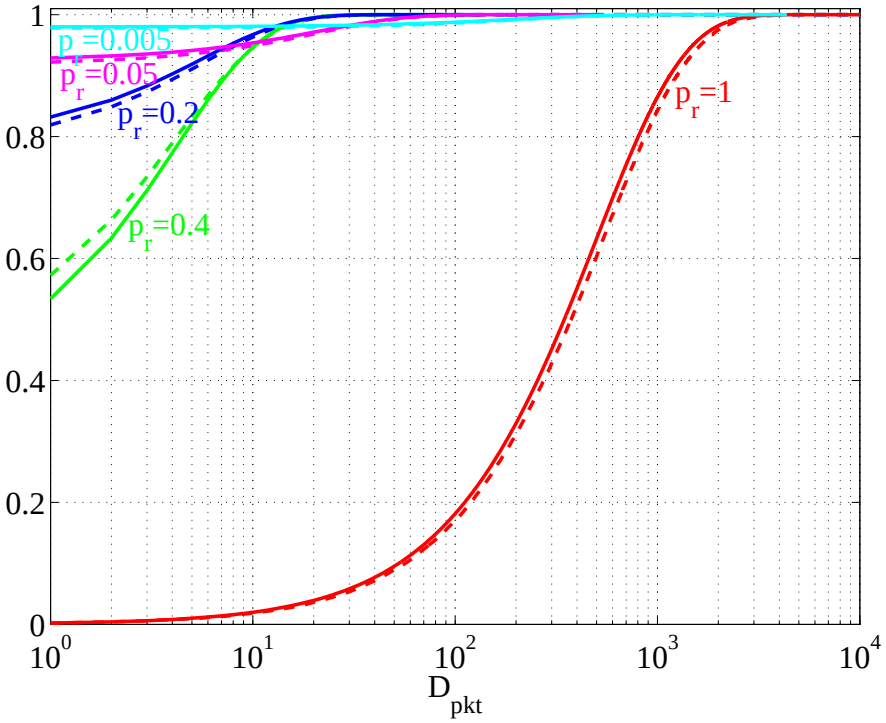

Figure 2.8: Packet delay cumulative distribution for CRDSA with $N_s = 100\ slots$, $I_{max} = 20$, $M = 350$ and $p_0 = 0.18$

have been correctly received. Therefore

$$p_{ij} = \sum_{t=0}^{M-j} \sum_{b=0}^{j} \binom{M-j}{t} p_0^t (1-p_0)^{M-j-t} \cdot \binom{j}{b} p_r^b (1-p_r)^{j-b} \cdot q(s|t+b) \tag{2.11}$$

where $q(s|t+b)$ is the probability that s packets are correctly decoded if $t+b$ packets are transmitted[3]. Let us then call Q the matrix with elements $q_{s,t+b}$ corresponding to probability $q(s|t+b)$.

In Figure 2.9 an example of the resulting P matrix is shown. According to the bidimensional representation used in paragraph 2.1, we can see here that there are two peaks corresponding to the two expected locally stable equilibrium points. However, it is more fruitful for our considerations to look at this graph from an (i,j) plane perspective plotting a line for $i = j$. Points below this line represent decrements of the number of backlogged packets while points above represent increments. Non-zero probability points look like a wake close to the line $i = j$, highlighting that possible transitions are found only for small changes in the number of backlogged packets compared to the total population M. Taking single values of j, we can roughly

[3] For the same reason previously claimed for the PLR, also $q(s|t+b)$ values are calculated from simulations over a big amount of runs (over 10^6 per $(t+b)$ value) since analytical formulas able to tightly describe the probability for a packet to be correctly decoded have not been found yet. Nevertheless in the followings a method to reduce this computational effort is introduced.

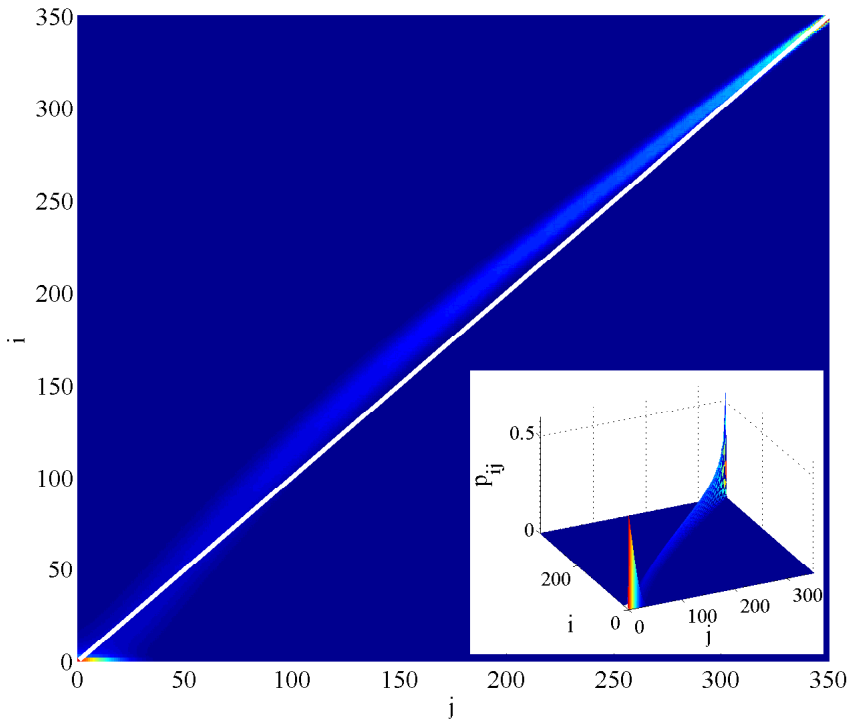

Figure 2.9: P matrix for CRDSA with $N_s = 100$, $I_{max} = 20$, $M = 350$, $p_0 = 0.143$, $p_r = 1$

identify 3 regions of the wake:

- for small values of j (close to the channel operating point) non-zero probabilities are found both for increase and decrease of N_B;
- for values of j close to M (i.e. close to the channel saturation point) non-zero probabilities are found both for increase and decrease of N_B;
- for the rest of the j values non-zero probabilities are almost exclusively found for $i > j$ so that the number of backlogged users monotonically increases.

Therefore in this particular case the system has probability zero of returning to the stability region after N_B crosses 120. We want to highlight here that the presence of a *no-return* point is scenario-dependent in the sense that for a different set of values M, p_0 , p_r , N_s it is not necessarily true that the probability of coming back from a certain value N_B is zero: sometimes could be negligible, sometimes could not, even though for the typical settings used in these scenarios the last case is really rare. Nevertheless this highlights one of the advantages of calculating the P matrix: it tells us theoretically if there is any probability of coming back to the region of stability and in the case the answer is no, tells us what is the *no-return* value of N_B.

2.4.2 State probability matrix and FET calculation

Based on the P matrix, it is now possible to calculate the probability B_i^{f+1} to be in a certain state $N_B = i$ at frame $f+1$, given a certain probability distribution $B^f = [B_0^f \; B_1^f \; \cdots \; B_M^f]$ at frame f:

$$\begin{bmatrix} B_0^{f+1} \\ B_1^{f+1} \\ \vdots \\ B_M^{f+1} \end{bmatrix} = \begin{bmatrix} p_{0,0} & \cdots & p_{0,M} \\ p_{1,0} & & \vdots \\ \vdots & \ddots & \vdots \\ p_{M,0} & \cdots & p_{M,M} \end{bmatrix} \cdot \begin{bmatrix} B_0^f \\ B_1^f \\ \vdots \\ B_M^f \end{bmatrix} \tag{2.12}$$

Generalizing Equation 2.12, the state distribution at each frame $(f+1)$ can always be calculated from the initial probability distribution $B^0 = [B_0^0 \; B_0^1 \; \cdots \; B_0^M]$ and the matrix P^{f+1}. Given the state probability matrix, it is now possible to calculate the average and cumulative distribution of the FET from a given initial state. In this example we consider as initial state $B^0 = [\, 1 \; 0 \; 0 \; \cdots \; 0 \,]$ that is the case in which the communication starts with zero backlogged users.

Figure 2.10 reports the evolution frame after frame of the state probability for the P illustrated in Figure 2.9. As we can see, when f increases the probability of being around the locally stable point in the region of high throughput decreases while the probability of being in saturation increases.

2.4.3 Reduced transition matrix

The entire description of any state of this Markov chain is of great interest but most of the times impractical, mainly because the dimension of the P matrix is equal to M^2. Therefore it could take a huge computational effort to calculate it. Nevertheless it is of interest to know the probability that the stability region around the operational point has been left in a certain moment, regardless of the actual state once we enter the region that yields to saturation.

In fact, it has been already pointed out in the description of Figure 2.9 that the further the communication gets from the first point of local stability, the smaller is the probability that the communication will come back to the stability region. For this reason, as a first approximation, it is possible to consider an absorbing state $N_B^{abs} = \lceil N_B^U \rceil + 1$ that groups all the probabilities for states from $\lceil N_B^U \rceil + 1$ to M. Doing so, our P matrix can be rewritten as

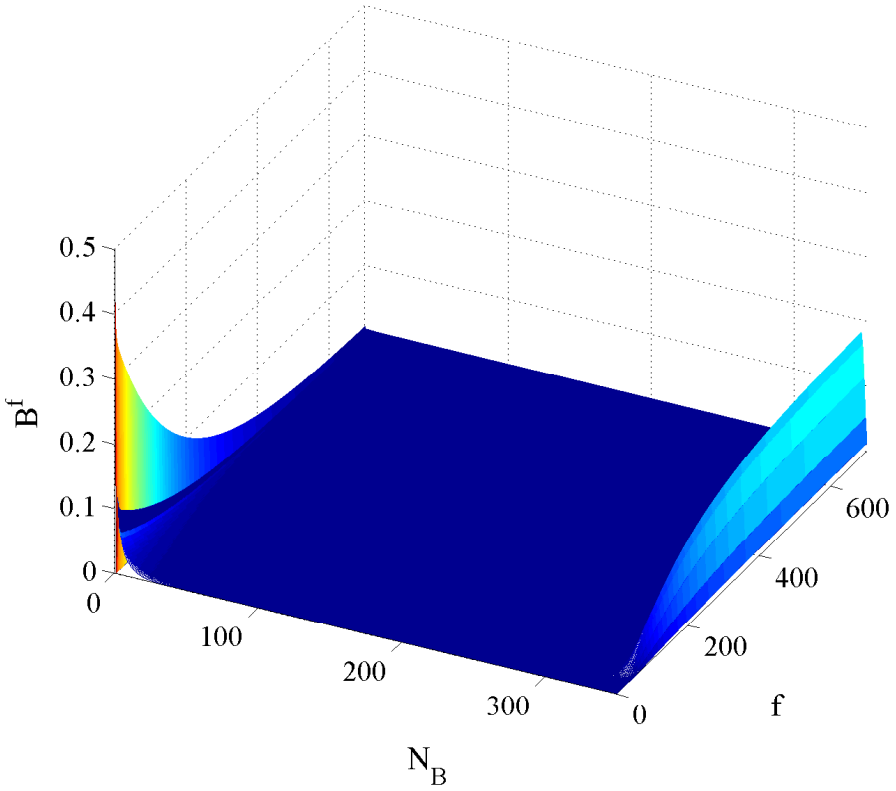

Figure 2.10: Evolution of B^f for the P matrix in figure 2.9

$$P = \begin{bmatrix} p_{0,0} & \cdots & p_{0,N_B^U} & 0 \\ \vdots & \ddots & \vdots & \vdots \\ p_{N_B^U,0} & \cdots & p_{1,N_B^U} & 0 \\ 1-(\sum_{\alpha=0}^{N_B^U} p_{\alpha,0}) & \cdots & 1-(\sum_{\alpha=0}^{N_B^U} p_{\alpha,N_B^U}) & 1 \end{bmatrix} \tag{2.13}$$

The P matrix in Equation 2.13 takes much less effort than calculating the entire P matrix since only $(\lceil N_B^U \rceil + 1)^2$ elements need to be computed thus speeding up calculations. Considering that $\sum_{\alpha=0}^{N_B^U} p_{\alpha,j}$ must be equal to 1, the probability to get to the absorbing state N_B^{abs} from a certain state j can be computed as $p_{i,j} = 1-(\sum_{\alpha=0}^{N_B^U} p_{\alpha,j})$. Moreover, since N_B^{abs} is an absorbing state, any probability to leave this state is zero while the probability of staying in the absorbing state is equal to 1.

2.4.4 Absorbing state validity

Since reducing the transition matrix by means of an absorbing state is an approximation, we now aim at verifying the validity of this approximation. Figure 2.11 shows the distribution for

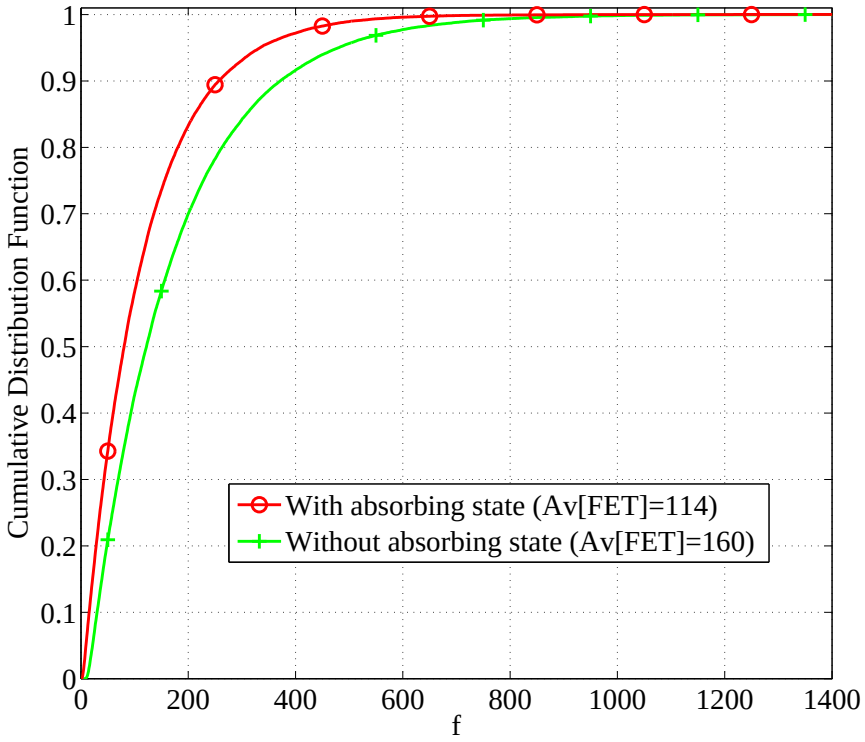

Figure 2.11: FET cumulative distribution for CRDSA with $N_s = 100$, $I_{max} = 20$, $M = 350$, $p_0 = 0.18$, $p_r = 1$

the results obtained with the reduced matrix and the simulated results. Regarding simulations, if N_B crosses the value $\lceil N_B^U \rceil$ but it comes back to the stability region, the FET is reset and the next exit is waited to set it again. For the analytic results the FET is calculated accordingly to the reduced matrix in Equation 2.13.

As already pointed out in the description of Figure 2.9, when the number of backlogged packets N_B is still close to the unstable equilibrium point, a certain probability that the communication will come back from the instability region is present. This is the reason why in Figure 2.11 the two curves show a noticeable difference. However, this problem can be solved by considering $N_B^{abs} = \lceil N_B^U \rceil + 1 + \Delta$ as absorbing state, where Δ is a positive integer big enough to ensure that the probability of false exits from the stability region (i.e. the probability that N_B crosses the stability region but comes back to values $< N_B^{abs}$) is sufficiently low. Doing so, simulation and analytical results with the approximation of absorbing state perfectly match. Figure 2.12 shows how the difference among the two average FETs decreases while increasing the chosen value for N_B^{abs}.

In conclusion, we can state that analytic results with the approximation of absorbing state represent a lower bound for the actual FET. Therefore during this kind of analysis a tradeoff between tightness of the results and simplicity of computation is present.

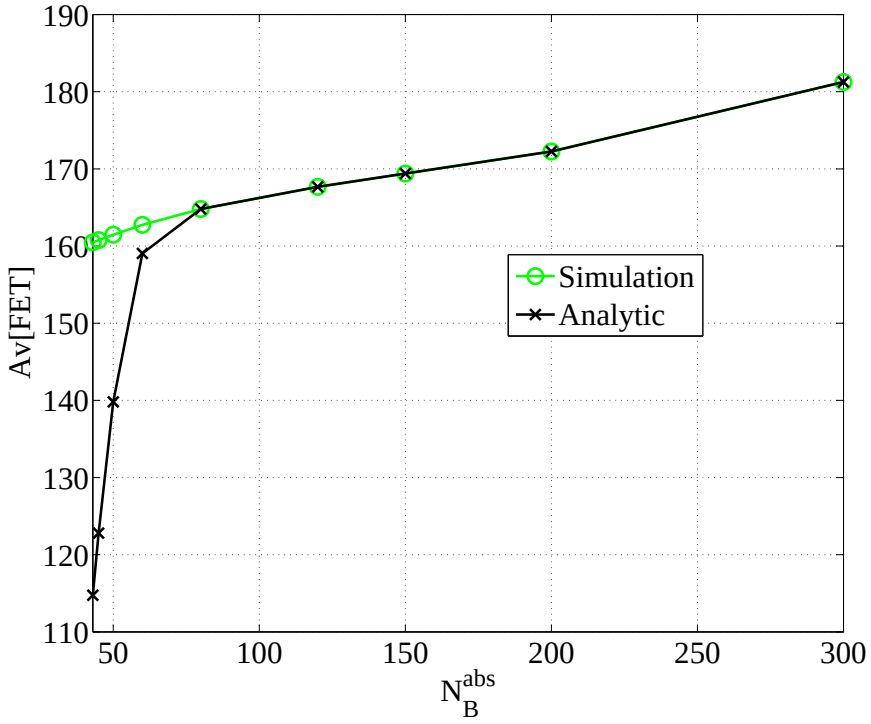

Figure 2.12: Simulated and analytic average FET when increasing N_B^{abs} for CRDSA with $N_s = 100$, $I_{max} = 20$, $M = 350$, $p_0 = 0.18$, $p_r = 1$

2.4.5 Reduced transition matrix for infinite population

The model presented is also adaptable to the case of infinite population. In fact the probability transition matrix P can be adapted by considering

$$p_{ij} = \sum_{t=0}^{\infty} \sum_{b=0}^{j} \frac{\lambda^t e^{-\lambda}}{t!} \cdot \binom{j}{b} p_r^b (1-p_r)^{N_B - b} \cdot q(s|t+b) \tag{2.14}$$

Although in this case P has infinite size, it has been just shown that is possible and practical to reduce the P matrix by means of an absorbing state. With this expedient, also this case can be treaten since P is transformed to an equivalent matrix with finite size.

2.5 Design settings

In this paragraph we will resume the role of some crucial parameters such as M, p_0, p_r and explain how the communication state changes when changing them and what are the relations to be considered when designing DVB-RCS2 communications in RA mode. In fact, since optimization depends on *constraints* and *degrees of freedom* of the particular study case, a deep investigation of the relation among these crucial parameters is needed in order to understand

tradeoffs that have to be faced. Moreover, the same discussion is introductory to understand how control policies can help to obtain better performance and a stable channel even in case of statistical fluctuations that could yield to instability.

2.5.1 Degrees of freedom

Consider Figure 2.13. The first thing we can notice is that M and p_0 only influence the channel load line while changing p_r corresponds to modifying the equilibrium contour. In Figure 2.13(a) we can see that p_0 influences the slope of the channel load line that becomes steeper when increasing p_0. This is intuitive to understand since for fixed M, if $p_0^A < p_0^B$ then $G_T^A < G_T^B$. Figure 2.13(b) shows that M shifts the channel load line up and down if the population size is respectively increasing or decreasing. From Equation 2.3 we can notice that the value M is equal to what is known in literature as q, i.e. the intersection of the line with the y-axis. Finally p_r determines a shift upward of the channel load line for smaller values of p_r (Figure 2.13(c)). As already shown, if the value p_r is sufficiently small, it is possible to stabilize a channel initially unstable. This represents the ground base for one of the control policies shown in the next section.

2.5.2 Constraints

Concerning possible *constraints*, we can identify the followings

1. stability
2. maximize p_0 or guarantee a value $p_0 \geq p_0^{min}$
3. maximize M or guarantee a value $M \geq M^{min}$
4. minimize the delay or guarantee that a certain value $Av[D_{pkt}]^{max}$ is not exceeded
5. maximize the throughput or guarantee a value $G_{OUT} \geq G_{OUT}^{min}$

For constraint 1) it has been previously shown that the stability corresponds to having a single intersection between the channel load line and the equilibrium curve (i.e. a single point of equilibrium) before the throughput peak. Constraints from 2) to 5) can be graphically represented on the (G_T,N_B) plane by the following formulas:

2.
$$\frac{G_T \cdot N_s}{M - N_B} \geq p_0^{min} \tag{2.15}$$

3.
$$\frac{G_T \cdot N_s}{p_0} + N_B \geq M^{min} \tag{2.16}$$

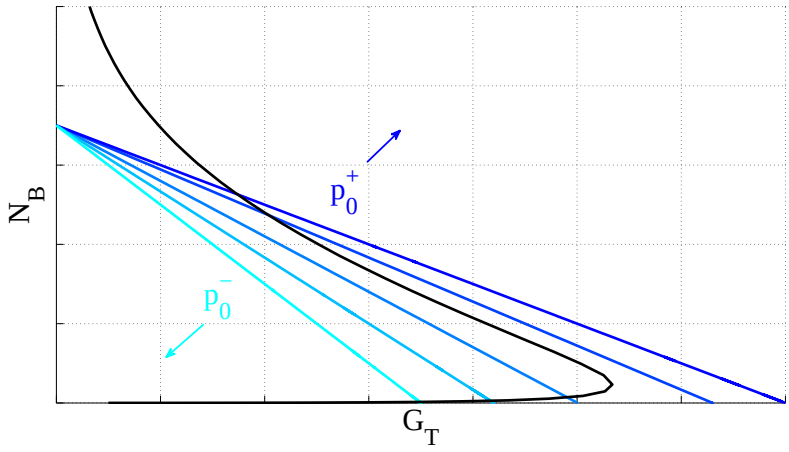

(a) Changing p_0

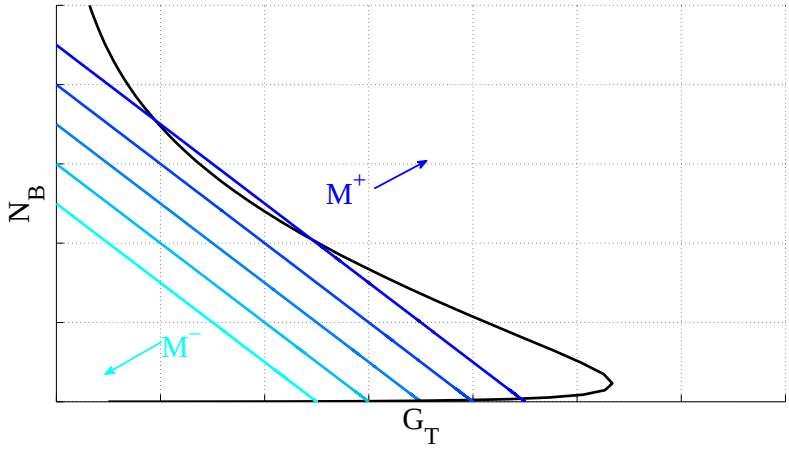

(b) Changing M

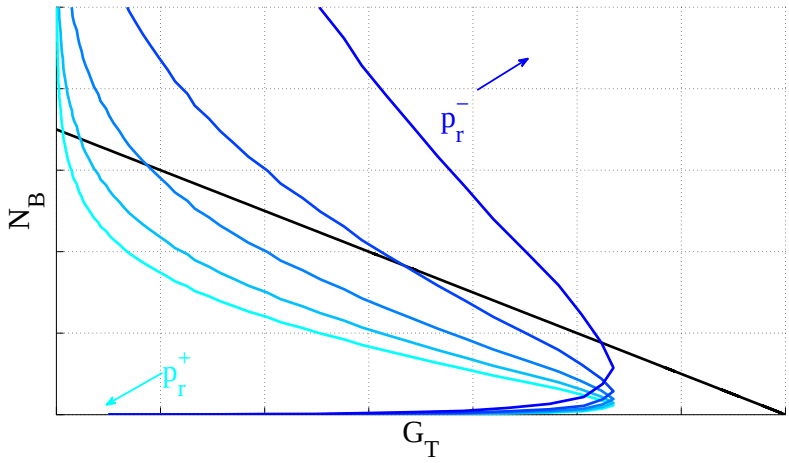

(c) Changing p_r

Figure 2.13: Graphical representation of the changes in the (G_T,N_B) plane when increasing or decreasing one of the parameters' values

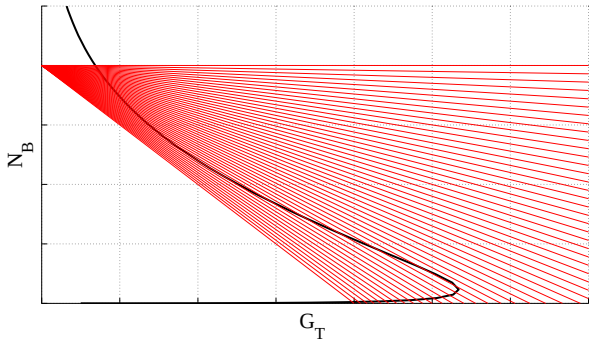

(a) p_0 constraint

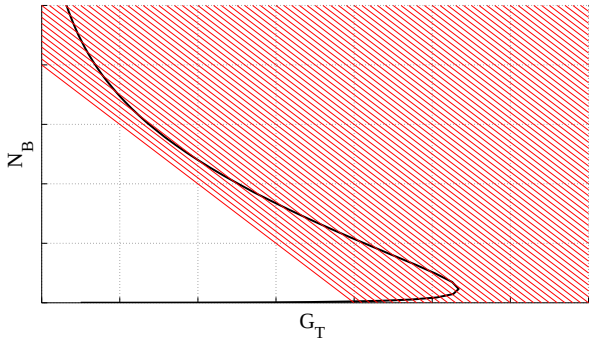

(b) M constraint

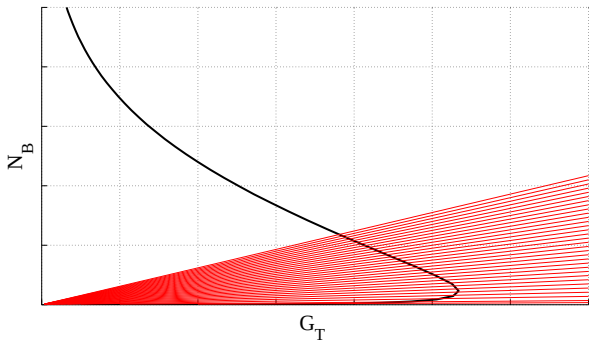

(c) Delay constraint

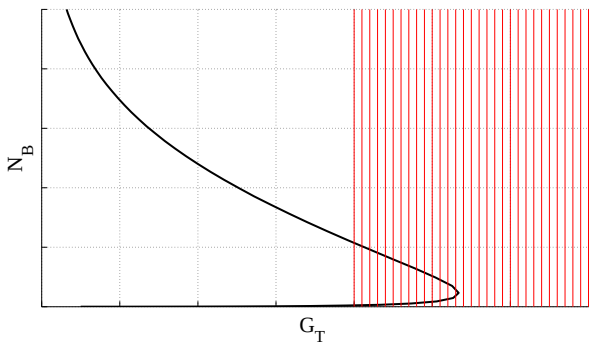

(d) Throughput constraint

Figure 2.14: Graphical representation of the admissible areas for various constraints

4.
$$\frac{N_B}{G_T \cdot N_s} \leq Av[D_{pkt}]^{max} \tag{2.17}$$

5.
$$G_T \geq G_{OUT}^{min} \tag{2.18}$$

In other words, each formula simply represents an admissible area where the operational point has to be, as illustrated in Figure 2.14.

Any study case will be characterized by one or more *degrees of freedom* and one or more *design constraints*. In case of more than one design constraint, the resulting constraint will be the intersection of the respective admissible areas. Therefore we can conclude that the designed model not only allows to forecast stability and throughput of the communication, but also to easiliy represent its constraints. This enables a design that does not need any use of complicated formulas in order to understand feasible settings.

Notice that the choice of N_s has not been considered as a design parameter. This choice have basically two reasons: first of all in DVB-RCS2, the number of slots allocated for RA is dynamically decided by the NCC; secondly, the best choice for N_s can always be considered between 100 and 200 since a lower value would degrade too much the throughput performance while a bigger value would degrade too much the delay performance.

2.6 Packet degree and RA technique

In the previous paragraphs we have concentrated on the best selection of p_0, p_r and M once the number of replicas per packet (packet degree) is chosen. However also the number of packet copies is a design parameter[4]. For this reason, this section analyzes the choice on the number of copies per packet to be sent. Moreover, a comparison on the advantages and disadvantages of CRDSA with regard to SA are outlined.

Figure 2.15 shows that up to moderate channel loads, a greater packet degree is always convenient not only in terms of PLR but also in terms of throughput and packet delay. But considering stability to be one of our constraints, we can see from Figure 2.16 that for $p_r = 1$ SA offers the most reliable performance since after the throughput peak any CRDSA curve rapidly degrades with N_B while SA degrades in a slow-paced manner. As a result, for moderate channel load lines with $G_T \leq 0.4$ for $N_B = 0$, SA is able to support up to approximately

[4]In this work we compare various packet degrees under the assumption of equal received power per replica. For discussion on the power efficiency when considering transponder's average power limits refer to [51]. Moreover the additional overhead due to the need of more pointers when more copies are sent has been omitted, since it can be considered neglibile with regard to the burst size especially when few copies (no more than 4 or 5) are considered.

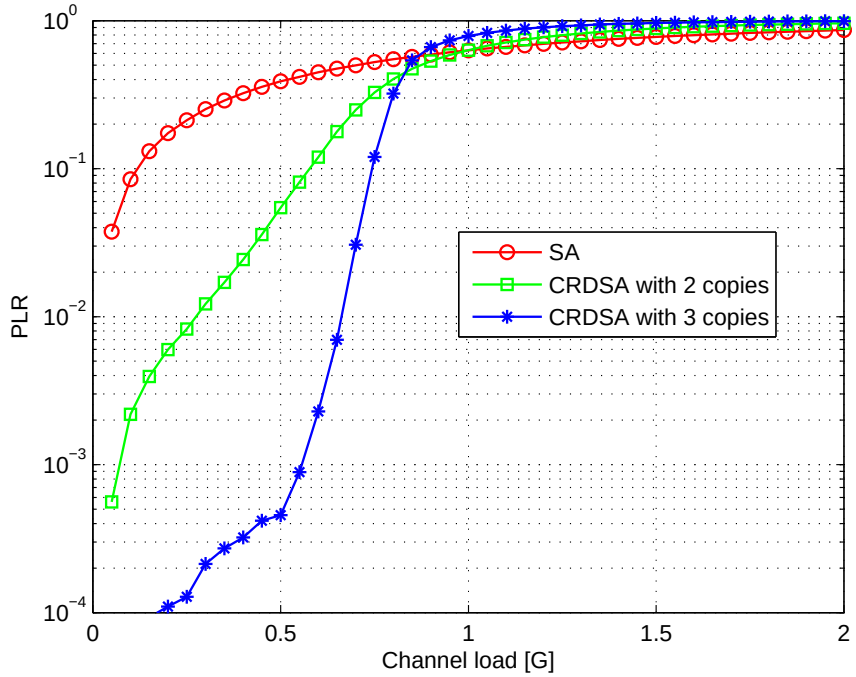

Figure 2.15: Packet Loss Ratio for different packet degrees when $N_S = 100$ slots

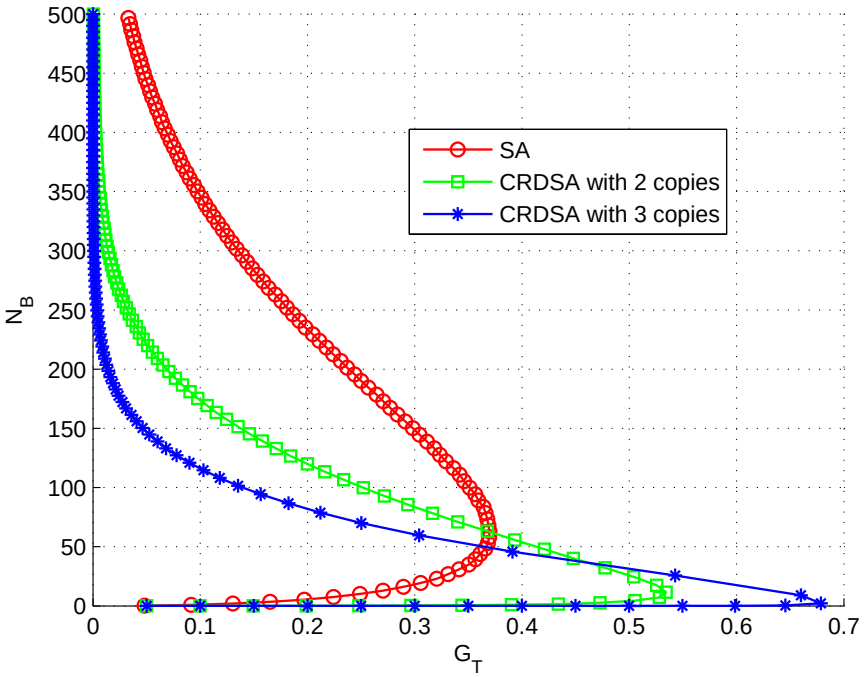

Figure 2.16: Equilibrium contour for different packet degrees when $N_S = 100$ slots

450 users ensuring stability, while for CRDSA with 2 replicas the admissible population is approximately 50% less and for CRDSA with 3 replicas the admissible M is less than 150.

However, as previously said, the operational point for CRDSA always occurs in a point with higher throughput, smaller backlogged size and smaller packet delay. Moreover in para-

graph 2.4 it has been shown that depending on the channel load line the actual FET could be so big that instability could be accepted. For example, for $M = 450$ and $p_0 = 0.089$ the computed FET is practically zero, in the sense that even though we know that a certain probability exists, it is so small that the computation resulted to be zero due to its littleness.

Considering $M = 250$ and $p_0 = 0.2$ SA presents a globally stable behaviour around its throughput peak ($G_{OUT} = 0.36$) for $N_B^G = 65$ while CRDSA with 3 replicas presents a locally stable equilibrium point with throughput equal to 0.5 , N_B^S close to 0 and unstable equilibrium point for $N_B^U \approx 43$.

Using formulas in 2.4 the obtained average FET is approximately 10^4 frames. In this case, if we are willing to maintain the advantages of CRDSA with 3 replicas (e.g. its lower PLR) some countermeasures to ensure stability are required. In the next paragraphs simple yet effective control policies able to counteract the event of drift to saturation will be shown. After that, the convenience of using such a dynamic policy in the case of finite and infinite users' population will be discussed.

2.7 Control Limit Policies

If we are in the case in which the considered channel is not stable, some kind of solution to counteract the possibility of drift to saturation is required. Two straightforward solutions could be: use a smaller value for the retransmission probability giving then rise to a larger backlogged population for the same throughput value; allowing a smaller user population size M thus resulting in a waste of capacity.

A third solution is the use of control limit policies to control unstable channels by applying the countermeasures above in a dynamic manner. In this section we analyze control procedures of the limit type [46] able to ensure stability in the case of stationary parameters. However the same reasoning can also be applied in the case of dynamic ones (such as non-stationary M) with the necessary modifications.

Two simple yet effective dynamic control procedures are considered: the input control procedure (ICP) and the retransmission control procedure (RCP). These two control procedures are based upon a subclass of policies known as control limit policies, in which the space of the policies is generally composed of two actions plus a critical state that determines the switch between them, known as *control limit*. In this case the *control limit* is a critical threshold for a certain number of backlogged users $\hat{N}_B$.

2.7.1 Input Control Procedure

This control procedure deals with new packets to transmit. In particular, two possible actions are possible: accept (action a) or deny (action d) and the switch between them is determined by the threshold $\hat{N}_B$ as previously mentioned.

2.7.2 Retransmission Control Procedure

As the name says, the retransmission control procedure deals with packets to retransmit and in particular with their retransmission probability. In particular two different retransmission probabilities p_r and p_c are defined that represent respectively the action taken in normal retransmission state (action r) and in critical state (action c). From the definition above it is straightforward that it must be $p_r > p_c$. The switch between these two modes is determined once again by the threshold $\hat{N}_B$.

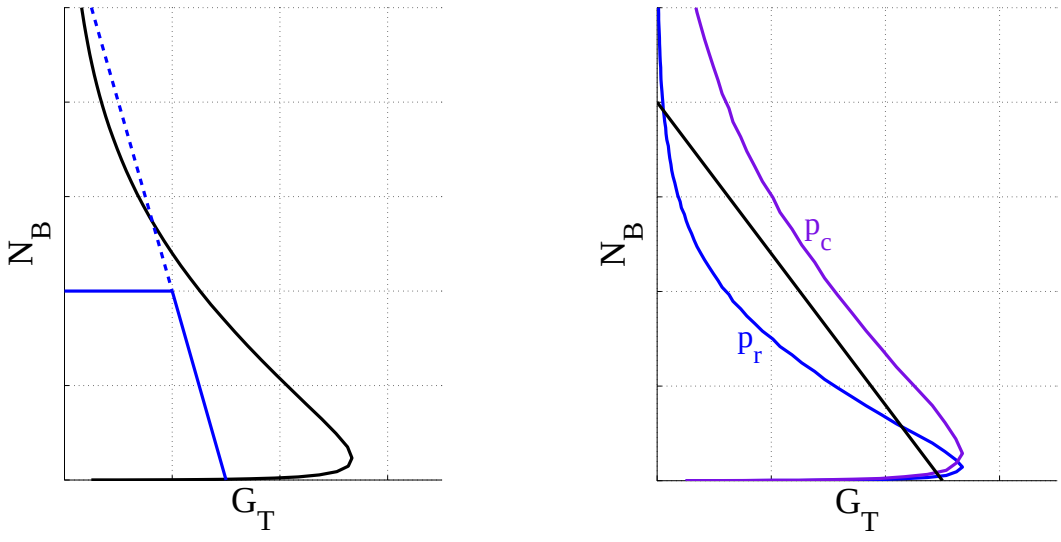

(a) ICP (b) RCP

Figure 2.17: Examples of control limit policies

Figure 2.17 graphically represents these 2 cases. As we can see both policies accomplish the same task of ensuring channel stability. However, while ICP controls the access of thinking users, RCP controls the access of backlogged users.

2.8 Dynamic control policies for finite population

In this paragraph the result of the application of dynamic control policies for CRDSA with 2 and 3 replicas is discussed and compared to SA as well as to the case of static design ($p_r = p_c$) when a finite population is assumed. Consider the case previously analyzed in paragraph 2.6 and reported in Figure 2.18 with $M = 250$, $p_0 = 0.2$ and $p_r = 1$. Moreover we assume $p_c = 0.75$ for CRDSA with 2 copies and $p_c = 0.53$ for CRDSA with 3 copies, that are the biggest values for p_c that ensure stability in the two respective cases.

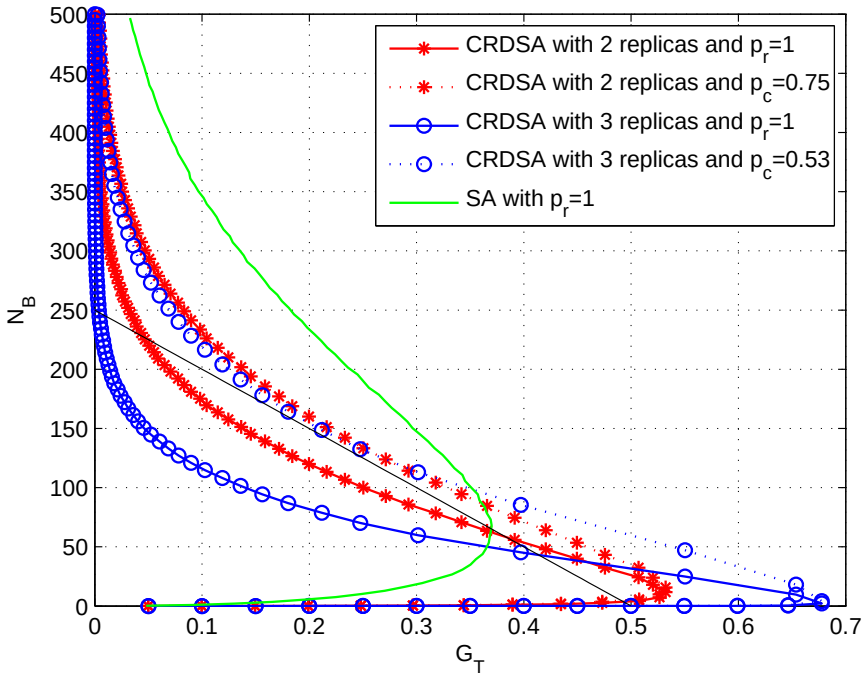

Figure 2.18: Equilibrium contour for SA and CRDSA with 2 and 3 replicas in normal and critical RCP state

Figures 2.19 and 2.20 show the results in terms of throughput and average packet delay when varying the threshold of the control limit policy $\hat{N}_B$. As we can see the results among the various cases are similar in terms of maximum throughput and minimum delay achieved, except for ICP with 3 replicas that shows slightly higher throughput and lower delay than the other cases.

For SA instead, the resulting channel for $M = 250$ and $p_0 = 0.2$ does not need any dynamic control policy since it is globally stable with throughput equal to 0.369 and delay equal to 1.76 frames. It is now clear that despite instability that needs to be controlled, the time spent in critical state is so small that results shown for CRDSA with 2 and 3 replicas are better than SA. Therefore we can affirm that CRDSA always gets better performance than SA despite instability.

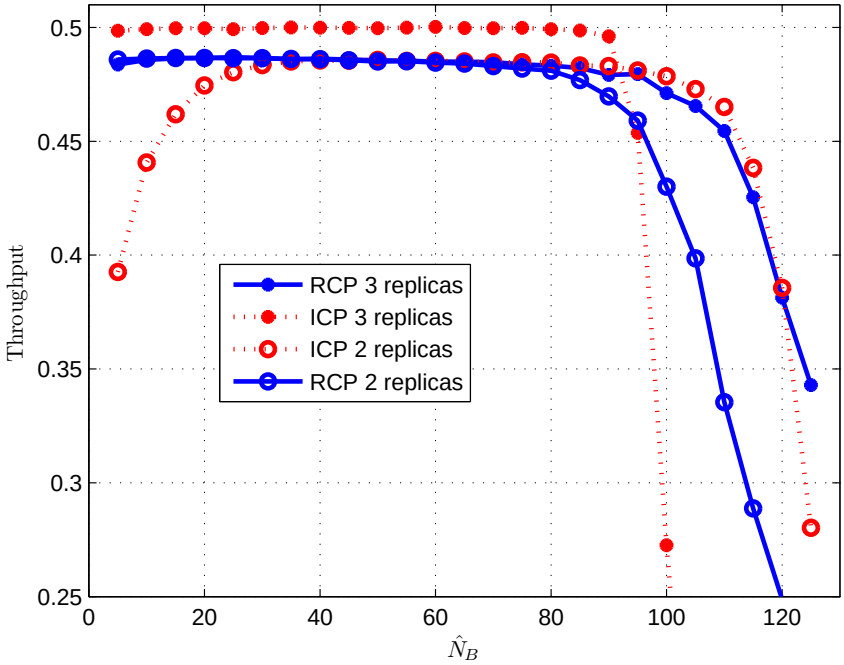

Figure 2.19: Throughput over $\hat{N}_B$ for dynamic retransmission policies

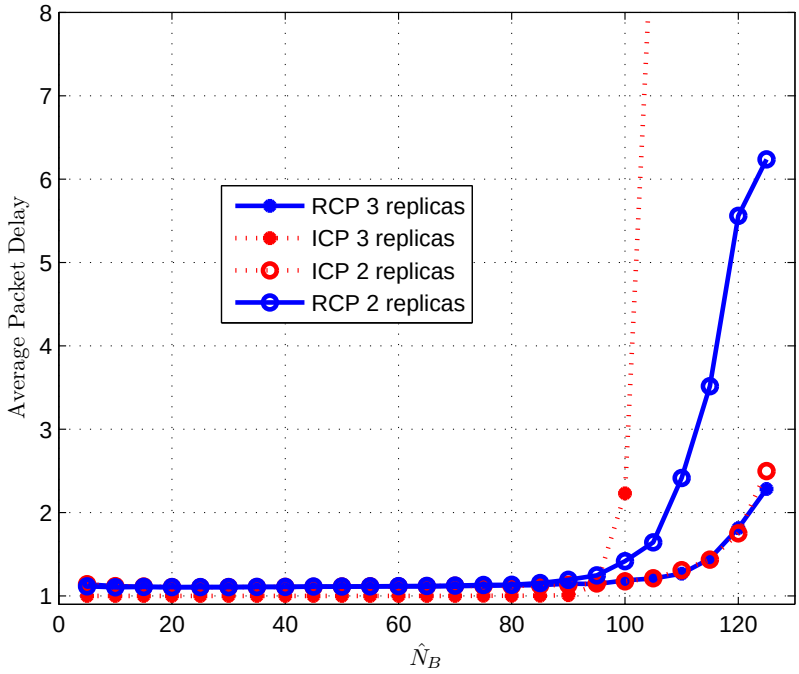

Figure 2.20: Packet delay over $\hat{N}_B$ for dynamic retransmission policies

It can also be noticed that in any case considered here, there is a certain range of flatness around N_B^U. This range changes depending on the policy applied, the number of replicas, the time spent in critical state and the performance degradation between normal and critical state. The width of this flat region is really important since in real satellite communications large

propagation delay has to be considered.

2.8.1 Control policies in case of propagation delay

Differently from the case of immediate feedback assumed so far throughout the paper, when the $\hat{N}_B$ threshold is crossed the control limit policy needs a certain propagation time from the NCC to the satellite terminals before it is applied. As a result the effective threshold is not $\hat{N}_B$ but some value $\hat{N}_B + \delta$, where δ depends on the drift of the number of backlogged users for the particular case and on the propagation delay. Therefore the wider is the flat region, the less the performance optimality of the controlled channel will be influenced by the propagation delay [53].

Moreover, we can see that in the case of 2 replicas a degradation of the throughput is also found for $\hat{N}_B < N_B^U$. In general terms, when a control limit policy is applied it does not make sense to choose $\hat{N}_B < N_B^U$, therefore this result does not seem to be of interest for our analysis. However, when $N_B < \hat{N}_B$ the control limit policy switches back to normal state, but as previously mentioned users do not immediately receive the acknowledgment for this new change due to the propagation delay so that the critical policy might actually be left for some value $\hat{N}_B - \delta$ resulting in the possibility of suboptimal performance (see ICP with 2 copies per packet).

2.8.2 On the use of dynamic control policies over static design

Let us now discuss the results when instead of dynamic control limit policy, the channel is designed by statically decreasing the retransmission probability so that the channel is always stable. Differently from SA, in this case decrementing p_r has really small influence on the overall performance especially when the first point of intersection between the equilibrium contour and the channel load line takes place before the throughput peak and sufficiently far from it. As a matter of fact with $p_r = 0.53$ for CRDSA with 2 replicas and with $p_r = 0.75$ for CRDSA with 3 replicas the following results are obtained:

- CRDSA with 2 replicas: $G_{OUT} = 0.49$; $Av[D_{pkt}] = 1.01$
- CRDSA with 3 replicas: $G_{OUT} = 0.5$; $Av[D_{pkt}] = 1$

In conclusion we can say that with stationary values of M and p_0, in most of the cases the use of dynamic policies for CRDSA does not appear to be a convenient solution compared to a static design if a choice can be made. This can be affirmed also in light of the more realistic case of non-immediate feedback in which a certain performance degradation is present. The only

case in which dynamic policies could be really necessary with stationary M and p_0 is when M is so big that the required p_r rendering the channel stable really degrades the performance thus requiring the use of dynamic policies. Nevertheless the analysis above is useful for future work on the case of non-stationary p_0 and M that does not allow to a-priori set the retransmission probability in order to be sure that the channel is always stable. Moreover the analysis presented for the case of finite M is introductory to understand the application of dynamic policies to the case of infinite population.

2.9 Dynamic control policies for infinite population

Finally we discuss the use of dynamic control policies in order to provide stability in the case of infinite population. As a matter of fact this case is closer to the real DVB-over-satellite application scenario in which a big number of users is expected to generate new traffic independently of whether previous transmissions are still pending or not, so that actual channel traffic can be modeled as a Poisson process.

In the case of infinite population, ICP is the only policy that can ensure stability since decreasing p_r could not be sufficient to recover stability. In fact, RCP might be used as a mean to recover the channel communication from instability by setting p_c so that the operational point falls again in the region of stability. However such a procedure does not always ensure stability from a theoretical point of view since due to the satellite propagation delay, the switch from and to critical state need some time to propagate meanwhile the number of backlogged users will continue to rapidly and indefinitely increase so that at the end the chosen value for p_c could not be anymore sufficient.

$\lambda = 65$	$\lambda = 60$	$\lambda = 55$	$\lambda = 50$
$N_B^U = 11$	$N_B^U = 18$	$N_B^U = 25$	$N_B^U = 32$

Table 2.2: Points of unstable equilibrium for CRDSA with 3 copies depending on λ

Figure 2.21 and 2.22 show throughput results depending on the number of new packet arrivals λ at each frame. As we can see the bigger the λ value, the higher the throughput but also the narrower the flat region. The reason for such a result is similar to what has been explained in the previous sections for the finite population case. In particular we can see from Table II that the closer the operational point is to the throughput peak, the smaller is the value of N_B^U.

Figure 2.22 shows that obtained results concerning delay reflect throughput results since

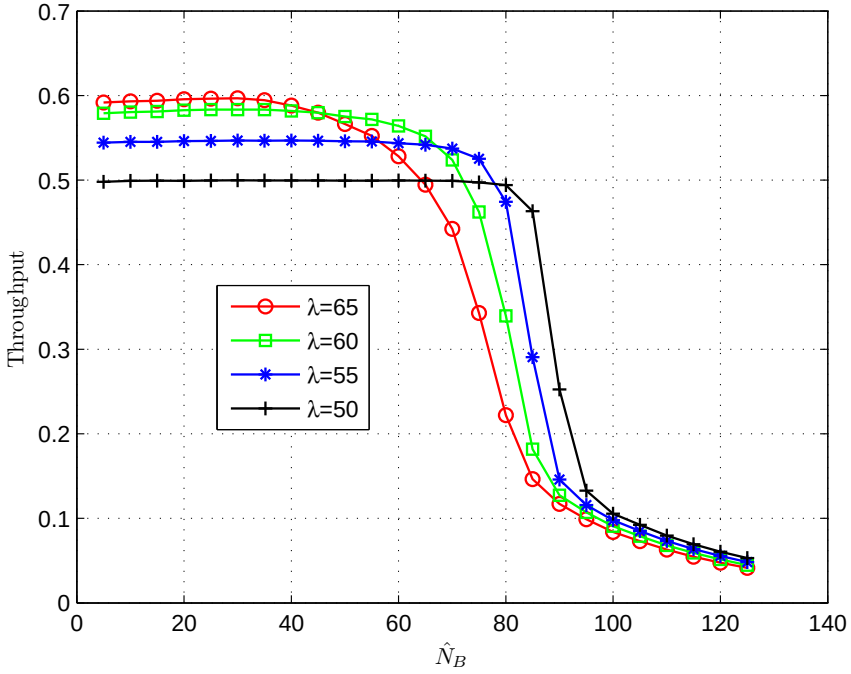

Figure 2.21: Throughput over $\hat{N}_B$ for ICP in case of infinite population

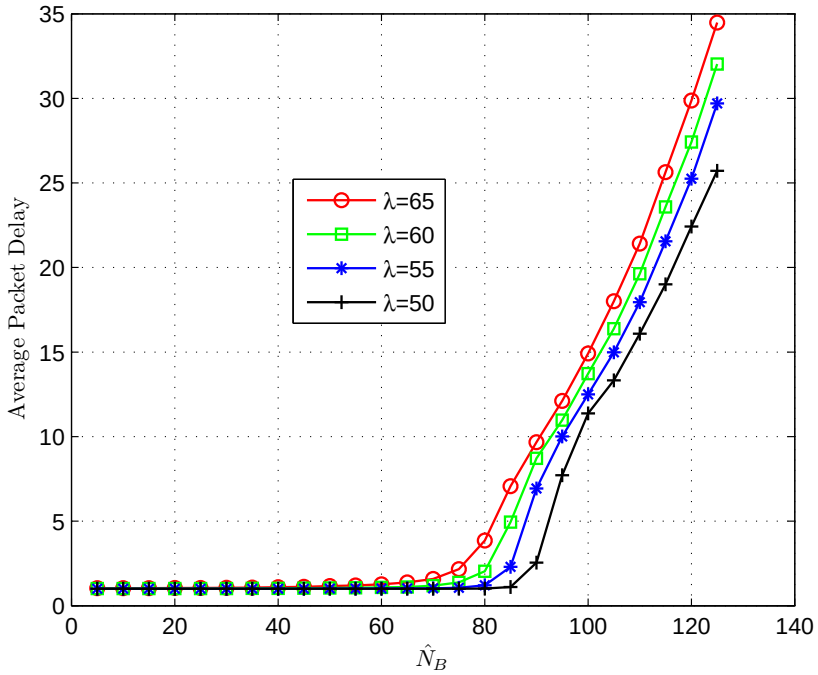

Figure 2.22: Packet delay over $\hat{N}_B$ for ICP in case of infinite population

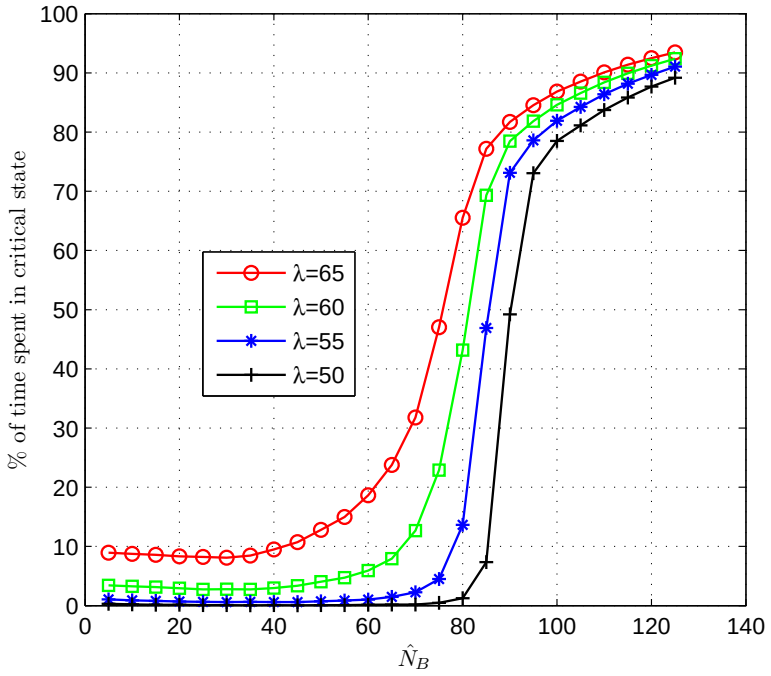

Figure 2.23: Percentage of time spent in critical state over $\hat{N}_B$ for ICP in case of infinite population

the wider is the flat region for the throughput, the wider is the flat region with delay equal to 1. Finally Figure 2.23 shows that for bigger values of λ users spend some time in critical state also in the flat throughput region giving place on one hand to the possibility of suboptimality due to the propagation delay and on the other hand increasing the overall PLR by reason of rejected packets.

2.10 Conclusions

In this chapter a model for design of a congestion-free system using CRDSA as RA mode in DVB-RCS2 has been outlined. This model allows to study and predict stability and to calculate the expected throughput as well as the expected delay at the channel operating point. Moreover, this kind of representation allows a simple yet effective view of how the communication behaves when changing one or more of the key parameters thus allowing a design that can easily consider the tradeoff among multiple constraints.

A simplified framework for the calculation of the First Exit Time has also been introduced and its importance for the evaluation of unstable channels has been highlighted. All the presented models and tools can be extended to consider a different frame size, power unbalance, the introduction of FEC or any other modification. The central part of the paper discusses design settings and the convenience of using CRDSA over SA.

In the last part, dynamic retransmission policies of the control limit type have been introduced and their effectiveness and convenience have been discussed against static design. In particular, concerning the case of finite user population, found results have shown that differently from SA in which dynamic retransmission policies are generally preferred, in the case of CRDSA a static design that ensures stability (i.e. by decreasing the retransmission probability for backlogged packets) is generally more convenient. Finally, dynamic retransmission policies have been applied to the case of infinite user population. Found results have shown that control limit policies are able to stabilize the channel also in the case of infinite user population while ensuring a performance close to the best achievable even in presence of large propagation delay as it is the case in a geostationary satellite system used for DVB-RCS communications.

Chapter 3

Stability of asynchronous Random Access schemes

Recently the same concept behind CRDSA has been applied to Pure Aloha giving birth to a technique renamed here Contention Resolution Aloha (CRA) [27], that is able to boost the performance in case of asynchronous RA schemes. In this chapter, throughput as well as packet delay and related stability for asynchronous ALOHA techniques under geometrically distributed retransmissions are analyzed both in case of finite and infinite population. Moreover, a comparison between pure ALOHA, CRDSA and CRDSA techniques is presented, in order to give a measure of the achievable gain that can be reached in a closed-loop scenario with respect to the previous state of the art. This analysis uses the same tools adopted for synchronous access schemes, with the necessary modifications needed in order to take into account the differences between the two techniques. The chapter is organized as follows. In paragraph 3.1 an overview of the considered asynchronous access scheme is given. Paragraph 3.2 presents the definition of stability as well as the model used for the measure of the stability when using retransmissions. Paragraph 3.3 deals with a model for the computation of the delay associated to received packets. Finally, in paragraph 3.4 a comparison both in terms of stability and in terms of delay is carried out between CRDSA, CRA and pure ALOHA. Paragraph 3.5 concludes the paper.

3.1 System Overview

The scenario considered in this chapter is a multi-access channel, in which a certain number of terminals communicate to a gateway (e.g. a ground station) via satellite. Differently from synchronous access schemes, in this case the channel is divided into frames but each frame is not subdivided into slots. When a terminal has a packet to transmit, it waits for the beginning of the next available frame in order to place d copies of that packet. Let us call t_0 the beginning of a frame, T_F the frame duration and τ a generic burst duration. The d copies of a packet are placed

with starting time within the interval $[t_0;t_0 + T_F - \tau]$, with uniformly distributed probability and so that burst copies belonging to the same packet are not overlapping.

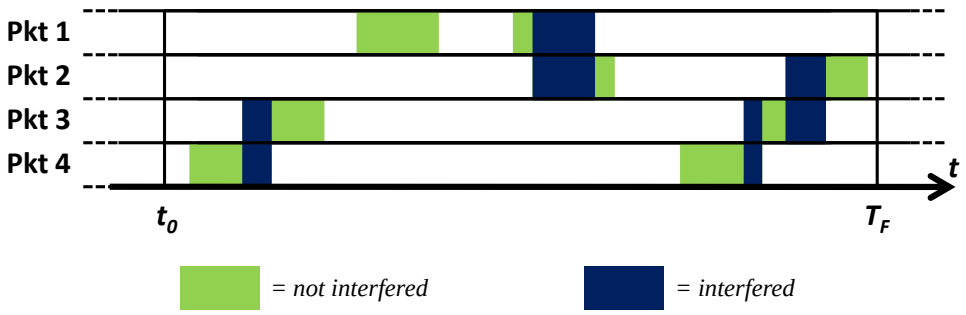

Figure 3.1: Example of a generic frame at the receiver for CRA

At the receiver, each frame contains a certain number of bursts as depicted in Figure 3.1. Any burst will have or not a certain degree of interference due to transmission time overlap with other bursts. Notice that differently from CRDSA, in which interference can only occur for the whole burst, in this case also partial interference can occur. In [27] two cases are analyzed: the first case assumes that any overlap results in entire loss of the packet's burst; the second case considers the application of a strong FEC able to allow decoding if the amount of interference is limited. In any case, similarly to what happens in CRDSA, an iterative IC process is started at the receiver in order to remove bursts belonging to correctly decoded packets thanks to the knowledge of their location within the frame from the correctly decoded burst.

Consider the assumption of ideal channel estimation and perfect IC. In the first case (i.e. where no FEC is used), at each iteration packet bursts are attempted to be decoded only if the burst is not overlapping with other bursts. In Figure 3.1, $Packet\ 1$ has a copy that did not interfere during transmission, therefore it can be decoded and the interference of the other burst copy can be removed in order to recover the content of $Packet\ 2$. In the second case in which a strong FEC is applied, not only bursts without interference, but also those satisfying a certain threshold in terms of amount of interference power are decoded. Let us define as in the original CRA paper [27] the rate $R = R_C \cdot log_2 M$ where R_C is the coding rate and M the modulation index. Moreover the normalized MAC channel load is defined as $G_{IN} = \frac{N_{tx} \cdot \tau}{T_F}$ with N_{tx} indicating the number of transmitted packets, while $G_{OUT} = G_{IN}[1 - PLR(G_{IN})]$ represents the throughput in terms of portion of load successfully decoded. Notice that PLR (i.e. the Packet Loss Ratio) depends on the frame size T_F, the burst degree distribution (defined from [26] as the probability of having a certain number of copies per packet through the following polynomial $\Lambda(x) = \sum_d \Lambda_d x^d$, where Λ_d is the probability that a given packet will have burst degree d), the rate R, the maximum number of iterations for the decoding process I_{max} and the $SNIR$. In [27] the decoding threshold has been approximated with the Shannon bound.

As claimed by the authors, even though this threshold is quite optimistic, it can be considered valid for moderate to high SNIR with properly designed schemes and represents the ground base for the study of the performance with real codes. Setting $C_{ref} = R = log_2(1 + SNIR)$, the decoding threshold is $SNIR_{dec,dB} = 10 \cdot log_{10}(2^R - 1)$. In order for a burst to be decoded, its $SNIR$ must be at least equal to $SNIR_{dec}$. The $SNIR$ of each burst can be computed as

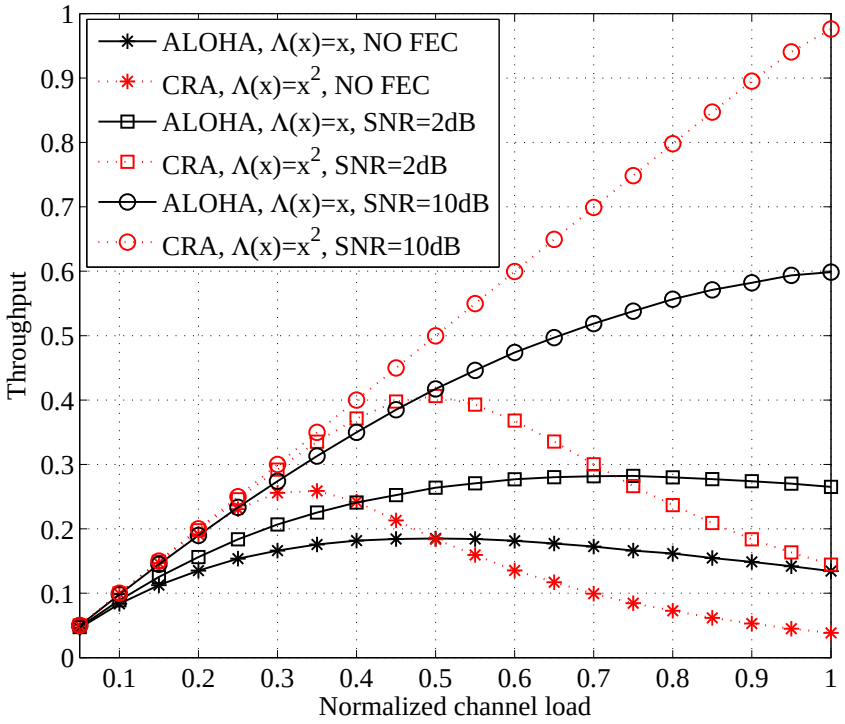

Figure 3.2: Open loop throughput results

$$SNIR = \frac{P}{x \cdot P + N} = \frac{SNR}{x \cdot SNR + 1} \tag{3.1}$$

where x represents the degree of interference for a certain burst as a sum over all interference contributions expressed with a value between 0 and 1. For example, in case of no interference $x = 0$, in case of 50% overlapping with another burst $x = 0.5$ and in case of 50% interference with n other bursts, $x = 0.5 \cdot n$. In Figure 3.2 results for an open loop scenario (i.e. without retransmission of lost contents) are illustrated for ALOHA and the representative case of CRA with $\Lambda(x) = x^2$. The parameter values chosen for simulations are $T_F = 100\ ms$, $\tau = 1\ ms$ for every packet, $M = 4$ (QPSK), $R_C = 1/2$, $I_{max} = 50$ and a number of simulation rounds per channel load point equal to 10^4.

3.2 Stability

Assume the case in which CRA has been chosen as RA scheme and a certain number of users M (either finite or infinite) participate in the described scenario. We assume each user to be in one of two possible states: Thinking (T) or Backlogged (B).

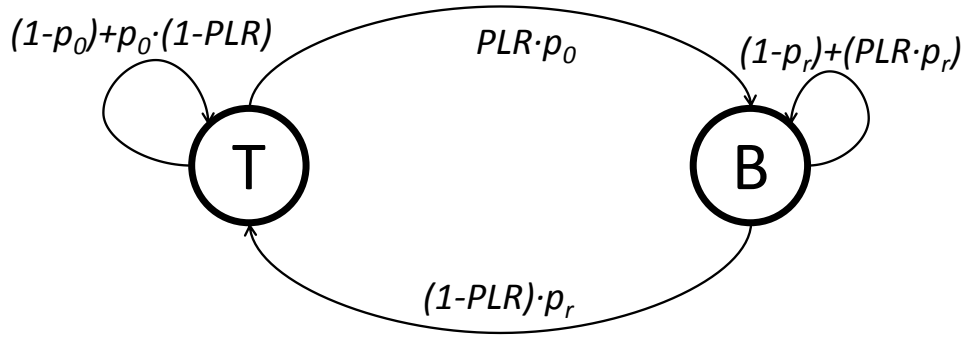

Figure 3.3: Markov Chain for user state

Users in T state send a packet at the beginning of the next frame with probability p_0. Assuming that users are acknowledged about the outcome of the transmission at the end of the frame in which they transmitted, if the packet is correctly decoded the user stays in T state. Therefore the probability of staying in Thinking state is equal to the probability that a user does not send any packet plus the probability that a user sends a packet that is correctly received at the first attempt. On the other hand, if a user is unsuccessful in its first attempt, it switches to backlogged state. In B state, a user attempts retransmission with probability p_r. In case the retransmission ends up successfully the user comes back to Thinking state at the end of the frame in which it retransmitted its packet while in case of no retransmission or unsuccessful retransmission, it stays in B state.

Let us define N_B^f as the number of backlogged packets at the end of frame f and M as the total number of users, so that

$$G_B^j = \frac{N_B^{(f-1)} \cdot \tau \cdot p_r}{T_F} \tag{3.2}$$

is the expected channel load in frame f due to retransmissions and

$$G_T^f = \frac{(M - N_B^{(f-1)}) \cdot \tau \cdot p_0}{T_F} \tag{3.3}$$

is the expected channel load of frame f due to new transmissions. Finally $G_{IN}^f = G_T^f + G_B^f$ is the expected total channel load of frame f.

The aim of the definitions above is to find the *equilibrium contour* in a plane having as axis the number of backlogged users and the channel load due to new transmissions. As a matter of fact, *equilibrium contour* is defined as the locus of points for which the expected channel load

due to new transmissions is equal to the expected throughput, so that the communication can be considered as stable and the total expected channel load G_{IN}^{f} is equal frame after frame. The expected number of new transmissions at the equilibrium can be defined as

$$G_T = G_{OUT} = G_{IN}\,[1 - PLR(G_{IN})] \tag{3.4}$$

In stability conditions, also the number of backlogged users remains the same frame after frame. Therefore

$$N_B = N_B(1 - p_r) + \frac{G_{IN} \cdot T_F}{\tau} PLR(G_{IN}) \tag{3.5}$$

from which

$$N_B = \frac{G_{IN} \cdot PLR(G_{IN}) \cdot T_F}{\tau \cdot p_r} \tag{3.6}$$

Equations (3.4) and (3.6) describe the *equilibrium contour*. This contour, together with the expected channel load due to new transmissions in Equation 3.3 (known as channel load line) gives a model for the computation of the stability.

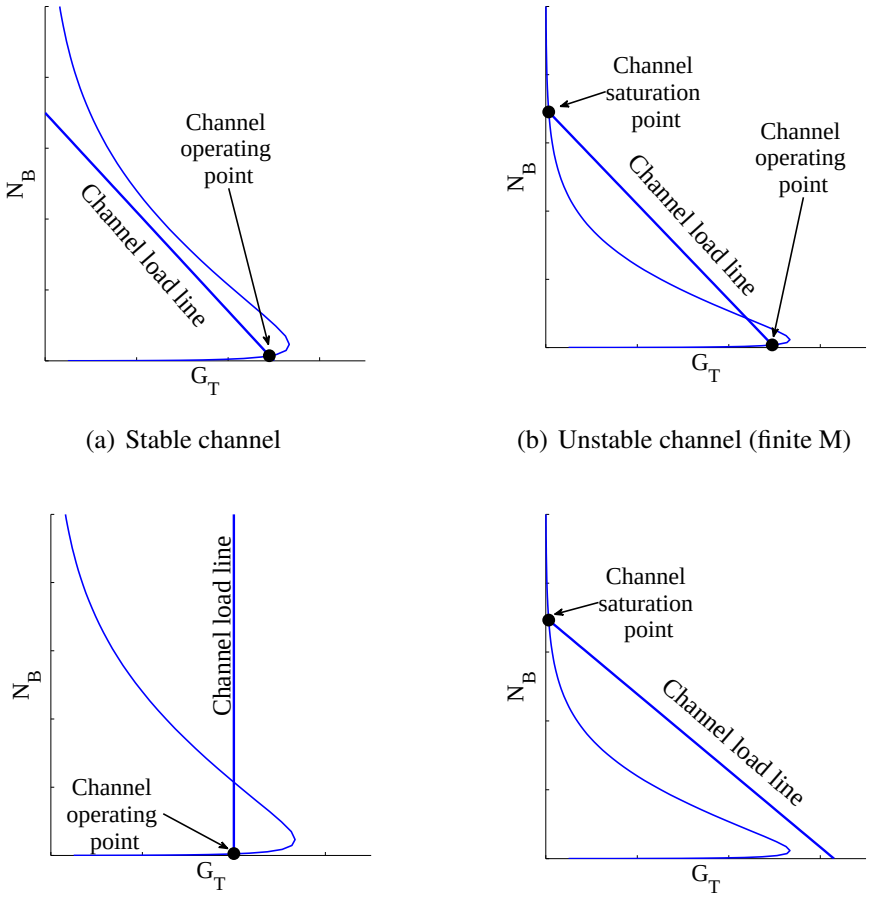

(a) Stable channel

(b) Unstable channel (finite M)

(c) Unstable channel (infinite M)

(d) Overloaded channel

Figure 3.4: Examples of stable and unstable channels

Consider the examples in Figure 3.4. Each channel load line can intersect the equilibrium contour in one or more points (i.e. for one or more N_B values). These intersections are referred to as equilibrium points since $G_{OUT} = G_T$ holds. The rest of the points of the channel load line belong to one of two sets: those on the left part of the plane with regard to the equilibrium contour represent points for which $G_{OUT} > G_T$, thus situations that yield to decrease of the backlogged population; those on the right part of the plane with regard to the equilibrium contour represent points for which $G_{OUT} < G_T$, thus situations that yield to growth of the backlogged population.

Therefore, an intersection point is defined as a *stable equilibrium point* with coordinates (G_T^S,N_B^S) if it enters the left part of the plane for increasing N_B since for $N_B < N_B^S$ the result is that $G_{OUT} < G_T$ and for $N_B > N_B^S$ we find that $G_{OUT} > G_T$ so that the equilibrium point acts as a sink. With the same reasoning, an intersection point is defined as an *unstable equilibrium point* with coordinates (G_T^U,N_B^U) if it enters the right part of the plane for increasing N_B. In this case it can be proven that as soon as a statistical fluctuation from the equilibrium point occurs, the number of backlogged users N_B diverges from (G_T^U,N_B^U). As a matter of fact, as explained in [44], the model is based on the expected behavior while in reality the obtained values oscillate around the expected value.

In Figure 3.4(a) an example of stable equilibrium point is given. Being this point the only one of intersection it is also a *globally stable equilibrium point* and we consider the related channel as stable since the communication will keep operating indefinitely around that point. On the other hand, if the point of equilibrium is not the only one as in Figure 3.4(b) it takes the name of *locally stable equilibrium point*. In particular the illustrated example shows two locally stable equilibrium points: one for a good throughput value, thus called channel operating point in the sense that is the point in which we want the communication to operate; one for throughput close to zero called channel saturation point since in that state too many users are in backlogged state and thus any packet transmission has hard times in being successful. Consider a scenario in which the communication starts from $N_B = 0$. The communication will keep being around the operating point as long as statistical fluctuations are small enough to keep $N_B < N_B^U$. At a certain point however, the instability point will be crossed and in small time the saturation point will be reached. Depending on the communication settings, there is also a certain probability to exit from the state of saturation and come back around the channel operating point. However, this probability is generally small and considered negligible. Figure 3.4(c) represents the same scenario as in Figure 3.4(b) (i.e. the case of unstable channel) but for an infinite number of users. In this case the channel load due to new transmissions is independent on the actual number of backlogged users. Nevertheless the same discussion as for the case with finite number of users is valid and we can assume that the point of saturation is found for $N_B \to \infty$. Notice that in this

case the formula for the channel load used so far is no longer valid. However, if Poisson arrivals with expected value λ in terms of new packets to transmit are considered, the channel load line can be expressed as

$$G_T = \frac{\lambda \cdot \tau}{T_F} \tag{3.7}$$

As a matter of fact, for a finite number of users the number of new transmissions is binomially distributed, while for a number of users that goes to infinity we can consider the binomial distribution converging towards the poissonian one. Finally Figure 3.4(d) shows another example of globally stable equilibrium point. However, in this case the intersection point occurs for throughput close to zero. Therefore the point is defined as channel saturation point and the channel is considered overloaded.

3.3 Packet Delay in stable channels

Assuming a stable channel so that only a globally stable and operating point is present, it is of interest to know the delay associated to successfully transmitted packets. For a generic packet, it is possible to do so using the discrete-time Markov chain in Figure 3.3. T_F is assumed to be our discrete time unit. Therefore, the packet delay D_{pkt} can be calculated as the number of frames that elapse from the beginning of the frame in which the packet was transmitted for the first time, till the end of the one in which the packet was correctly received.

$$Pr\{D_{pkt} = f\} = \begin{cases} 1 - PLR, & \text{for } f = 1 \\ PLR\,[p_r\,(1 - PLR)]\cdot & \\ \cdot[1 - p_r + PLR\,p_r]^{f-2}\,, & \text{for } f > 1 \end{cases} \tag{3.8}$$

Based on Equation 3.8 the expected packet delay can be written as

$$Av[D_{pkt}] = \sum_{f=1}^{\infty} f \cdot Pr\{D_{pkt} = f\} \tag{3.9}$$

Equation 3.9 can also be rewritten in a form that is more practical for our analysis, by means of Little's Theorem. As a matter of fact, in a stable system the average number of users in B state is equal to the average time spent in backlogged state multiplied by the arrival rate of new packets G_T (that we know to be equal to G_{OUT} at the operational point). Therefore

$$Av[D_{pkt}] = \frac{N_B \cdot \tau}{G_{OUT} \cdot T_F} \tag{3.10}$$

where the presence of T_F/τ in the formula has the aim of normalizing the delay to the frame unit.

3.4 Comparison of Random Access techniques

Before starting the analysis of the results, it is useful to have a more solid comprehension of the role of three key parameters for the communication: the probability of new transmission p_0, the probability of retransmission p_r and the total population M. The first two parameters have influence on the channel load line while the retransmission probability influences the shape of the equilibrium contour. In particular, defining a generic line $y = m \cdot x + q$ with $x = G_T$ and $y = N_B$, p_0 is inversely proportional to m. Therefore, fixing q, a decrement of p_0 determines a change for the slope of the channel load line that becomes steeper while an increment of p_0 has the opposite effect on the slope. M has the same graphical meaning of q. In other words, fixing p_0 (i.e. the line slope) changing M corresponds to changing the point of intersection with the y-axis since for $G_T = 0$, $N_B = M$. Finally, as shown in Figure 3.5(c), a decrement of the retransmission probability determines a shift upwards of the equilibrium contour.

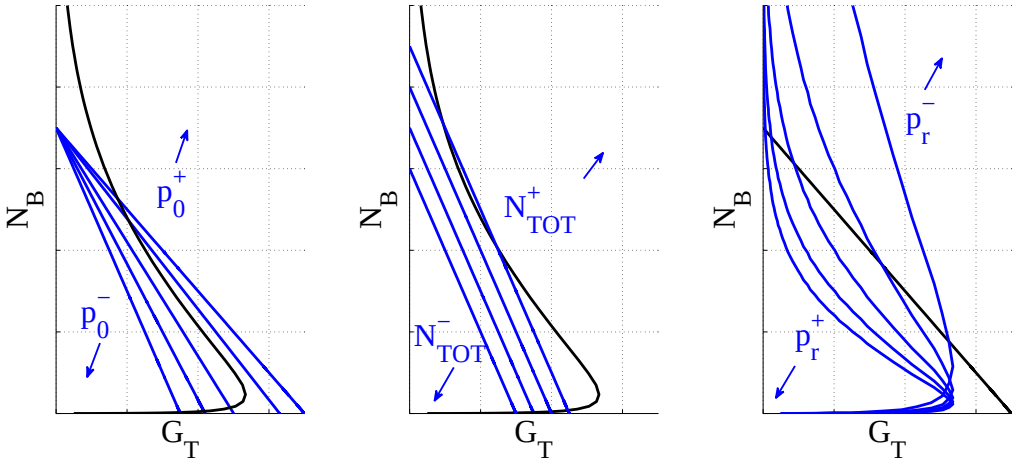

(a) Changing p_0 (b) Changing M (c) Changing p_r

Figure 3.5: Graphical representation of the result for increments and decrements of p_0, M and p_r

Figures 3.6 - 3.8 show results for the settings outlined in paragraph 3.1. In the same figures, also the results for SA and CRDSA are reported, assuming the same settings and a comparable frame size of 100 slots, since $\frac{T_F}{\tau} = 100$. Notice that the aim of this section is to give a qualitative analysis rather than precise numerical results. In fact, the obtained results are based on the Shannon Bound while in practical implementations a real code must be considered. Therefore a quantitative analysis would be of unnoticeable importance. On the other hand a qualitative

analysis is still of big value since it can prove the general validity of the technique and highlight pros and cons with regard to the state of the art.

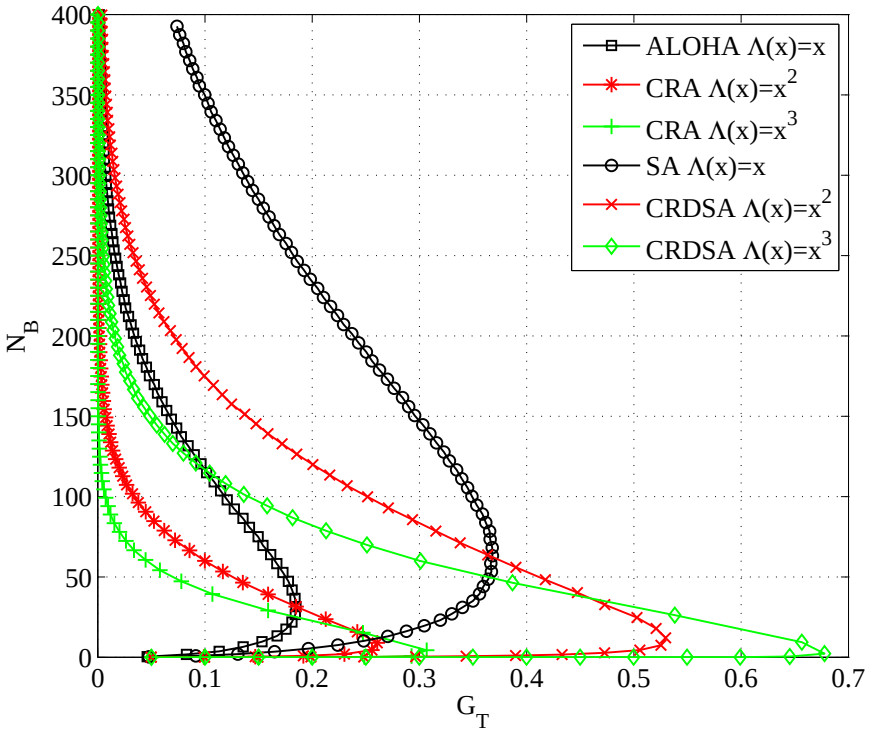

Figure 3.6: Equilibrium contour for pure ALOHA and CRA when no FEC is used

Figure 3.6 shows that even when no FEC is used, CRA can reach higher values of throughput than Pure Aloha, if the communication is designed properly so that the channel is stable. However, throughput results are far from those obtained for CRDSA. In addition, having a stable channel in CRA assumes that the total number of users participating is small enough so that only one point of intersection is present. For example, in the case of CRA with $\Lambda(x) = x^3$, if we want an expected throughput close to the peak (i.e. $T \simeq 0.3$) the total number of users must not be bigger than $M \simeq 60$; on the other hand we can see that for Pure Aloha, almost 400 users can take part in the communication still ensuring a channel operating point around the throughput peak. If the design constraints require the use of CRA together with a bigger number of users, we know from Figure 3.5(c) that it is possible to decrease the retransmission probability for backlogged users p_r. Nevertheless the stability comes at the cost of increased packet delay. This can be qualitatively understood considering that decreasing p_r, the peak throughput remains the same while the corresponding number of backlogged users N_B increases. Therefore from Little's theorem an increase in the average packet delay is expected. Finally, it can be seen that without the use of FEC the results of Aloha and CRA are worse than those for SA and CRDSA. As a matter of fact the results for synchronous techniques give place to equilibrium contour with identical shapes but bigger in value of throughput as well as in width of the curve below

the peak.

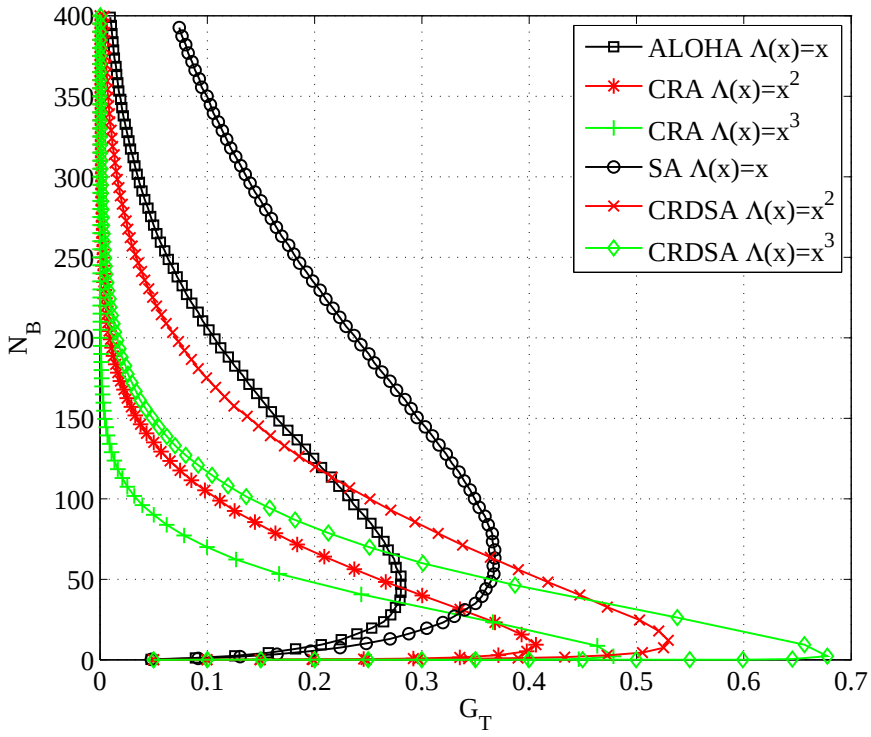

Figure 3.7: Equilibrium contour for ALOHA and CRA with associated FEC with $R_C = 1/2$ and $SNR = 2\ dB$

Similar considerations can be done in Figure 3.7 for the case in which FEC is used and the SNR is quite low ($2\ dB$). In fact, concerning asynchronous techniques the same reasoning as for the previous case applies. Moreover, concerning the comparison with synchronous techniques, we can see that SA and CRDSA still outperform asynchronous techniques even though the performance of the two gets closer.

Finally for high SNR ($10\ dB$) as in Figure 3.8, asynchronous techniques outperform synchronous ones. In particular, it can be noticed that while for CRDSA the burst degree distribution $\Lambda(x) = x^3$ is always better than $\Lambda(x) = x^2$, in CRA when the SNR is high enough $\Lambda(x) = x^2$ appears to be the best solution. However also in this case Pure Aloha still allows the participation in a stable communication of a higher number of users M with regard to CRA.

3.5 Conclusions

In this chapter a qualitative analysis of the stability in asynchronous RA schemes has been presented. In particular, stability results for CRA have been shown using a model based on the equilibrium contour. The obtained results have also been compared to Pure Aloha and CRDSA,

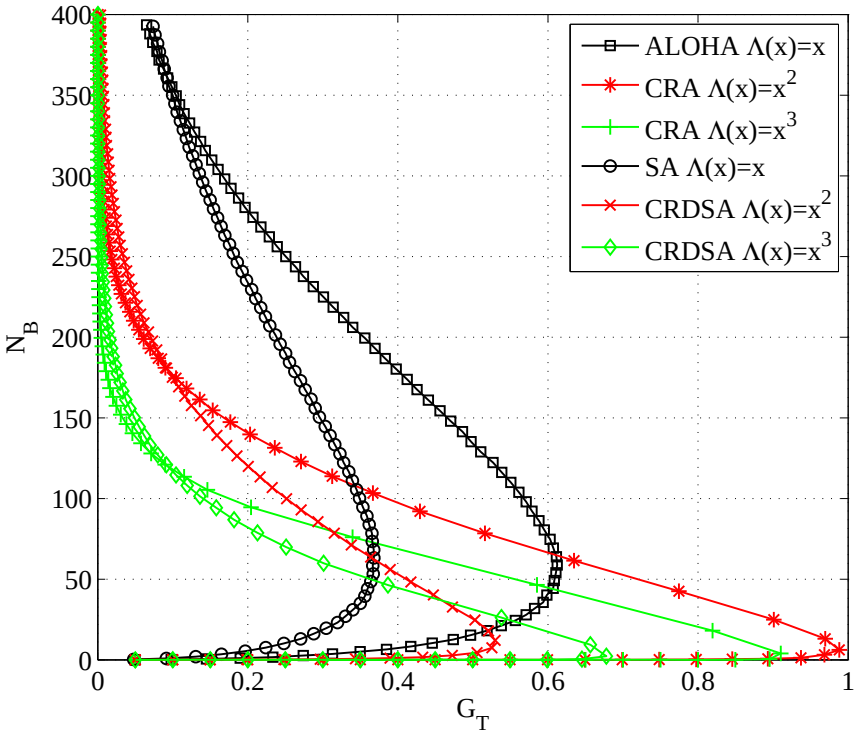

Figure 3.8: Equilibrium contour for ALOHA and CRA with associated FEC with $R_C = 1/2$ and $SNR = 10\ dB$

showing that under the constraint of channel stability, despite the obtained throughput boost CRA supports a smaller number of users than pure ALOHA and does not appear convenient in low SNR scenarios with respect to synchronous access schemes. As a matter of fact, designing CRA to support a bigger number of users requires a decrement of the retransmission probability that yields to an increase on the average packet delay. Therefore further studies could investigate if this increment of packet delay would still allow asynchronous access schemes to be more efficient than Pure Aloha or not from a packet delay perspective. We want to remark that obtained results for CRA represent an upper bound, since the Shannon Bound has been considered as decoding threshold for received bursts. This is the reason why in this work the analysis has been accomplished in a qualitative and graphical manner rather than comparing the various techniques and burst degree distributions with numerical strictness. A very recent work proposed in [84] and called Enhanced Contention Resolution Aloha (ECRA) shows the possibility to outperform CRA in terms of throughput and Packet Error Rate and sets the more realistic Random Coding Bound as decoding threshold. While those results still do not constitute a practical case using a real code, they constitute an interesting step forward towards the case of a real scenario. The presented analysis can be as well extended to this recent evolution and future works should consider these latest findings rather than CRA.

Chapter 4

Sliding Window Contention Resolution Diversity Slotted Aloha

In the previous chapters it has been shown that CRDSA and its burst degree variations are valid candidate for RA in multiaccess satellite channels. However all these techniques group slots in frames, implying that each user has to wait the beginning of the next frame to start sending its packets. This introduces an undesirable component of delay that is not present in the simplest form of SA and DSA, in which a packet (or the first copy of a packet) is typically sent in the next slot as soon as it is ready for transmission. Also the throughput performance is limited by frames, because users transmitting in the same frame share the same set of eligible slots to place their copies and this increases in a way the probability of unsolvable collisions. Therefore the idea for this new technique arises from the need of an unframed Contention Resolution Diversity Slotted ALOHA technique capable of achieving better throughput and packet delivery delay than in the framed case.

The chapter is organized as follows. In paragraph 4.1 the proposed RA scheme is presented. In paragraph 4.2 the advantages of the proposed technique are illustrated with respect to the throughput and the packet delay. Paragraph 4.3 motivates the degree distribution choices for the case of irregular repetitions. Paragraph 4.4 deals with the adopted simulation approach. In Paragraph 4.5 numerical results are compared in order to show performance improvements and to highlight the importance of proper selection for the key parameters of the access scheme. In paragraph 4.6 the concept of normalized efficiency is introduced together with the formulas used for its computation and simulation results are presented. Paragraph 4.7 concludes the chapter.

4.1 Proposed random access scheme

Consider a scenario in which a certain number of terminals communicate to a remote gateway via satellite using Single Carrier - Time Division Multiple Access (SC-TDMA) and have no

immediate knowledge either about the outcome of their transmission or about the status of the other terminals (transmitting or not). The proposed RA technique works in the following way: as soon as a user has a packet available for transmission, the first copy is sent in the next available slot while the other $d-1$ copies for the same packet are placed in the next $N_{sw}-1$ slots with equally distributed probability. N_{sw} represents the number of successive slots (comprehensive of the one with the first copy) in which a certain user can place its packet replicas and in this sense it can be considered as counterpart of the frame. We refer to this set of N_{sw} slots as Sliding Window, to underline that time after time, depending on their arrival, the set of slots considered by users to place the copies of their packets is gradually sliding. Therefore, only packets ready to be transmitted within the same slot interval have the same set, while those having an arrival difference of $\lceil T_{ij}/T_s \rceil$ slots (T_{ij} indicates the time difference between packet *i* and packet *j*) will share just $N_{sw} - \lceil T_{ij}/T_s \rceil$ slots. At the receiver side, an IC iterative process similar to the one for the classic CRDSA technique is started at the end of each slot or, in a more general case, with a period that is multiple of T_s.

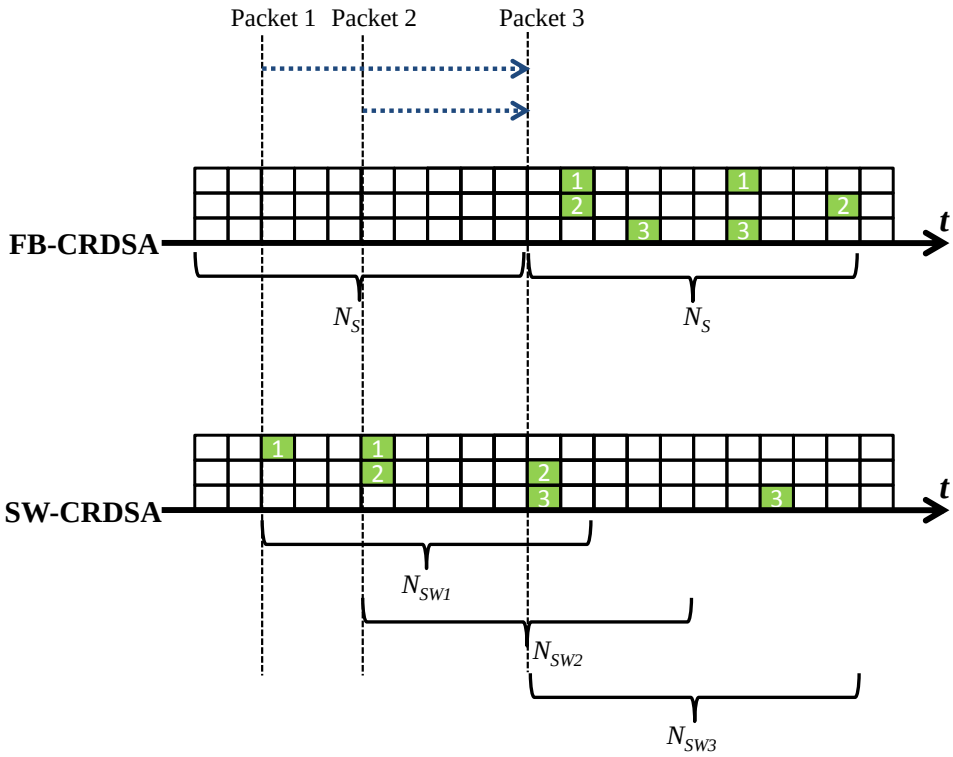

Figure 4.1: Example of access to the channel for FB-CRDSA and SW-CRDSA

4.2 Advantages of the proposed scheme

4.2.1 Throughput

Figure 4.1 illustrates the difference between the technique that groups slots in frames, i.e. Frame-Based CRDSA (FB-CRDSA), and the one using a Sliding Window, from now on indicated as Sliding-Window CRDSA (SW-CRDSA). In FB-CRDSA, packets ready to be transmitted would tipically wait until the beginning of the next frame to start sending their copies (the waiting interval is indicated with a dotted arrow). This implies that packets ready to be transmitted within the same frame, randomly choose the slots to place their replicas from an identical set of slots (i.e. the slots of the frame) and a so called *stopping set* is created with a certain probability. A *stopping set* [85] can be defined as a set of packets such that a certain set of slots contains all the copies of those packets and each slot contains at least two copies of different packets belonging to the stopping set.
On the contrary, as already described in the previous section and differently from FB-CRDSA, in the case of SW-CRDSA users consider the set of the next N_{sw} slots immediately after packet generation as set to put their packet's copies. Therefore each of them has a different slots' set to put the copies of their packets, unless more than one packet was ready for transmission within the same slot interval. The result is that the probability to form a stopping set in SW-CRDSA depends also on the moment in which packets are ready for transmission; thus a lower probability to have a stopping set involving a certain set of users is generally found up to moderate channel loads. In fact, if the equivalent graph representation given in [26] is considered, the resulting graph for SW-CRDSA has infinite size and a more tree-like structure than the corresponding graph for FB-CRDSA, demonstrating that the probability of unsolvable collisions is smaller if the same settings (e.g. number of copies per packet) and $N_{sw} = N_s$ are assumed.

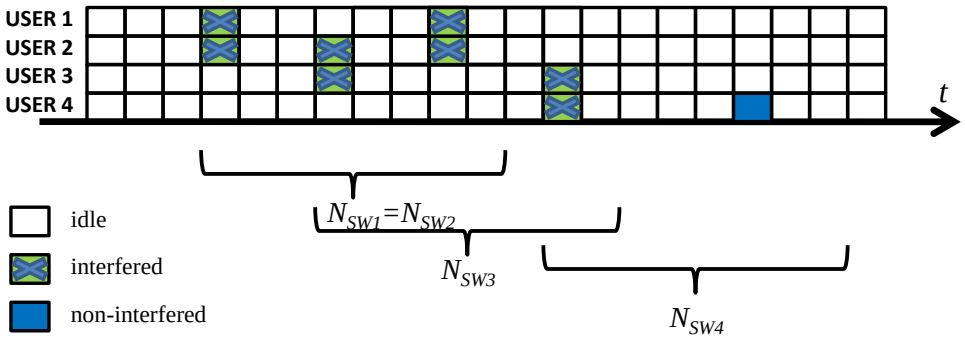

Figure 4.2: Example of SW-CRDSA with irregular repetitions

Consider Figure 4.2, representing an example with irregular number of replicas. If perfect channel estimation and interference cancellation are assumed, each slot can be in one of three

states:

- no copies have been transmitted in a given slot, thus the slot is idle;
- only 1 copy has been transmitted in a given slot, thus the packet did not interefere and is correctly decoded;
- more than 1 copy has been transmitted in a given slot, thus interfering and resulting in loss of all the copy in that slot.

User 1's packet copies are all interfering as well as User 2's and User 3's packet copies, but User 4 has a copy that did not collide. Therefore the content of the packet from User 3 can be restored thanks to IC of User 4's copies and in a waterfall manner also User 2's and User 1's packets will be restored. Notice that the IC process can be done only if all the slots containing the interfered copies are still memorized at the receiver. Thus, the receiver needs to memorize more than N_{sw} slots so that restorable packet's copies are not lost. While adding a cost due to the need to keep in memory more packets at the receiver, this results in a better throughput performance as it will be shown in the next paragraphs.

4.2.2 Packet Delivery Delay

In SW-CRDSA, the usage of a different Channel Access Algorithm allows users to send their packets without waiting for the beginning of the next frame, whereas in the FB-CRDSA case each user has to wait a time between 0 and T_F (i.e. the frame time duration) to start transmitting. Moreover, there is another delay component comprised between T_s and T_F, that depends on the placement of the packet copies over the frame, on the probability of recovering them at each IC process and on the frequency in the employment of the IC process (e.g. at the end of each frame or at the end of each slot). These two components together with the propagation delay T_p represent the total packet delivery delay. In summary, the range for the packet delay D_{pkt} in the FB-CRDSA case is

$$T_p + T_s < D_{pkt} \leq T_p + 2\,T_F \tag{4.1}$$

In the proposed technique instead, the time delay varies from $T_p + T_s$ to $T_p + T_{rx}$, where T_{rx} is the number of slots memorized at the receiver (i.e. N_{rx}) times the slot duration T_s. Even though this range is wider, it will be shown by means of simulations that the average delay in the SW-CRDSA case is always smaller than the one for FB-CRDSA, if $N_s = N_{sw}$ is assumed.

4.3 Remarks on Irregular Repetitions for SW-CRDSA

In FB-CRDSA, the use of irregular repetitions (IRSA) can yield to even better throughput results than using regular repetitions [26]. Therefore, we want to extend the concept of IRSA also to the case of SW-CRDSA in order to demonstrate that SW-CRDSA overcomes FB-CRDSA both in delay and in throughput performance also when using irregular burst repetitions. Considering a certain maximum number of copies per packet, the choice has been to use the same repetition distributions given in [26]:

- $\Lambda(x) = 0.5102\,x^2 + 0.4898\,x^4$ for maximum number of copies per packet equal to 4;
- $\Lambda(x) = 0.5\,x^2 + 0.28\,x^3 + 0.22\,x^8$ for maximum number of copies per packet equal to 8;

where each term $\Lambda_d x^d$ of the polynomial indicates that the probability of having d burst replicas (namely burst degree) for a certain packet is Λ_d.

The motivation driving to this choice is the intention to use the results obtained in [26] for optimized burst repetitions, in order to have a comparison between SW-CRDSA and the best FB-CRDSA case for a given maximum number of copies per packet. Moreover, it is expected that the repetition optimization brought in [26] for an infinite frame size is still valid for SW-CRDSA on a first approximation. In fact, in the asymptotic case of SW-CRDSA ($N_{sw} = \infty$) we can assume the entire history of the transmission equal to a frame of infinite size ($N_s = \infty$), that is also the asymptotic case for FB-CRDSA. Assuming that these distribution optimizations calculated for FB-CRDSA with an asymptotic setting remain valid also for a finite sliding window size (as done in [26] for a finite frame size), the only thing that needs to be demonstrated is that the distribution of packet's copies over the slots in FB-CRDSA and SW-CRDSA is identical. In both cases, the polynomial representation of the degree distribution from the perspective of the slots is

$$\Psi(x) = \sum_d \Psi_d x^d \tag{4.2}$$

$$\Psi_d = \lim_{M\to\infty} \binom{M}{d} \left(\frac{\Psi'(1)}{M}\right)^l \left(1 - \frac{\Psi'(1)}{M}\right)^{M-d} \tag{4.3}$$

where $\frac{\Psi'(1)}{M} = P_{UinS}$ is the probability that a generic user puts a copy in a given slot. Therefore it remains to demonstrate that P_{UinS} is equal for the two cases (i.e. $P_{UinS}^{FR} = P_{UinS}^{SW}$) . Defining:

- $P_i^N = \frac{1}{N-i+1}$ probability of putting the i^{th} replica in a given slot over N possible slots (the i^{th} replica can be put only in those slots not yet occupied by copies of the same packet);
- $P_{NOT(j)}^N = \frac{N-1}{N}\frac{N-2}{N-1}\cdots\frac{N-j}{N-j+1} = \frac{N-j}{N}$ probability that none of j replicas has been put in a given slot over N possible slots;
- $P_{first}^N = \frac{Nsw-1}{N}$ probability that the first replica in the case of SW-CRDSA has been put no more than $N_{sw}-1$ slots before, so that one of the other copies can be put in the considered slot with a certain probability greater than zero (i.e. the considered slot belongs to the sliding window of that packet).

The probability that a generic user sends a burst copy within a given slot in the FB-CRDSA case is

$$P_{UinS}^{FR} = P_1^{N_s} + P_{NOT1}^{N_s} P_2^{N_s} + P_{NOT(l-1)}^{N_s} P_l^{N_s} = \frac{l}{N_s} \tag{4.4}$$

while in the SW-CRDSA case

$$P_{UinS}^{SW} = P_1^{N_s} + P_{first}^{N_s}(P_{NOT1}^{N_{sw}-1} P_2^{N_{sw}-1} + P_{NOT(l-1)}^{N_{sw}-1} P_l^{N_{sw}-1}) = \frac{l}{N_s} \tag{4.5}$$

Therefore $P_{UinS}^{FR} = P_{UinS}^{SW}$ that demonstrates the validity of the assumption.

4.4 Simulation Approach

In order to compare FB-CRDSA and SW-CRDSA, numerical simulations have been performed. All the simulations regard only the MAC layer. Moreover perfect channel estimation and interference cancellation have been assumed, so that bursts are either colliding or correctly received. This means that capture effects[1] and sources of disturbance such as noise have not been considered ($SNR = \infty$). Differently from usual simulations for FB-CRDSA, we do not suppose a fixed channel load on each frame but Poisson Arrivals with a given mean arrival rate λ (mean number of packet arrivals per slot interval). In fact, to achieve comparable results for FB-CRDSA and SW-CRDSA, the same assumptions on packet arrivals have to be made. Since in

[1] Capture effects may lead to better results especially in scenarios where power unbalance among different users is present. In fact, in this case a packet might be decodable even though it belongs to a stopping set.

the case of SW-CRDSA it is not possible to fragment the entire history of the transmission into smaller independent parts (frames), a theoretically infinite time has to be considered together with a realistic packet arrivals distribution. For this reason, we assume an infinite population generating packets according to a Poisson distribution with a given mean λ, that is the commonly used model for RA communications when packet arrivals are independent from each other and can be generated at any time with equal probability. Therefore, the number of users on each frame for FB-CRDSA will vary according to the abovementioned Poisson distribution.

Concerning simulation settings, we consider a satellite communication system with GEO bent-pipe satellites with $T_s = 1\ ms$ assumed as time unit and propagation time from the source to the gateway $T_p = 250\ ms$. Moreover, the receiver starts an IC process at the end of each slot both in the case of FB-CRDSA and in the case of SW-CRDSA, and waiting intervals for the beginning of the next slot are assumed to be negligible. Concerning the maximum number of iterations for the IC iterative process, we have assumed $I_{max} = 50$, a value big enough in order to make sure that the results are independent on the number of iterations of the IC process, since this is not the aim of this work. Finally, the simulations have been performed for an *open loop* communication scenario. Thus neither congestion control nor retransmissions have been considered.

4.5 Numerical Results

4.5.1 Memory Size at the Receiver

The first thing to highlight is the importance of having a memorization of more than N_{sw} slots at the receiver. Consider Figure 4.3, showing the throughput in the case of regular burst degree distribution with two replicas per packet. For a memorization of slots at the receiver of the same size of the SW-CRDSA, the resulting throughput is worse than in FB-CRDSA. However, the performance with SW-CRDSA already overtakes the one in the framed case for $N_{rx} = 2N_{sw}$ and the throughput increases even more for bigger N_{rx} values. This happens up to a point (in this case $5 \cdot N_{sw}$) in which there is no more improvement for the throughput even though bigger N_{rx} values are assumed. This depends on the fact that the possibility of restoring packets is no longer dependent on the size of the receiver. In other words, even though an infinite number of slots is memorized at the receiver, those packets would not be decoded because the problem concerns the presence of stopping sets and is not related to the receiver size.

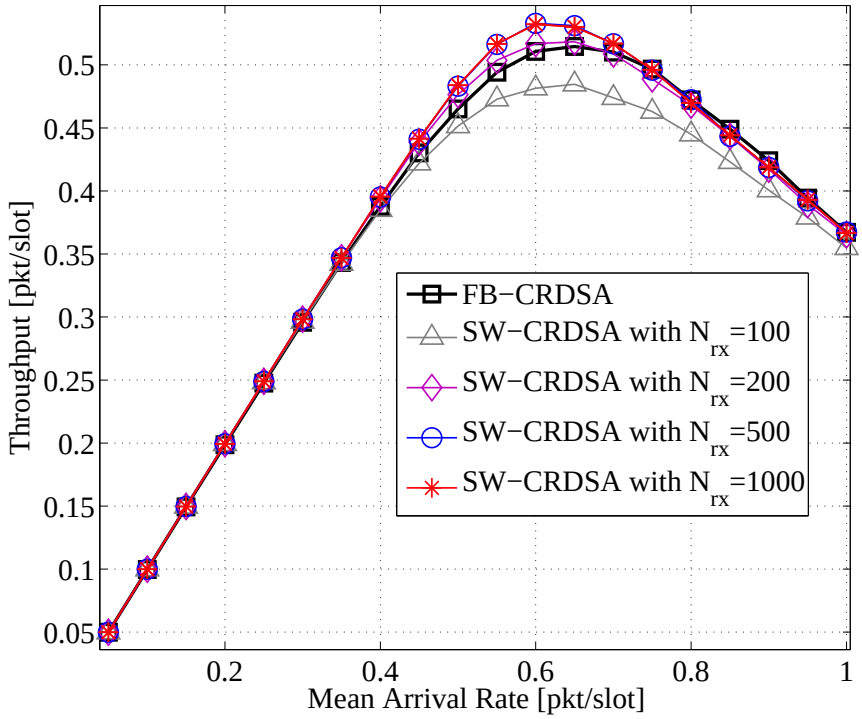

Figure 4.3: Simulation results for the throughput in case of 2 copies per packet with $N_s = N_{sw} = 100$ slots

4.5.2 Size of the Sliding Window

Also the choice of the number of slots for N_s and N_{sw} influences the resulting throughput, although with different dependences. Figure 4.4 shows that increasing the frame and sliding window size, FB-CRDSA's throughput is more influenced than SW-CRDSA's one. Moreover Figure 4.5 shows that while in the FB-CRDSA case the average packet delay has higher dependence on the frame size, the delay in case of SW-CRDSA is remarkably influenced by the value of N_{sw} only for moderate to high arrival rates, but it is still less influenced compared to FB-CRDSA.

4.5.3 Packet Delay Distribution

Another important aspect in the comparison of FB-CRDSA and SW-CRDSA is the distribution of packet delay occurrencies. Figure 4.6 shows an example of packet delay occurrences normalized over the number of correctly received packets for SW-CRDSA and FB-CRDSA as well as its cumulative distribution, in order to verify the probability that a certain delay threshold is exceeded or not. The distribution of received packets for SW-CRDSA can be divided in three sets:

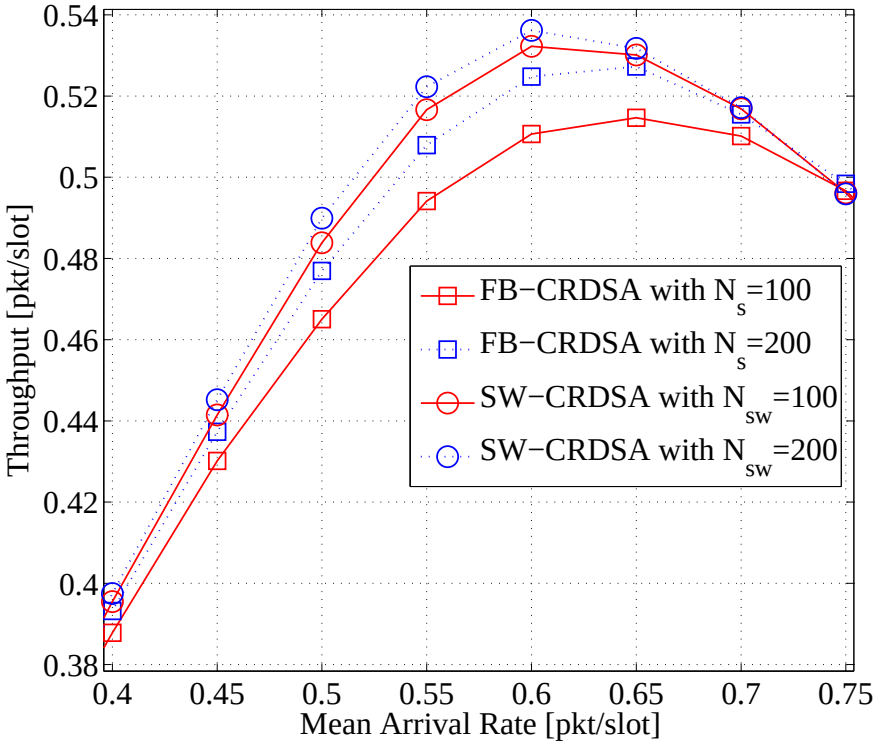

Figure 4.4: Simulation results for the throughput in case of 2 copies per packet with $N_{rx} = 500$ slots for the SW-CRDSA case

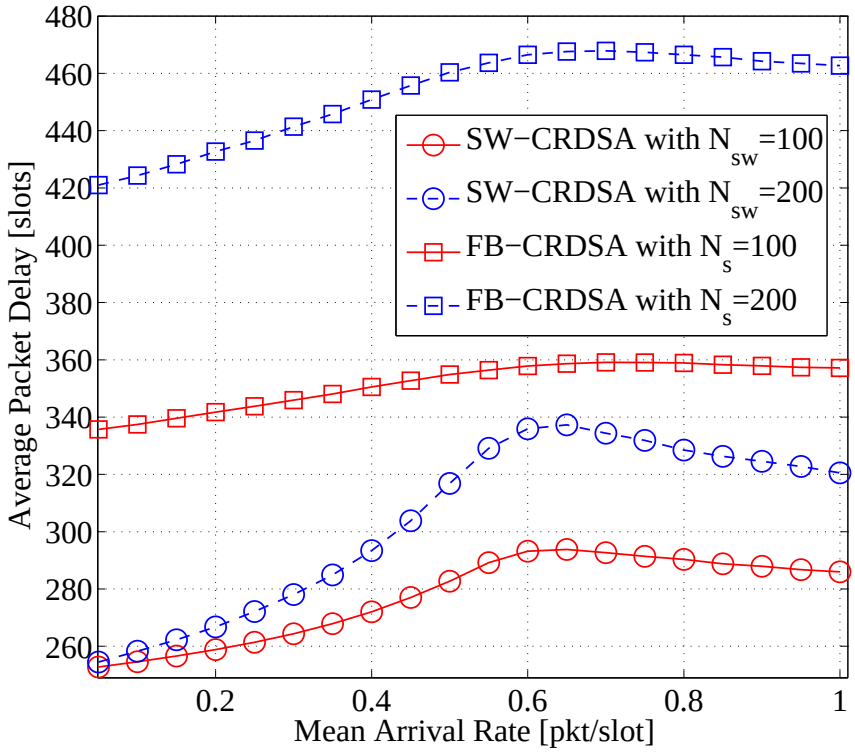

Figure 4.5: Simulation results for the delay in case of 2 copies per packet with $N_{rx} = 500$ slots for the SW-CRDSA case

- $T_p + T_s$ (the most occurring value) represents the lowest achievable delay, i.e. the case in which the first replica is immediately decoded because it is alone in the slot or together with copies belonging to already decoded packets;
- values of delay between $T_p + 2 \cdot T_s$ and $T_p + T_s \cdot N_{sw}$ have more or less equal occurrence distribution, reflecting the fact that in this interval packet content is restored with more or less equally distributed probability among slots;
- values greater than $T_p + T_s \cdot N_{sw}$ present an exponential-like distribution highlighting that the number of occurrencies quickly decreases after this value.

Regarding FB-CRDSA, as expected the packet delay is distributed between $T_p + T_s$ and $T_p + 2 \cdot (T_s \cdot N_s)$. In particular, the distribution is almost symmetric, it has its maximum at $350\ ms$ (that is $T_p + T_s \cdot N_s$) and an occurrence ratio that linearly decreases when considering values away from the maximum in both directions. Consider now the cumulative probability distribution in the small window. Given a certain timeout T_{to} for the packet delay, SW-CRDSA gets much better results than FB-CRDSA in terms of ratio of received packets with delay $\leq T_{to}$, up to timeout values close to $T_p + 2 \cdot T_s \cdot N_s$. However, it is necessary to verify that the better throughput performance of SW-CRDSA is not invalidated, considering the dependency shown in 4.5.1.

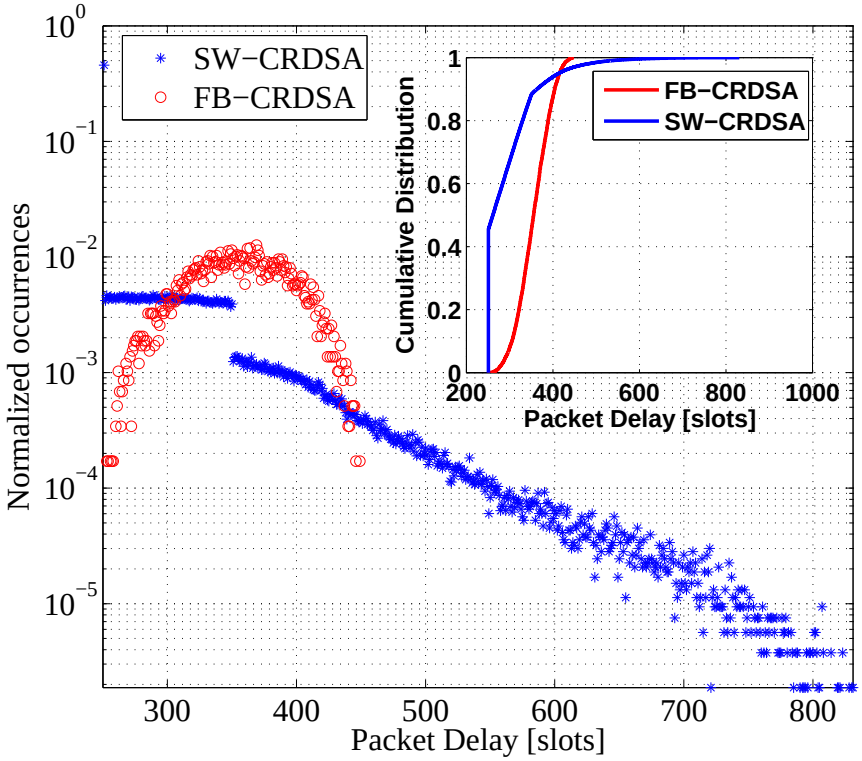

Figure 4.6: Normalized packet delay occurrencies and cumulative distribution for correctly received packets in CRDSA with $N_{sw} = N_s = 100$ slots, $\lambda = 0.6[pkt/slot]$ and $N_{rx} = 500$ slots for the SW-CRDSA case

4.5.4 Overall Results

Finally, in this section the throughput and average packet delay performance of FB-CRDSA and SW-CRDSA for various regular and irregular burst repetition distributions are compared. Figure 4.7 shows throughput curves for different cases. As it can be seen, SW-CRDSA outperforms FB-CRDSA. In particular, while for SW-CRDSA a modest 2% gain is obtained, for the other burst degree distributions a 13% gain is achieved. Moreover the peak throughput is shifted to bigger values of mean arrival rate, showing that SW-CRDSA operates at its optimal point in bigger traffic conditions than FB-CRDSA. Also the region in which the throughput is almost linear, corresponding to successful decoding of almost all packets sent, is extended to bigger mean arrival rates. The only part in which it would be convenient to use FB-CRDSA instead of SW-CRDSA is for very high mean arrival rates. However this is a zone of congestion in which it is not desirable to have the channel falling into because of the low throughput. Figure 4.8 shows the average packet delay performance for the same cases considered in Figure 4.7. As we can see, SW-CRDSA gets always much smaller delay than FB-CRDSA. In particular, the average packet delay for SW-CRDSA is at least $100\ ms$ less than the corresponding value for FB-CRDSA, up $\lambda = 0.8$. Moreover it can be seen that the use of 2 replicas per packet is the best burst degree choice when $\lambda > 0.7$. On the contrary, for smaller values a bigger mean number of copies pays off in terms of diminished average packet delay both in the FB-CRDSA and SW-CRDSA case.

4.6 Average power limitations

The results presented so far in this chapter assume the same peak transmission power for all schemes and burst degree repetitions. As already pointed out in [15] and [26], this assumption is correct for many applications in which the only limit resides on the peak power available and the main interest regards the effect of the interference due to multiple access. However there are cases in which a limit on the average power is present. For example, in satellite systems the average power available at the transponder represents a fundamental limitation for transmission in the downlink path (i.e. from the satellite to the earth receiver). For this reason, it is of interest to analyze the throughput of this new medium access scheme assuming the same average signal power received at the earth station.

4.6.1 Normalized efficiency computation

Let us define the normalized efficiency η similarly to [15], as the ratio of the capacity C_i (with i indicating the considered Random Access Scheme) to the Gaussian capacity C_{ref} (i.e. the

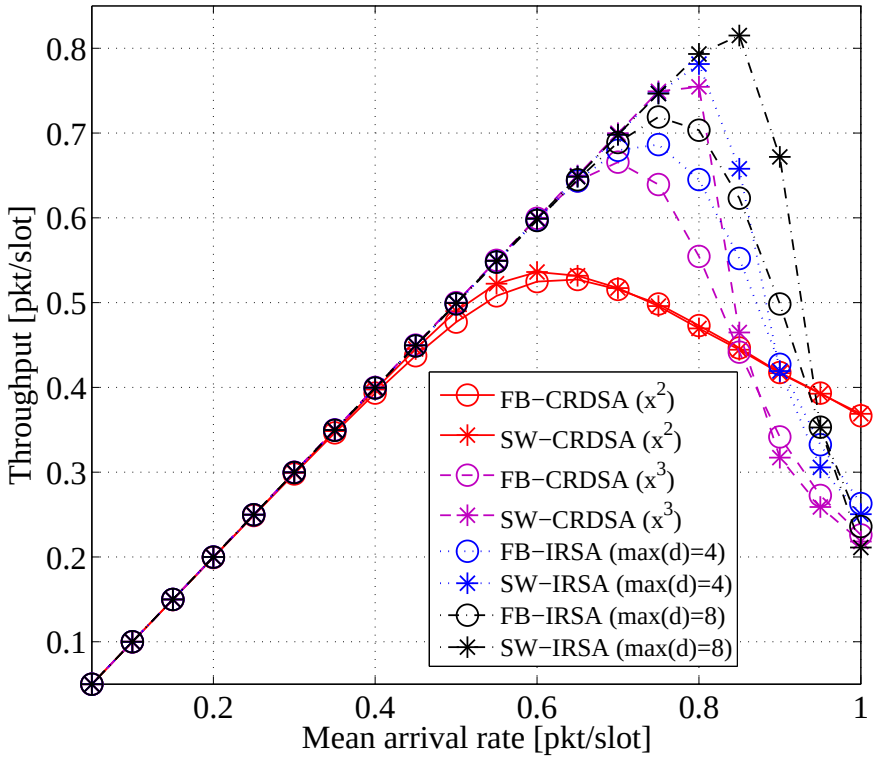

Figure 4.7: Simulated throughput for FB-CRDSA and SW-CRDSA with $N_s = N_{sw} = 200$ slots and $N_{rx} = 500$ slots for the SW-CRDSA case

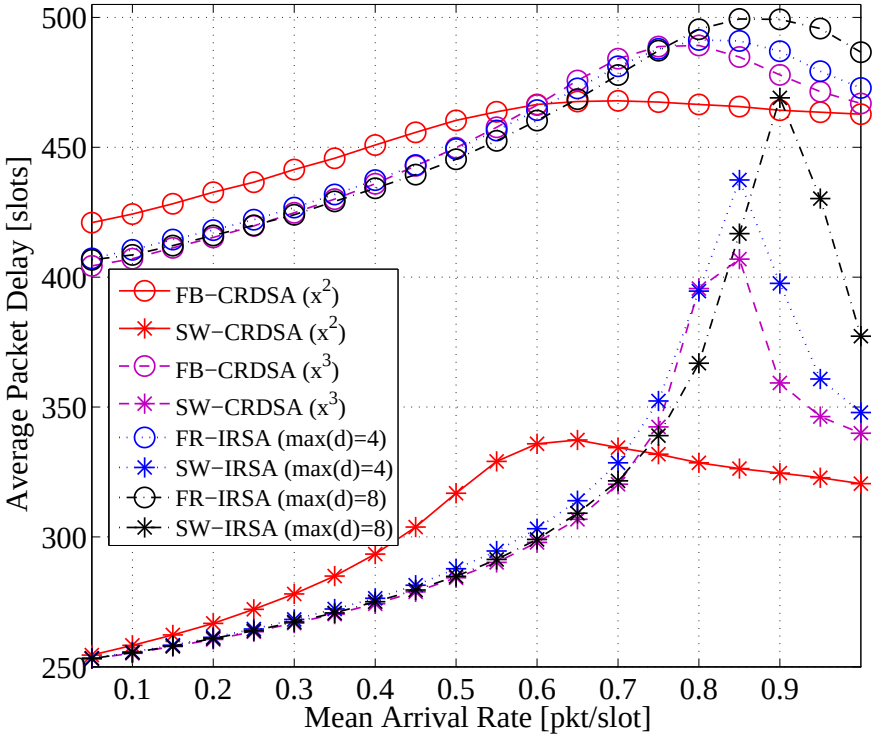

Figure 4.8: Simulated delay for FB-CRDSA and SW-CRDSA with $N_s = N_{sw} = 200$ slots and $N_{rx} = 500$ slots for the SW-CRDSA case

capacity of the satellite channel under the assumption that the transponder transmits continuously):

$$\eta = \frac{C_i}{C_{ref}} \tag{4.6}$$

The Gaussian channel capacity C_{ref} is expressed as

$$C_{ref} = W \cdot log\left(1 + \frac{P_{agg}}{N}\right) \tag{4.7}$$

where W is the channel bandwidth, P_{agg} is the average aggregate signal power at the receiver and N is the noise power. Moreover, from [26] the capacity of the considered RA scheme can be evaluated as

$$C_i = W \cdot G_{OUT-i}(G_{IN}) \cdot log\left(1 + \frac{P_{agg}}{N \cdot D_i}\right) \tag{4.8}$$

where G_{IN} is the normalized MAC channel load, $G_{OUT-i}(G_{IN})$ the related throughput and D_i is the ratio between the average transmitted power and the power used for the transmission of a packet copy. Therefore in SA $D_{SA} = G_{IN}$, in CRDSA with a regular number d of replicas $D_{CRDSA} = (d \cdot G_{IN})$ and in the more general case of irregular repetitions $D_{IRSA} = (\Lambda'(1) \cdot G_{IN})$ where $\Lambda'(1)$ is the average burst degree as defined in [26].

4.6.2 Simulation Results

Based on the definition of normalized efficiency given in 4.6.1, simulation results in terms of normalized efficiency depending on the normalized MAC channel load (i.e. logical channel load regardless of the actual physical number of bursts per packet content) are now shown for various SNR values and under the constraint of equal average power at the receiver. The following simulations have been obtained through implementation in a numerical computing environment, assuming for each point of the resulting curve that the total arrivals of packets to be transmitted are Poisson distributed with aggregate channel load value per each point equal to the mean value of the corresponding Poisson distribution. As already outlined, a typical scenario where these simulations could be applied is the case of a certain number of terminals that send bursty and infrequent data to a remote gateway via satellite using SC-TDMA.

Figures 4.9 - 4.12 show that the obtained results are highly dependent on the utilized burst degree distribution as well as on the SNR. While from a general point of view we can immediately state the convenience in using SW-CRDSA instead of FB-CRDSA, a more in-depth

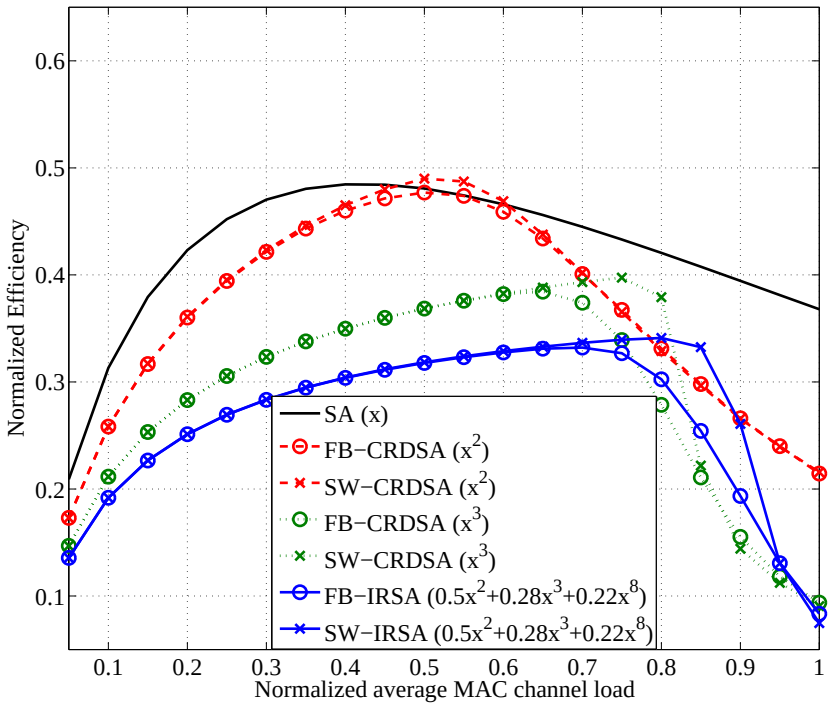

Figure 4.9: Normalized Efficiency for SA and various Frame Based and Sliding Window packet replicas distributions with $N_s = N_{sw} = 200$ slots, $I_{max} = 50$ and $SNR = 0\ dB$

analysis on the best burst degree distribution needs a discussion of the presented figures.

Figure 4.9 shows that for $SNR = 0\ dB$, FB-CRDSA with 2 replicas gets worse results than SA and only equals it in terms of normalized efficiency for $G_{IN} = 0.55$. SW-CRDSA with 2 replicas instead, outperforms SA both in terms of normalized efficiency in the range between $G_{IN} = [0.45, 0.6]$ and in terms of normalized efficiency peak. The nice thing about SW-CRDSA outperforming SA precisely in this range comes from the fact that this is the region around the throughput peak, i.e. the area in which we want our communication system using CRDSA as Random Access method to operate from a throughput maximization perspective. The use of other burst degree distributions than $\Lambda(x) = x^2$ yields to bad results over the entire range of load values, compared to SA. For $SNR = 6\ dB$, the convenience of using CRDSA(x^2) becomes more and more evident while also the choice of a greater number of replicas is found to be a better choice with respect to SA if the operating point is around the throughput peak. However, at $SNR = 6\ dB$ the use of more than 2 replicas per packet still does not appear to be the best choice with respect to CRDSA(x^2). Finally for $SNR = 12\ dB$ using SW-CRDSA(x^3) becomes the best choice while from $SNR = 18\ dB$ SW-IRSA with maximum burst degree equal to 8 begins to outperform the normalized efficiency of CRDSA with regular burst distribution.

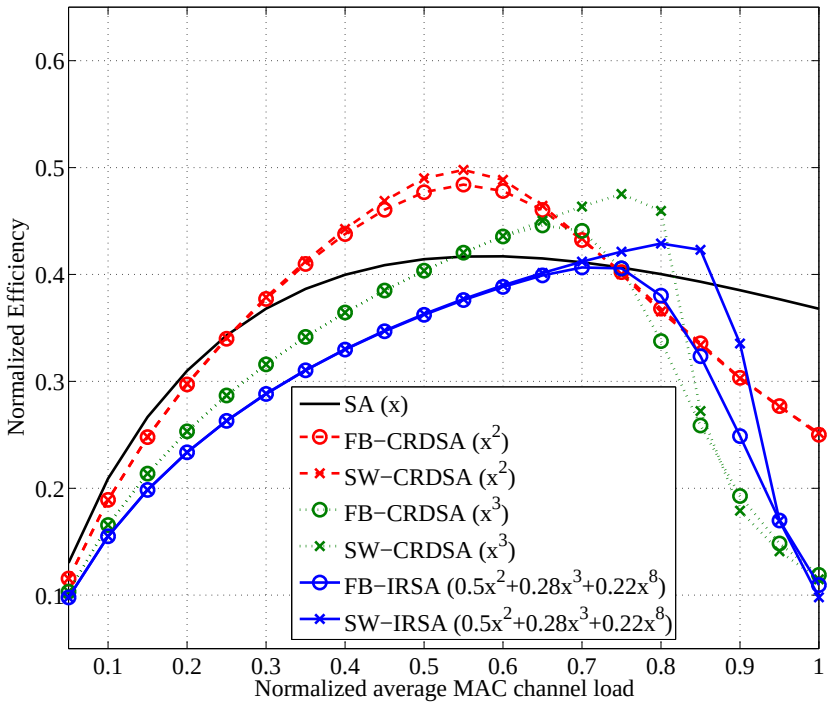

Figure 4.10: Normalized Efficiency for SA and various Frame Based and Sliding Window packet replicas distributions with $N_s = N_{sw} = 200$ slots, $I_{max} = 50$ and $SNR = 6\ dB$

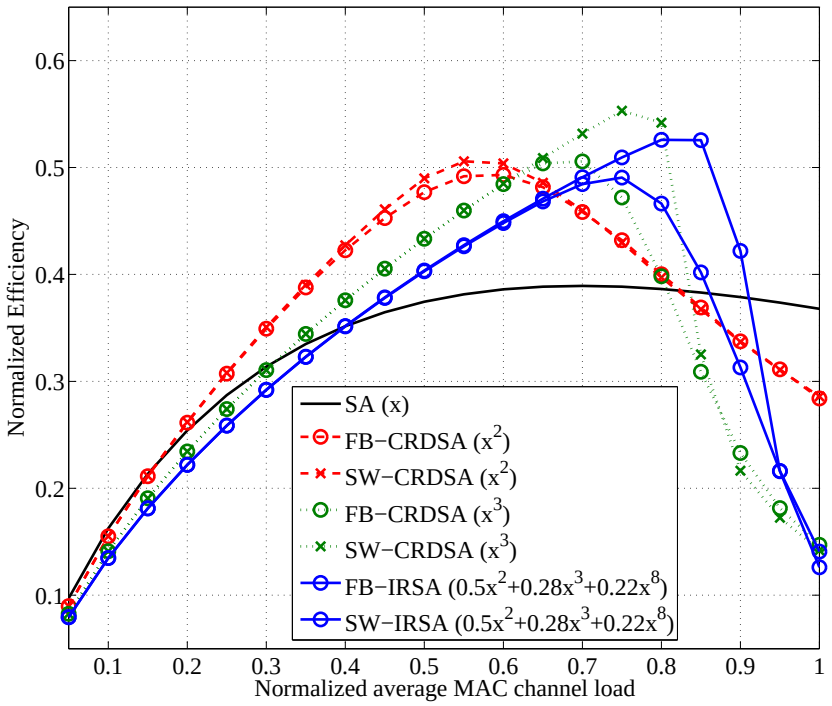

Figure 4.11: Normalized Efficiency for SA and various Frame Based and Sliding Window packet replicas distributions with $N_s = N_{sw} = 200$ slots, $I_{max} = 50$ and $SNR = 12\ dB$

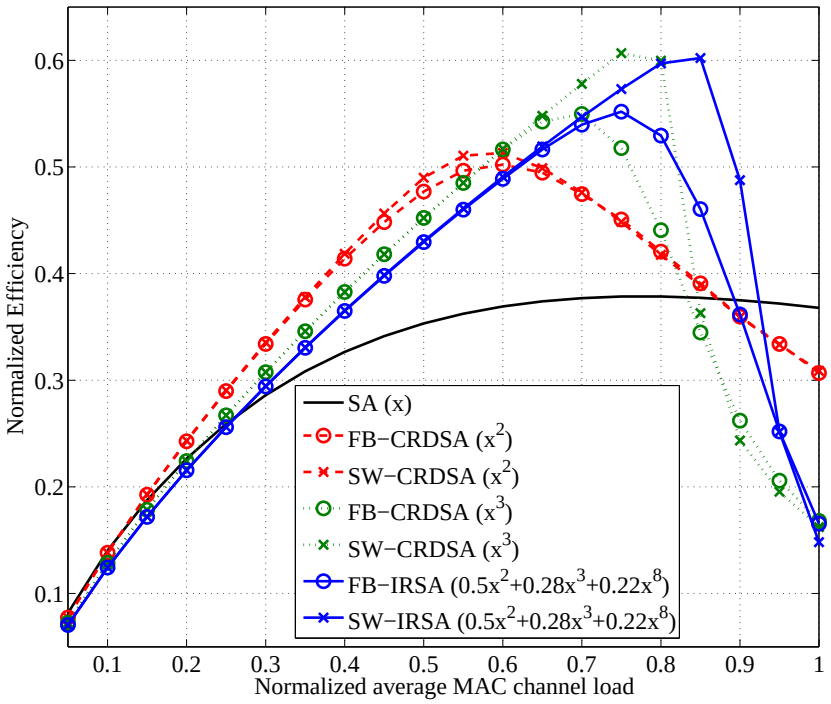

Figure 4.12: Normalized Efficiency for SA and various Frame Based and Sliding Window packet replicas distributions with $N_s = N_{sw} = 200$ slots, $I_{max} = 50$ and $SNR = 18\ dB$

4.7 Conclusions

In this chapter a new channel access scheme for Contention Resolution Diversity SA techniques has been introduced. This novelty shows a throughput performance up to 13% greater than the one using frames; moreover, with this new access scheme, the throughput curve has a wider linear region and also the throughput peak is shifted to greater values of mean arrival rate. Also the average packet delay is greatly reduced, rendering this scheme attractive for delay critical applications especially in cases in which retransmission is not convenient or even impossible because of propagation delay issues as in satellite communications. The presented scheme can also be extended to the more general case in which also the first replica is distributed with equal probability over the sliding window set. However it is believed that this choice would not really improve the throughput while the delay performance would get worse due to additional time before the first replica is sent. This comes from the consideration that, up to moderate channel loads, simultaneous transmissions of the first copy of a packet are not really probable. In the second part of the chapter an analysis in terms of normalized efficiency for the Sliding Window - CRDSA technique has been presented. The need for such an analysis finds its reason in the use of Contention Resolution Diversity Slotted Aloha as Random Access communication technique for transmission in scenarios with limits on the average power (e.g. transponder's

energy limitations in satellite communications). For this reason, a comparison that takes into account fairness in the use of available energy (in this case at the relay) is needed. Found results clearly show that the use of an unframed access to the channel is more convenient than a division of the channel in frames since Sliding Window - CRDSA outperforms Frame Based - CRDSA regardless of the actual burst degree distribution chosen. Moreover while with Frame Based techniques SNR greater than $6\ dB$ is needed in order to get better results than SA in terms of normalized efficiency, with the use of Sliding Window - CRDSA better results around the throughput peak are already found for $SNR = 0\ dB$. The obtained results find application in open loop scenarios as well as in the case of retransmission of unresolvable packets, under the assumption that the channel is globally stable.

Chapter 5

Conclusions

In this thesis, Advanced Random Access techniques for Satellite Communications have been studied. In the last years, new advances in multi-access communication protocols together with the increasing need for bidirectional communications in consumer type of interactive satellite terminals have revived the interest for a set of schemes able to guarantee high-speed and low latency communication in bursty traffic conditions. In this work, starting from the latest findings on Aloha-based Random Access schemes, the optimization of such techniques and their use in closed-loop scenarios have been investigated with particular regard to the Return Channel over Satellite of Digital Video Broadcasting.

The thesis starts in chapter 1 with a summary on the state of the art of Demand Assignement and Random Access techniques as well as on the recent evolution from the first to the second version of the Return Channel over Satellite of Digital Video Broadcasting specification. In chapter 2 a stability and packet delay model for channel analysis and design have been presented showing that proper design through this tools can ensure high performance of this new access scheme. The use of control limit policies has also been introduced and their use has been thoroughly discussed both for finite and infinite users population showing that, differently from Slotted Aloha, in some cases static design over dynamic policies has to be preferable especially if long propagation delay is present. In chapter 3 the same models and tools introduced for CRDSA are extended to the case of asynchronous Random Access schemes and a comparison of the two families of schemes is put in place demonstrating that asynchronous techniques are convenient only when the signal-to-noise ratio is high enough to ensure decodability of partially colliding packets. However, similarly to the synchronous case, also asynchronous schemes can ensure a stable channel for a smaller number of users than pure Aloha protocol. In chapter 4 a new access scheme currently patent pending is presented. In this scheme terminals access the channel in an unframed manner. It has been shown that such a change brings improvements that further diminish latency due to immediate transmission of the first replica and further boost

throughput because the number of loops on the corresponding bipartite graph representation is mitigated.

In light of the improvements presented throughout this work, the need for a new discussion of resource allocation in multi-access satellite communication scenarios such as DVB-RCS2 arises. It is believed that in the next future Return Channel Satellite Terminals and Nework Control Centers will use mechanisms to jointly use Demand Assignement and Random Access techniques in a smarter manner. This will provide differentiated services for a range of applications with different Quality of Service requirements (e.g. delay-constrained versus delay-tolerant traffic sources) while reaching higher throughput. As a matter of fact, applications with small traffic and strict latency requirements may enjoy low propagation delay of Random Access while heavy-traffic applications can exploit the high spectral efficiency of Demand Assignment.

The doctorate research conducted in this three years has been financed by the Sardinian Regional Government through the program *"P.O.R. Sardegna F.S.E. 2007-2013 - Axis IV Human Resources, Objective l.3, Line of Activity l.3.1."* and it has been mainly conducted at the University of Cagliari except for a period of six months spent at the German Aerospace Center (Deutsche Zentrum für Luft- und Raumfahrt) in Oberpfaffenhofen.

Appendix A

Acronyms

DAMA	Demand Assignment Multiple Access
GEO	Geostationary Earth Orbit
DVB	Digital Video Broadcasting
RA	Random Access
SA	Slotted Aloha
DSA	Diversity Slotted Aloha
IC	Interference Cancellation
CDMA	Code Division Multiple Access
CRDSA	Contention Resolution Diversity Slotted Aloha
IRSA	Irregular Repetition Slotted Aloha
MAC	Medium Access Control
RCS	Return Channel over Satellite
DVB-RCS	Digital Video Broadcasting - Return Channel over Satellite
DVB-RCS2	Digital Video Broadcasting - Return Channel over Satellite version 2
NCC	Network Control Center
RCST	Return Channel Satellite Terminals
VSAT	Very Small Aperture Terminals
IPoS	Internet Protocol over Satellite
S-DOCSIS	Data over Cable Service Interface Specification over Satellites
RSM-A	Regenerative Satellite Mesh
DSP	Digital Signal Processors
FEC	Forward Error Correction
IP	Internet Protocol
LL	Lower Layer
HL	Higher Layer
RTT	Round Trip Time
TDMA	Time Division Multiple Access
CRA	Constant Rate Allocation
SLA	Service Level Agreement

RBDC	Rate Based Dynamic Capacity
VBDC	Volume Based Dynamic Capacity
AVBDC	Absolute VBDC
FCA	Free Capacity Allocation
CSMA	Carrier Sense Multiple Access
SREJ-Aloha	Selective Reject Aloha
LDPC	Low Density Parity Check
R-Aloha	Reservation Aloha
TDM	Time Division Multiplexed
LAN	Local Area Network
MF-TDMA	Multi-Frequency Time Division Multiple Access
BoD	Bandwidth on Demand
CR	Capacity Request
FET	First Exit Time
ICP	Input Control Procedure
RCP	Retransmission Control Procedure
CRA	Contention Resolution Aloha
ECRA	Enhanced Contention Resolution Aloha
SC-TDMA	Single Carrier - Time Division Multiple Access
FB-CRDSA	Frame Based - CRDSA
SW-CRDSA	Sliding Window - CRDSA

Appendix B

Notation

G_{IN}	Normalized logical channel load
G_{OUT}	Throughput (i.e. part of logical channel load correctly decoded)
M	Population size
N_s	Number of slots in a frame
T_s	Slot time interval
p_0	New packet generation probability over a frame interval
I_{max}	Maximum number of iteration for the IC process
T	Thinking state
B	Backlogged state
p_r	Packet retransmission probability over a frame interval
f	Frame number
N_B	Number of backlogged users
G_B	Logical channel load due to users in B state
G_T	Logical channel load due to users in T state
PLR	Packet Loss Ratio
d	Burst degree (i.e. number of copies per packet)
λ	Mean of the Poisson process
(G_T^G, N_B^G)	Globally stable equilibrium point
(G_T^S, N_B^S)	Locally stable equilibrium point
(G_T^U, N_B^U)	Unstable equilibrium point
t	Number of transmitting users in T state
b	Number of transmitting users in B state
D_{pkt}	Packet delay
P	Transition matrix
p_{ij}	Transition probability from j to i backlogged users
Q	Success probability matrix
s	Number of packets correctly received
$q(s\|t+b)$	Probability that s packets are correctly received if $t+b$ are transmitted
B_i	Probability of being in state i

N_B^{abs}	Absorbing state
$\hat{N}_B$	Critical threshold for control limit policies
p_c	Retransmission probability in critical state
t_0	Frame start
T_F	Frame duration
τ	Burst duration
R	Channel rate
C_{ref}	Gaussian capacity
R_C	Coding rate
M	Modulation Index
N_{tx}	Number of transmitting packets in a certain frame
$\Lambda(x)$	Burst degree distribution
Λ_d	Probability of burst degree d
SNR	Signal to noise ratio
$SNIR$	Signal to noise plus interference ratio
$SNIR_{dec}$	SNIR decodability threshold
x	Interference degree
N_{sw}	Sliding window size
T_{ij}	Packet arrival difference between packet i and j
T_p	Propagation delay
T_{rx}	Memory time at the receiver
N_{rx}	Number of slots memorized at the receiver
$\Psi(x)$	Slot degree distribution
Ψ_d	Probability of slot degree d
P_{UinS}	Probability that a generic user puts a copy in a given slot
P_i^N	Probability of putting the i^{th} replica in a given slot over N possible
$P_{NOT(j)}^N$	Probability that none of j copies has been put in a given slot over N possible
P_{first}^N	Probability that the first SW-CRDSA copy has been put no more than $N_{sw}-1$ slots before
T_{to}	Packet timeout a the receiver
η	Normalized efficiency
C_i	Capacity of Random Access scheme i
W	Channel Bandwidth
P_{agg}	Aggregate signal power
N	Noise power
D_i	Average-to-copy power ratio

Bibliography

[1] J. Puente, W. Schmidt, and A. Werth, "Multiple-access techniques for commercial satellites," *Proceedings of the IEEE*, vol. 59, no. 2, pp. 218–229, 1971.

[2] R. Gallager, "A perspective on multiaccess channels," *Information Theory, IEEE Transactions on*, vol. 31, no. 2, pp. 124–142, 1985.

[3] E. R. Cacciamani, "The spade system as applied to data communications and small earth station operation," *COMSAT Technical Review*, vol. 1, 1971.

[4] T. Le-Ngoc and S. V. Krishnamurthy, "Performance of combined free/demand assignment multi-access (cfdama) protocol with pre-assigned request slots in integrated voice/data satellite communications," in *Communications, 1995. ICC '95 Seattle, 'Gateway to Globalization', 1995 IEEE International Conference on*, vol. 3, 1995, pp. 1572–1576.

[5] ——, "Performance of combined free/demand assignment multiple-access schemes in satellite communications," *International Journal of Satellite Communications*, vol. 14, no. 1, pp. 11–21, 1996.

[6] T. Le-Ngoc and I. Jahangir, "Performance analysis of cfdama-pb protocol for packet satellite communications," *Communications, IEEE Transactions on*, vol. 46, no. 9, pp. 1206–1214, 1998.

[7] N. Abramson, "Packet switching with satellites," in *Proceedings of the June 4-8, 1973, National Computer Conference and Exposition*, ser. AFIPS '73, 1973, pp. 695–702.

[8] T. Pratt, C. W. Bostian, J. E. Allnutt *et al.*, *Satellite communications*. Wiley New York et al., 1986.

[9] O. Herrero, G. Foti, and G. Gallinaro, "Spread-spectrum techniques for the provision of packet access on the reverse link of next-generation broadband multimedia satellite systems," *Selected Areas in Communications, IEEE Journal on*, vol. 22, no. 3, pp. 574–583, 2004.

[10] P. E. Jackson and C. D. Stubbs, "A study of multiaccess computer communications," in *Proceedings of the May 14-16, 1969, Spring Joint Computer Conference*, 1969, pp. 491–504.

[11] S. S. Lam, "A carrier sense multiple access protocol for local networks," *Computer Networks*, vol. 4, no. 1, pp. 21 – 32, 1980.

[12] G. Bianchi, "Performance analysis of the ieee 802.11 distributed coordination function," *Selected Areas in Communications, IEEE Journal on*, vol. 18, no. 3, pp. 535–547, 2000.

[13] N. Abramson, "The aloha system: another alternative for computer communications," in *Proceedings Fall Joint Computer Conference*.

[14] L. Roberts, *ALOHA packet systems with and without slots and capture*. ARPANET System Note 8 (NIC11290), 1972.

[15] N. Abramson, "The throughput of packet broadcasting channels," *Communications, IEEE Transactions on*, vol. 25, no. 1, pp. 117–128, 1977.

[16] G. Choudhury and S. Rappaport, "Diversity aloha–a random access scheme for satellite communications," *Communications, IEEE Transactions on*, vol. 31, no. 3, pp. 450–457, 1983.

[17] R. Murali and B. Hughes, "Random access with large propagation delay," *Networking, IEEE/ACM Transactions on*, vol. 5, no. 6, pp. 924–935, 1997.

[18] B. Hajek, N. Likhanov, and B. Tsybakov, "On the delay in a multiple-access system with large propagation delay," *Information Theory, IEEE Transactions on*, vol. 40, no. 4, pp. 1158–1166, 1994.

[19] D. Raychaudhuri, "Stability, throughput, and delay of asynchronous selective reject aloha," *Communications, IEEE Transactions on*, vol. 35, no. 7, pp. 767–772, 1987.

[20] P. Patel and J. Holtzman, "Analysis of a simple successive interference cancellation scheme in a ds/cdma system," *Selected Areas in Communications, IEEE Journal on*, vol. 12, no. 5, pp. 796–807, 1994.

[21] E. Casini, R. De Gaudenzi, and O. Herrero, "Contention resolution diversity slotted aloha (crdsa): An enhanced random access schemefor satellite access packet networks," *Wireless Communications, IEEE Transactions on*, vol. 6, no. 4, pp. 1408–1419, 2007.

[22] O. Herrero and R. De Gaudenzi, "A high-performance mac protocol for consumer broadband satellite systems," in *Proceedings of the 27th International Communications Satellite Systems Conference (ICSSC) 2009, Edinburgh, Scotland*, 2009.

[23] R. De Gaudenzi and O. del Rio Herrero, "Advances in random access protocols for satellite networks," in *Satellite and Space Communications, 2009. IWSSC 2009. International Workshop on*, 2009, pp. 331–336.

[24] G. Liva, "A slotted aloha scheme based on bipartite graph optimization," in *Source and Channel Coding (SCC), 2010 International ITG Conference on*, 2010, pp. 1–6.

[25] ——, "Contention resolution diversity slotted aloha with variable rate burst repetitions," in *Global Telecommunications Conference (GLOBECOM 2010), 2010 IEEE*, 2010, pp. 1–6.

[26] ——, "Graph-based analysis and optimization of contention resolution diversity slotted aloha," *Communications, IEEE Transactions on*, vol. 59, no. 2, pp. 477–487, 2011.

[27] C. Kissling, "Performance enhancements for asynchronous random access protocols over satellite," in *Communications (ICC), 2011 IEEE International Conference on*, 2011, pp. 1–6.

[28] G. Liva, E. Paolini, and M. Chiani, "High-throughtput random access via codes on graphs," in *Future Network and Mobile Summit, 2010*, 2010, pp. 1–8.

[29] E. Paolini, G. Liva, and M. Chiani, "High throughput random access via codes on graphs: Coded slotted aloha," in *Communications (ICC), 2011 IEEE International Conference on*, 2011, pp. 1–6.

[30] G. Liva, E. Paolini, M. Lentmaier, and M. Chiani, "Spatially-coupled random access on graphs," in *Information Theory Proceedings (ISIT), 2012 IEEE International Symposium on*, 2012, pp. 478–482.

[31] E. Paolini, G. Liva, and M. Chiani, "Random access on graphs: A survey and new results," in *Signals, Systems and Computers (ASILOMAR), 2012 Conference Record of the Forty Sixth Asilomar Conference on*, 2012, pp. 1743–1747.

[32] M. Chiani, G. Liva, and E. Paolini, "The marriage between random access and codes on graphs: Coded slotted aloha," in *Satellite Telecommunications (ESTEL), 2012 IEEE First AESS European Conference on*, 2012, pp. 1–6.

[33] M. Hagh and M. Soleymani, "Application of raptor coding with power adaptation to dvb multiple access channels," *Broadcasting, IEEE Transactions on*, vol. 58, no. 3, pp. 379–389, 2012.

[34] ——, "Constellation rotation for dvb multiple access channels with raptor coding," *Broadcasting, IEEE Transactions on*, vol. 59, no. 2, pp. 290–297, 2013.

[35] "Next generation dvb-rcs standardization group; etsi en 301 790 v1.5.1; digital video broadcasting (dvb); interaction channel for satellite distribution systems," 2009. [Online]. Available: http://www.etsi.org/deliver/etsi_en/301700_301799/301790/01.05.01_60/en_301790v010501p.pdf

[36] C. Morlet and A. Ginesi, "Introduction of mobility aspects for dvb-s2/rcs broadband systems," in *Satellite and Space Communications, 2006 International Workshop on*, 2006, pp. 93–97.

[37] "Dvb-rcs standardization group; (etsi) en 301 545-2 v1.1.1 (2012-01); digital video broadcasting (dvb); second generation dvb interactive satellite system (dvb-rcs2); part 2: Lower layers for satellite standard," 2012.

[38] A. Rana, J. McCoskey, and W. Check, "Vsat technology, trends, and applications," *Proceedings of the IEEE*, vol. 78, no. 7, pp. 1087–1095, 1990.

[39] J. Puente, "The emergence of commercial digital satellite communications," *Communications Magazine, IEEE*, vol. 48, no. 7, pp. 16–20, 2010.

[40] J. Maisonneuve, M. Deschanel, J. Heiles, W. Li, H. Liu, R. Sharpe, and Y. Wu, "An overview of iptv standards development," *Broadcasting, IEEE Transactions on*, vol. 55, no. 2, pp. 315–328, 2009.

[41] A. Tambuwal, R. Secchi, and G. Fairhurst, "Exploration of random access in dvb-rcs," in *PostGraduate Symposium on the Convergence of Telecommunications, Networking and Broadcasting (PGNET)*, 2011.

[42] "Telecommunication industry association - ip over satellite tia-1008," 2003. [Online]. Available: www.tiaonline.org

[43] S. Lam, "Satellite packet communication-multiple access protocols and performance," *Communications, IEEE Transactions on*, vol. 27, no. 10, pp. 1456–1466, 1979.

[44] L. Kleinrock and S. Lam, "Packet switching in a multiaccess broadcast channel: Performance evaluation," *Communications, IEEE Transactions on*, vol. 23, no. 4, pp. 410–423, 1975.

[45] A. Carleial and M. Hellman, "Bistable behavior of aloha-type systems," *Communications, IEEE Transactions on*, vol. 23, no. 4, pp. 401–410, 1975.

[46] S. Lam and L. Kleinrock, "Packet switching in a multiaccess broadcast channel: Dynamic control procedures," *Communications, IEEE Transactions on*, vol. 23, no. 9, pp. 891–904, 1975.

[47] S. S. Lam and L. Kleinrock, "Dynamic control schemes for a packet switched multi-access broadcast channel," in *Proceedings of the May 19-22, 1975, National Computer Conference and Exposition*, ser. AFIPS '75, 1975, pp. 143–153.

[48] Y.-C.Jenq, "Optimal retransmission control of slotted aloha systems," *Communications, IEEE Transactions on*, vol. 29, no. 6, pp. 891–895, 1981.

[49] A. Meloni, M. Murroni, C. Kissling, and M. Berioli, "Sliding window-based contention resolution diversity slotted aloha," in *Global Communications Conference (GLOBECOM), 2012 IEEE*, 2012, pp. 3305–3310.

[50] A. Meloni and M. Murroni, "On the stability of asynchronous random access schemes," in *Wireless Communications and Mobile Computing Conference (IWCMC), 2013 9th International*, 2013, pp. 843–848.

[51] ——, "Average power limitations in sliding window contention resolution diversity slotted aloha," in *Wireless Communications and Mobile Computing Conference (IWCMC), 2013 9th International*, 2013, pp. 7–12.

[52] ——, "Crdsa, crdsa++ and irsa: Stability and performance evaluation," in *Advanced Satellite Multimedia Systems Conference (ASMS) and 12th Signal Processing for Space Communications Workshop (SPSC), 2012 6th*, 2012, pp. 220–225.

[53] ——, "Random access congestion control in dvb-rcs2 interactive satellite terminals," in *Broadband Multimedia Systems and Broadcasting (BMSB), 2013 IEEE International Symposium on*, 2013, pp. 1–6.

[54] ——, "Random access in dvb-rcs2: Design and dynamic control for congestion avoidance," *Broadcasting, IEEE Transactions on*, in press.

[55] "Viasat. surfbeam web-centric broadband satellite access network," 2009. [Online]. Available: http://www.viasat.com/files/assets/surfbeam_overview_017_lores.pdf

[56] "Tia: Regenerative satellite mesh-a (rsm-a) air interface, tia-1040.1.01," 2005. [Online]. Available: www.tiaonline.org

[57] P. Chini, G. Giambene, and S. Kota, "A survey on mobile satellite systems," *International Journal of Satellite Communications and Networking*, vol. 28, no. 1, pp. 29–57, 2010.

[58] O. Herrero and R. De Gaudenzi, "A high efficiency scheme for large-scale satellite mobile messaging systems," in *Proceedings of the 27th International Communications Satellite Systems Conference (ICSSC) 2009, Edinburgh, Scotland*.

[59] G. Fairhurst, A. Sathiaseelan, C. Baudoin, and E. Callejo, "Delivery of triple-play services over broadband satellite networks," *IET communications*, vol. 4, no. 13, pp. 1544–1555, 2010.

[60] G. Peters, "Satellite delivery of next generation broadband access to the uk," in *Advanced satellite multimedia systems conference (asma) and the 11th signal processing for space communications workshop (spsc), 2010 5th*. IEEE, 2010, pp. 141–146.

[61] A. Munari, G. Acar, C. Kissling, M. Berioli, and H. P. L., "Multiple access in dvb-rcs2 user uplinks," *International Journal of Satellite Communications and Networking*, 2013.

[62] D. Raychaudhuri, "Aloha with multipacket messages and arq-type retransmission protocols–throughput analysis," *Communications, IEEE Transactions on*, vol. 32, no. 2, pp. 148–154, 1984.

[63] A. Ijaz, A. Awoseyila, and B. Evans, "Signal-to-noise ratio estimation algorithm for advanced dvb-rcs systems," *Broadcasting, IEEE Transactions on*, vol. 58, no. 4, pp. 603–608, 2012.

[64] R. Gallager, "Low-density parity-check codes," *Information Theory, IRE Transactions on*, vol. 8, no. 1, pp. 21–28, 1962.

[65] J. Capetanakis, "Tree algorithms for packet broadcast channels," *Information Theory, IEEE Transactions on*, vol. 25, no. 5, pp. 505–515, 1979.

[66] W. Crowther, R. Rettberg, D. Walden, S. Ornstein, and F. Heart, "A system for broadcast communication: Reservation-aloha," in *Proc. 6th Hawaii Int. Conf. Syst. Sci*, 1973, pp. 596–603.

[67] D. Raychaudhuri, "Selective reject aloha/fcfs: An advanced vsat channel access protocol," *International Journal of Satellite Communications*, vol. 7, no. 5, pp. 435–447, 1989.

[68] L. Kleinrock and Y. Yemini, "An optimal adaptive scheme for multiple access broadcast communication," in *Proc. ICC*, vol. 78, 1978, pp. 7–2.

[69] C. J. Wolejsza, D. P. Taylor, M. Grossman, and W. P. Osborne, "Multiple access protocols for data communications via vsat networks," 1987.

[70] H. Peyravi, "Medium access control protocols performance in satellite communications," *Communications Magazine, IEEE*, vol. 37, no. 3, pp. 62–71, 1999.

[71] C. Kozierok, *The TCP/IP-Guide: A Comprehensive, Illustrated Internet Protocols Reference*. No Starch Press, 2005.

[72] M. Allman, V. Paxson, W. Stevens *et al.*, "Tcp congestion control," 1999.

[73] S. Oueslati-Boulahia, A. Serhrouchni, S. Tohmé, S. Baier, and M. Berrada, "Tcp over satellite links: Problems and solutions," *Telecommunication Systems*, vol. 13, no. 2-4, pp. 199–212, 2000.

[74] B. Metcalfe, "Steady-state analysis of a slotted and controlled aloha system with blocking," *SIGCOMM Comput. Commun. Rev.*, vol. 5, no. 1, pp. 24–31, 1975.

[75] L. Kleinrock and S. Lam, "Packet switching in a slotted satellite channel," in *AFIPS Conference Proceedings*.

[76] R. Rettberg, "A brief simulation of the dynamics of an aloha system with slots," *ARPA Satellite System Note 36*, 1972.

[77] J. W. Cohen, *The single server queue*. Access Online via Elsevier, 1982.

[78] D.-K. Hong and S. jin Kang, "Joint frequency offset and carrier phase estimation for the return channel for digital video broadcasting," *Broadcasting, IEEE Transactions on*, vol. 51, no. 4, pp. 543–550, 2005.

[79] L. Kleinrock, *Queueing Systems: Volume I Theory; Queueing Systems: Volume II Computer Applications*. Wiley Interscience, New York, 1975 - 1976.

[80] E. Parzen, *Stochastic Processes*. SIAM, 1962, vol. 24.

[81] M. Ferguson, "On the control, stability, and waiting time in a slotted aloha random-access system," *Communications, IEEE Transactions on*, vol. 23, no. 11, pp. 1306–1311, 1975.

[82] R. Howard, *Dynamic Probabilistic Systems: Vol.: 1: Markov Models*. John Wiley and Sons, Incorporated, 1971.

[83] ——, *Dynamic Probabilistic Systems: Vol.: 2.: Semi-Markov and Decision Processes*. John Wiley and Sons, Incorporated, 1971.

[84] F. Clazzer and C. Kissling, "Enhanced contention resolution aloha - ecra," in *Systems, Communication and Coding (SCC), Proceedings of 2013 9th International ITG Conference on*, 2013, pp. 1–6.

[85] C. Di, D. Proietti, I. Telatar, T. Richardson, and R. Urbanke, "Finite-length analysis of low-density parity-check codes on the binary erasure channel," *Information Theory, IEEE Transactions on*, vol. 48, no. 6, pp. 1570–1579, 2002.

List of Publications Related to the Thesis

- Meloni, A.; Murroni, M., ”CRDSA, CRDSA++ and IRSA: Stability and performance evaluation,” Advanced Satellite Multimedia Systems Conference (ASMS) and 12th Signal Processing for Space Communications Workshop (SPSC), 2012 6th, pp.220-225, 5-7 Sept. 2012
- Meloni, A.; Murroni, M., ”Random Access in DVB-RCS2: Design and Dynamic Control for Congestion Avoidance,” Broadcasting, IEEE Transactions on , no.99
- Meloni, A.; Murroni, M.; Kissling, C.; Berioli, M., ”Sliding window-based Contention Resolution Diversity Slotted ALOHA,” Global Communications Conference (GLOBECOM), 2012 IEEE, pp.3305-3310, 3-7 Dec. 2012***
- Meloni, A.; Murroni, M., ”On the stability of asynchronous Random Access Schemes,” Wireless Communications and Mobile Computing Conference (IWCMC), 2013 9th International, pp.843-848, 1-5 July 2013
- Meloni, A.; Murroni, M., ”Random access congestion control in DVB-RCS2 interactive satellite terminals,” Broadband Multimedia Systems and Broadcasting (BMSB), 2013 IEEE International Symposium on, pp.1-6, 5-7 June 2013
- Meloni, A.; Murroni, M., ”Average power limitations in Sliding Window Contention Resolution Diversity Slotted Aloha,” Wireless Communications and Mobile Computing Conference (IWCMC), 2013 9th International, pp.7-12, 1-5 July 2013

*** Part of this paper is currently patent pending with application number DE102012211433.

Alessio Meloni gratefully acknowledges Sardinia Regional Government for the financial support of his PhD scholarship (P.O.R. Sardegna F.S.E. Operational Programme of the Autonomous Region of Sardinia, European Social Fund 2007-2013 - Axis IV Human Resources, Objective l.3, Line of Activity l.3.1.).